

**MORPHOLOGICAL ASSESSMENT OF A SELECTED REACH OF
JAMUNA RIVER BY USING DELFT3D MODEL**

ORPITA URMI LAZ

**DEPARTMENT OF WATER RESOURCES ENGINEERING
BANGLADESH UNIVERSITY OF ENGINEERING AND
TECHNOLOGY (BUET), DHAKA – 1000**

December 2012

**MORPHOLOGICAL ASSESSMENT OF A SELECTED REACH OF
JAMUNA RIVER BY USING DELFT3D MODEL**

A thesis submitted by

ORPITA URMI LAZ

(Roll No.1009162021P)

In partial fulfillment of the requirements for the degree

of

Master of Science in Engineering (Water Resources)

DEPARTMENT OF WATER RESOURCES ENGINEERING

**BANGLADESH UNIVERSITY OF ENGINEERING AND
TECHNOLOGY (BUET), DHAKA – 1000**

December 2012

DECLARATION

This is to certify that the thesis on “Morphological assessment of a selected reach of Jamuna river by using Delft3d model” has been performed by Orpita Urmi Laz and neither this nor any part thereof has been submitted elsewhere for the award of any other degree or diploma.

Signature by the Candidate
Orpita Urmi Laz

CERTIFICATE OF APPROVAL

The thesis titled “**Morphological assessment of a selected reach of Jamuna river by using Delft3d model**” submitted by Orpita Urmi Laz, Roll No: 1009162021(P), Session: October 2009, has been accepted as fulfilling this part of the requirement for the degree of Master of Science in Water Resources Engineering on December 2012.

Dr. Umme Kulsum Navera
Professor and Head
Department of Water Resources Engineering
BUET, Dhaka

Chairman of the Committee
(Supervisor)

Dr. Md. Abdul Matin
Professor
Department of Water Resources Engineering
BUET, Dhaka

Member

Dr. Md. Sabbir Mostafa Khan
Professor
Department of Water Resources Engineering
BUET, Dhaka

Member

Mr. Abu Saleh Khan
Deputy Executive Director
Institute of Water Modelling
House No.496, Road 32
New DOHS, Mohakhali, Dhaka - 1206

Member
(External)

Table of Contents

	Page No.
<i>Declaration</i>	<i>iii</i>
<i>Certificate of Approval</i>	<i>iv</i>
<i>Table of Contents</i>	<i>v</i>
<i>List of Figures</i>	<i>xi</i>
<i>List of Tables</i>	<i>xiv</i>
<i>Acknowledgement</i>	<i>xv</i>
<i>Abstract</i>	<i>xvi</i>
Chapter 1. Introduction	
1.1 General	1
1.2 Origin of Jamuna River	6
1.3 Background of the study	11
1.4 Scope of mathematical modeling	14
1.5 Objectives of the study	17
1.6 Organization of the report	18
Chapter 2. Literature Review	
2.1 General	19
2.2 Channel patterns	19
2.2.1 Straight channel	20
2.2.2 Meandering river	21
2.2.3 Braided channel	22

2.3 Factors influencing river geometry	23
2.4 Sediment transport	23
2.5 Morphology of a river system	25
2.6 Previous researches on Jamuna River	26
2.7 Previous studies on different rivers	36
2.7.1 Studies in Bangladesh	36
2.7.2 Studies around the World	38
2.8. Mathematical modeling studies	39
2.8.1 Studies in Bangladesh	40
2.8.2 Studies around the World	43
2.9. Summary	45

Chapter 3. Theory and Methodology

3.1 General	47
3.2 The basic equations of fluid dynamics	47
3.2.1 The Continuum Hypothesis - Fluid Element	48
3.2.2 The Continuity Equation	48
3.2.3 Conservation of Momentum	50
3.3 Advection-Diffusion equation	54
3.4 Settling Velocity	54
3.5 Deposition and erodability on Delft3d	55
3.6 Sediment transport	58

3.6.1	Suspended and bed load transport	58
3.6.2	Bed load transport: Van Rijn' 84	60
3.7	Methodological steps	62
3.8	Profile of the study area	63
3.9	Data collection and analysis	65
3.9.1	Satellite image data	65
3.9.2	Description of the selected stations	66
3.10	Approach and methodology followed by Iwm during data collection	66
3.10.1	Coordinate System	66
3.10.2	Bench mark	66
3.10.3	Bathymetric survey	66
3.10.4	Char survey	66
3.10.5	Bankline (Alignment) survey	67
3.10.6	Water Level gauging	67
3.11	Data analysis	67
3.12	Mathematical modeling	69
3.12.1	Grid generation	69
3.12.2	Bathymetry development	69
3.12.3	Sensitivity Analysis	70
3.12.4	Calibration and validation of the model	70
3.12.4.1	Hydrodynamic calibration	70

3.12.4.2 Hydrodynamic validation	70
3.12.5 Simulation of the model	71
3.13 Summary	71
Chapter 4. Model Setup	
4.1 General	72
4.2 Numerical model	72
4.3 Description of the model used in this study	74
4.4 Modeling framework	77
4.5 Space and time variation	78
4.6 Model set-up	79
4.6.1 Land Boundaries	79
4.6.2 Grid set up of the study reach	80
4.6.3 Refine grid	81
4.6.4 Orthogonalise grid	82
4.6.5 Grid Smoothness (Aspect Ratio)	83
4.6.6 Bathymetry development	84
4.7 Flow module set-up	86
4.7.1 Dry Points and Thin Dams	87
4.7.2 Time Frame	87
4.7.3 Boundary set up	88
4.7.4 Initial conditions	91

4.7.5 Parameters in hydrodynamic module	92
4.7.6 Morphological updating	93
4.7.7 Morphological "Switch"	94
4.7.8 Monitoring option	94
4.8 Summary	96
Chapter 5. Results and Discussions	
5.1 General	97
5.2 Model calibration	98
5.2.1 Necessity of model calibration	98
5.2.2 Calibration data	99
5.3 Model verification	100
5.3.1 Necessity of model verification	100
5.3.2 Verification data	100
5.4 Simulation of the model	101
5.4.1 Comparison of observed and simulated bed elevations	102
5.4.2 Variation in velocity and sediment transport	106
5.4.3 Comparison of the simulated bathymetry in September 2011 by Mike21 and Delft	125
5.5 Sensivity Analysis	126
5.5.1 Bottom roughness	128
5.5.2 Eddy Viscosity	128

5.6 Summary	128
Chapter 6. Conclusions and Recommendations	
6.1 General	130
6.2 Conclusions	130
6.3 Recommendations for further Study	131
References	133
Appendix A	139

List of Figures

Figure No.		Page No.
Figure 1.1	River Systems of Bangladesh	4
Figure 1.2	Longitudinal profile of the Brahmaputra River	6
Figure 1.3	Brahmaputra-Jamuna River System within Bangladesh Territory	9
Figure 1.4	Catchment Area of Major Rivers	10
Figure 2.1	Channel patterns	20
Figure 2.2	Various features of channels	21
Figure 2.3	Development of the Bengal Delta	29
Figure 2.4	Low-stage plan forms of the Jamuna River	32
Figure 2.5	Movement of the main channel for the period 1973-1995 and planform in 1995	33
Figure 2.6	Relation between the elevation and the age of the land along the Jamuna River	34
Figure 2.7	Plan forms of low flow, bar full, dominant and minimum bank full as defined by FAP1 and FAP24 for the Jamuna River at the beginning of 1994	35
Figure 3.1	Mass fluxes entering and leaving an element	49
Figure 3.2	Surface stresses on a fluid element in 2 dimensions	51
Figure 3.3	Schematization of flux on the kmx layer	56
Figure 3.4.	Schematic overview Delft3D calculation steps	62
Figure 3.5	Study Area on the Jamuna River	64
Figure 3.6	Water level gauge on the River Jamuna	67
Figure 4.1	Computer Modelling cycle from prototype to the Modeling results	73
Figure 4.2	Interaction among the main Delft3D modules	75
Figure 4.3	Structure of Delft3D	77
Figure 4.4	Land Boundary for selected reach of Jamuna River	80
Figure 4.5	Flow grids for selected reach of Jamuna River	81

Figure 4.6	Grids Refinement for selected reach of Jamuna River	82
Figure 4.7	Orthogonality of grids for selected reach of Jamuna River	83
Figure 4.8	Aspect ratio of grids for selected reach of Jamuna River	84
Figure 4.9	Measured bathymetry used in the model	85
Figure 4.10	Interpolated bathymetry used in the model	86
Figure 4.11	Courant number variation as function of the grid size	88
Figure 4.12	Flow Boundaries	86
Figure 4.13	Time series hydrographs from April to July 2010 used in the model as Boundary conditions for calibration period	90
Figure 4.14	Time series hydrographs from April to October 2011 used in the model as Boundary Conditions for Validation Period	91
Figure 4.15	Observation points and cross sections	95
Figure 5.1	Comparison of simulated and measured water levels of Jamuna River for calibration at Sirajganj	99
Figure 5.2	Comparison of simulated and measured water levels of Jamuna River for validation at Sirajganj	101
Figure 5.3	Cross Sections shown in Bathymetry of selected reach of the Jamuna River for comparison	102
Figure 5.4	Comparison of Cross-Section at (Sec a-a)	103
Figure 5.5	Comparison of Cross-Section at (Sec b-b)	103
Figure 5.6	Comparison of Cross-Section at (Sec c-c)	104
Figure 5.7	Comparison of Cross-Section at (Sec d-d)	104
Figure 5.8	Comparison of Cross-Section at (Sec e-e)	105
Figure 5.9	Comparison of Cross-Section at (Sec f-f)	105
Figure 5.10	Comparison of Cross-Section at (Sec g-g)	106
Figure 5.11	Depth Averaged Velocity in 29/7/2010	108
Figure 5.12	Total Sediment Transport in 29/7/2010	108

Figure 5.13	Depth Averaged Velocity in 27/1/2011	109
Figure 5.14	Total Sediment Transport in 27/1/2011	109
Figure 5.15	Depth Averaged Velocity in 27/7/2011	110
Figure 5.16	Total Sediment Transport in 27/7/2011	110
Figure 5.17	Depth Averaged Velocity in 25/1/2012	111
Figure 5.18	Total Sediment Transport in 25/1/2012	111
Figure 5.19	Depth Averaged Velocity in 24/7/2012	112
Figure 5.20	Total Sediment Transport in 24/7/2012	112
Figure 5.21	Bathymetry of selected reach of the Jamuna River in April 2010	114
Figure 5.22	Initial bed level in (1 April 2010)	115
Figure 5.23	Simulated bed level in (25 September 2010)	115
Figure 5.24	Simulated bed level in (23 September 2011)	116
Figure 5.25	Simulated bed level in (28 September 2012)	116
Figure 5.26	Cross-section at Section 1	117
Figure 5.27	Cross-section at Section 2	119
Figure 5.28	Cross-section at Section 3	120
Figure 5.29	Cross-section at Section 4	121
Figure 5.30	Cross-section at Section 5	123
Figure 5.31	Simulated bathymetry by Mike 21 (September 2011)	125
Figure 5.32	Simulated bathymetry by Delft 3D (September 2011)	125
Figure 5.33	Influence of Manning parameter on amplitudes of water level	127
Figure 5.32	Influence of Eddy viscosity on amplitudes of water level	128

List of Tables

Table No.		Page No.
Table 1.1	Losses of livelihoods	12
Table 1.2	Losses of cultivated land	12
Table 2.1	Grain size (mm) of bed material collected in 1993- 1994 by FAP24 (1996)	27
Table 4.1	Hydraulic parameters used in model	92
Table 5.1	Average sediment transport rate of the river for various seasons	113
Table 5.2	Average erosion and deposition of observed and simulated bathymetry	123
Table 5.3	Bed level changes for the selected sections	124
Table A.1	Observed and simulated water level data for calibration	139
Table A.2	Observed and simulated water level data for validation	140

Acknowledgements

I express my deepest thanks and appreciation to my supervisor Dr. Umme Kulsum Navera, Professor and Head, Department of Water Resources Engineering, BUET for her constant supervision, valuable guidance and unlimited encouragement during the period of research work. It was a great opportunity for me to work with Prof. Dr. Umme Kulsum Navera, whose unfailing eagerness made the study a success.

Sincere thanks also goes to the Members of the Examination Committee, Dr. M.A. Matin, Professor, Department of Water Resources Engineering, BUET; Dr. Md. Sabbir Mostafa Khan, Professor and Head of WRE Department, BUET and Mr. Abu Saleh Khan, Deputy Executive Director of Institute of Water Modelling, for their special interest, valuable comments and suggestions regarding the study.

I am indebted to all the officials of the River Engineering Division, IWM, Dhaka and to the officials of River Hydrology and Research Circle, BWDB, Dhaka for their help and cooperation in collecting the required data and information.

I would also like to express my gratitude to my parents and my husband for their sincere support, sacrifice, inspiration and help during the entire period of this study.

Finally I am grateful to almighty Allah.

Abstract

Simulation of sediment transport rate at the river Jamuna and variation of bed level along the river is carried out by using a two dimensional morphological model. Non-cohesive sediment transport module of Delft 3D Flow is used for the simulation. The upstream boundary of the model is taken at 30 Km upstream of Bangabandhu Bridge and downstream boundary is taken at 20 Km downstream of Bangabandhu Bridge.

Simulation period is taken from April 2010 to December 2012. Simulation is carried out for hydrodynamic calibration and for sediment transport rates. The cross-sections are taken at the locations which are vulnerable, such as Subaghacha, Sirajganj, Jamuna Bridge and also in the upstream near Kazipur and downstream near Chauhali etc. In the Morphology tab, the morphological scale factor has been set to 8.25 which extend the 121 days hydrodynamics to about 1000 days of morphological change. Calibration and validation are carried out against field observations (water level) of 2010 and 2011 respectively. Comparisons between simulated and observed water level are taken at the Sirajgonj station. The results showed satisfactory agreement with observed values.

For hydrodynamic and morphological computation, a time series discharge data is used at the upstream boundary and water level data as downstream boundary. Observed and simulated bed level elevation of 2010 has been compared and the comparison showed a very good agreement. After calibration of the model, the net amount of erosion and deposition along the river reach is computed. Finally, cross-sectional variation of bottom level during the monsoon seasons from 2010 to 2012 has been observed.

Results reveal that erosion takes place in the channel bed and the deposition mainly takes place to the adjacent char areas and increased its width and area. It is also evident that the channel has been shifted westwards of the reach due to shifting of the bank line of the river. Many tributary and distributaries have been appeared due to progressive erosion. In Sirajgonj, the sediment transport capacity seems to be the

highest due to higher velocity of flow. The zones of higher velocity has higher sediment transport capacities therefore occurs more erosion

CHAPTER 1

INTRODUCTION

1.1 General

Bangladesh is a riverine country with hundreds of rivers overlaying its landscape. Because of its inherent alluvium nature, the rivers of Bangladesh are morphologically dynamic characterized by erosion and sedimentation, which results in changes in hydraulic geometry; plan form and longitudinal profile of the rivers (Habibullah, 1987). Aggradations, degradation or change in plan forms; change in river bed and meandering characteristics are most common features in the rivers of Bangladesh, affecting the major rivers as well as the medium and the minor rivers. When bank erosion of a river takes place the drainage capacity of the river and navigation is hampered and consequently a large number of populations are directly or indirectly affected. A simple solution could be through local protective measures for the time being but properly designed river control and training structures are required to reduce the loss of lands. Before intervening with the natural behavior of a river, the consequences in both the near future and the long run should be considered. Each river style is characterized by a distinctive set of attributes, analyzed in terms of channel plan form, the geomorphic units that make up a reach, and bed material texture. The identification and interpretation of geomorphic units allows interpretation of processes that reflect the range of behavior of a river style. Thus helps in understanding of the behavior of the river in natural and disturbed conditions in an effective manner.

Bangladesh is a country blessed with abundant natural source of fresh sweet water. The three major rivers originating from Himalayas (Indus, Ganges and Brahmaputra) and flowing down the Northern regions of Indian Sub-continent reaches the Bay of Bengal through Bangladesh (Rahman et al., 2007). These rivers frequently flood the vast plain of Bangladesh, deposit silt and contributed largely to create the fertile soil. People of this land use the water from these rivers and their tributaries for cultivation and livelihood. For thousands of years, people settled in this fertile and easily

cultivable land along the rivers. There are 405 rivers in total, Brahmaputra, Padma, Meghna, Jamuna, Karnafuli are the bigger rivers among all. Total length of rivers is 24,140 Km. In an average yearly 844,000 million cubic meters of water flows into the country, the sediment load that comes along the flow is more than a billion ton (Imran, 2011).

The profusion of rivers can be divided into five major networks. The Jamuna originates as the Yarlung Tsangpo River in China's Xizang Autonomous Region (Tibet) and flowing through India's state of Arunachal Pradesh, where it becomes known as the Brahmaputra ("Son of Brahma"). There it turns to south into Asam. In flood plain of Asam, it flows towards west and then again veers into south and then enters Bangladesh through Kurigram district (at the border of Kurigram Sadar and Ulipur upazilas). Presently the Brahmaputra continues southeast from Bahadurabad (Dewanganj upazila of Jamalpur district) as the Old Brahmaputra and the river between Bahadurabad and Aricha is the Jamuna, not Brahmaputra. The Hydrology Directorate of the Bangladesh Water Development Board (BWDB) refers to the whole stretch as the Brahmaputra-Jamuna. Tista, Dudhkumar, Korotoa-Atrai, Hurasagar etc. are the main tributaries of Jamuna River.

The total length of the Tsangpo-Brahmaputra-Jamuna River up to its confluence with the Ganges is about 2,700 km. Within Bangladesh territory, Brahmaputra-Jamuna is 276 km long, of which Jamuna is 205 km. It receives waters from five major tributaries that total some 740 kilometers in length.

The second system is the Padma-Ganges originated in the Gangotri Glacier of the Himalaya, the Ganges runs through Himachal Pradesh, Uttar Pradesh, Bihar and West Bengal in India. For some 110 km the Ganges River forms the western boundary between India and Bangladesh before it enters Bangladesh at Durlavpur Union in Shibganj Upazila in the district of Chapai Nababganj to the Bay of Bengal. Just west of Shibganj, the distributary Bhagirathi emerges and flows southwards as the Hooghly. After the point where the Bhagirathi branches off, the Ganges is officially referred to as the Padma.

Further downstream, in Goalando, 2200 km away from the source, the Padma is joined by the mighty Jamuna (Lower Brahmaputra) and the resulting combination flows with the name Padma further east, to Chandpur. Here, the widest river in Bangladesh, the Meghna, joins the Padma, continuing as the Meghna almost in a straight line to the south, ending in the Bay of Bengal. Its main tributary is the Mahananda; its principal distributary is the Madhumati (called the Garai in its upper course) at right bank and Ichamati, Boral, Badai, Khalshadingi at left bank.

The third network is the Surma-Meghna River System. Surma River rises in the Manipur Hills in northern Manipur state, India, where it is called the Barak, and flows west and then southwest into Mizoram state. There it veers north into Assam state and flows west past the town of Silchar. At the border with Bangladesh, where the river divides, the north-eastern branch is called the Surma River and the south-eastern the Kushiya River. The Surma is also known as the Baulai River after it is joined by the Someswari River at Sukhair Rajapur Union in Dharmapasha Upazila in Sunamganj District. When the Surma and the Kushiya rejoin above Bhairab Bazar, the river is known as the Meghna River, which flows south past Dhaka and enters the lower Padma River. Near Muladhuli in Barisal district, the Safipur River is an offshoot of the Surma. At Sarail of Brahmanbaria District, the river Titas emerges from Meghna and after circling two large bends by 240 km, falls into the Meghna again near Nabinagar Upazila. Titas forms as a single stream but braids into two distinct streams which remain separate before re-joining the Meghna.

In Daudkandi, Comilla, Meghna is joined by the great river Gomoti, created by the combination of many streams. The Dakatia River is also part of this river in Comilla district. (BWDB, 2011)

Barak River flows separately to North-eastern as Surma River and to South-Eastern at Jakiganj Upazila in Sylhet District, originating from the hilly regions of eastern India. The Meghna is formed inside Bangladesh by the joining of the Surma and Kushiya rivers at Bajitpur in Keshoreganj. Down to Matlab in Chandpur, Meghna joins with Padma River and is hydrographically referred to as the Upper Meghna.

After the Padma joins, it is referred to as the Lower Meghna and finally it flows to the Bay of Bengal.

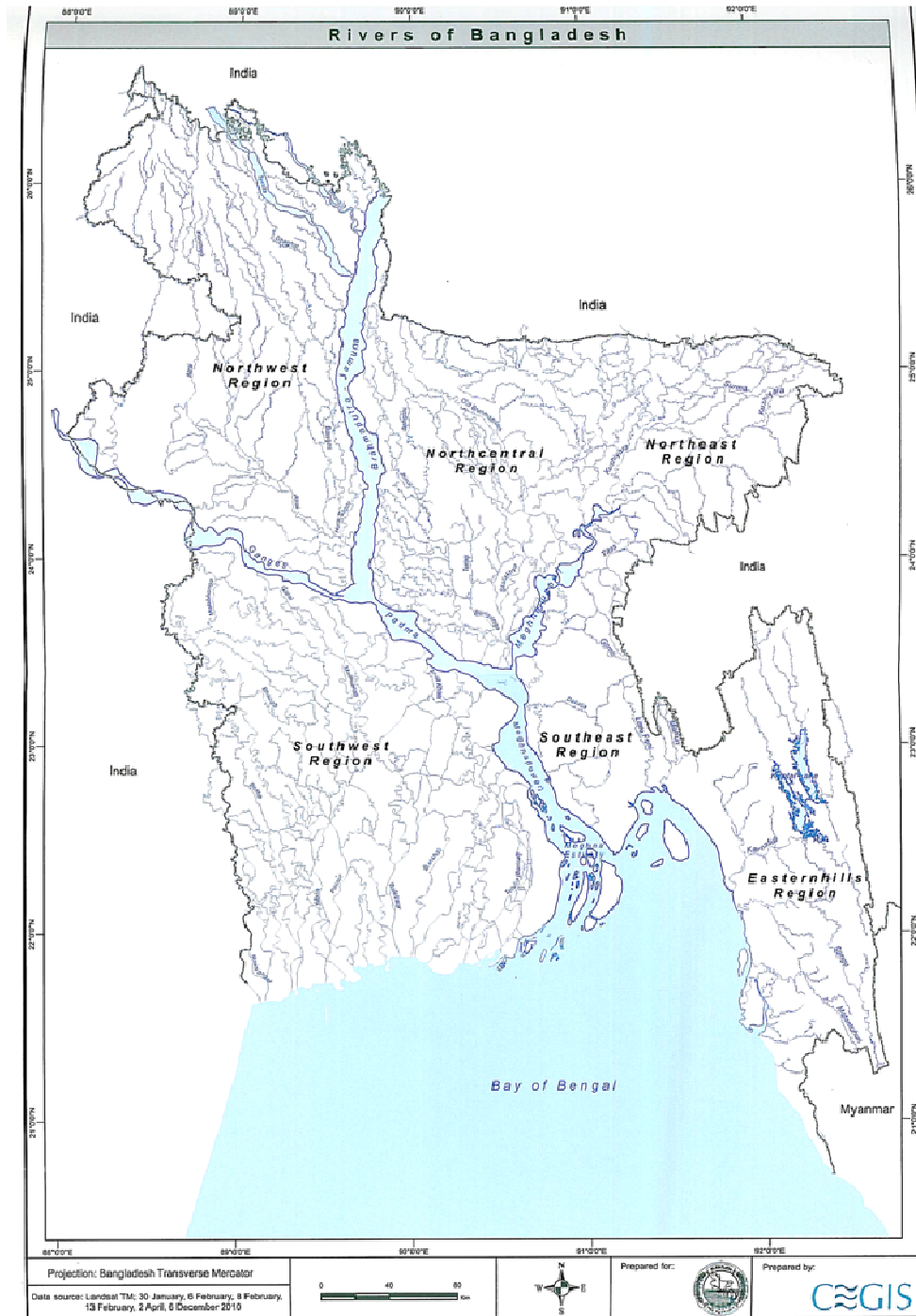


Figure 1.1: River Systems of Bangladesh (Source: CEGIS, 2010)

Meghna is reinforced by the Dhaleshwari before Chandpur as well. The name for the largest distributary of the Ganges in Bangladesh is the Padma River. When the Padma joins with the Jamuna River, the largest distributary of the Brahmaputra, and they join with the Meghna in Chandpur District, the result in Bangladesh is called the Lower Meghna.

After Chandpur, when the river has the combined flow of the Padma and Jamuna it moves down to the Bay of Bengal in an almost straight line. In her course from Chandpur to Bay of Bengal, the Meghna braids into a number of little rivers including the Pagli, Katalia, Dhonagoda, Matlab and Udhamodi. All of these rivers flow out from the Meghna and rejoin again at points downstream. When the Padma and Meghna join together, they form the fourth river system.

A fifth river system, unconnected to the other four, is the Karnaphuli. Karnaphuli River is one of the most important rivers in Chittagong hill tracts. This river originates from the Lushai hills in Mizoram, India and enters Bangladesh through Barkal Upazila in Rangamati District to Kaptai Lake in Balukhali Union. Then it follows a zigzag course before it forms two other prominent loops, the Dhuliachhari and the Kaptai.

After coming out from the Kaptai loop the river follows another stretch of tortuous course through the Sitapahar hill range and flows across the plain of Chittagong after emerging from the hills near Chandraghona. Therefore, the river drains into the Bay of Bengal cutting across several hill ranges, viz the Barkal, Gobamura, Chilardak, Sitapahar and Patiya of the Chittagong Hill Tracts and Chittagong. The maximum depth of this river is up to 20 m depending on tidal effect located at Patenga.

It has possibly maintained its older course keeping pace with the uplift of the hill ranges and can be classified as an antecedent river. The Karnafuli is narrow and straight from Prankiang to Waggachhari along Kaptai-Chandraghona road. The straightness of the river is probably due to a fault, which controlled the channel from Prankiang to Wagga. The main tributaries of the Karnafuli are the Kasalong, Chengi, Halda and Dhurung on the right and the Subalong, Kaptai, Rinkeong and Thega on

the left. Flowing to the west through Rangunia Upazila and then keeping Raozan Upazila on the north and Boalkhali Upazila on the south, it receives the waters of the Halda River at Kalurghat just above the railway bridge. It then turns south, receives the waters of the Boalkhali and other khals and turns west circling round the eastern and southern sides of Chittagong Town. From the extreme corner of the Chittagong Port to the west, it moves southwest to fall into the Bay of Bengal 16.89 km below.

The river meets Padma River in Chandpur District. Major tributaries of the Meghna include the Dhaleshwari River, Gumti River, and Feni River. The Meghna empties into the Bay of Bengal via four principal mouths, named Tetulia, Shahbazpur, Hatia, and Bamni.

1.2 Origin of Jamuna River

The Brahmaputra, also called Tsangpo-Brahmaputra is a transboundary river and one of the major rivers of Asia. The 3000 km long river springs in the western part of the Tibet Autonomous Region [Xizang] of China not far from the sources of the Ganges River and Indus River (Figure 1.2).

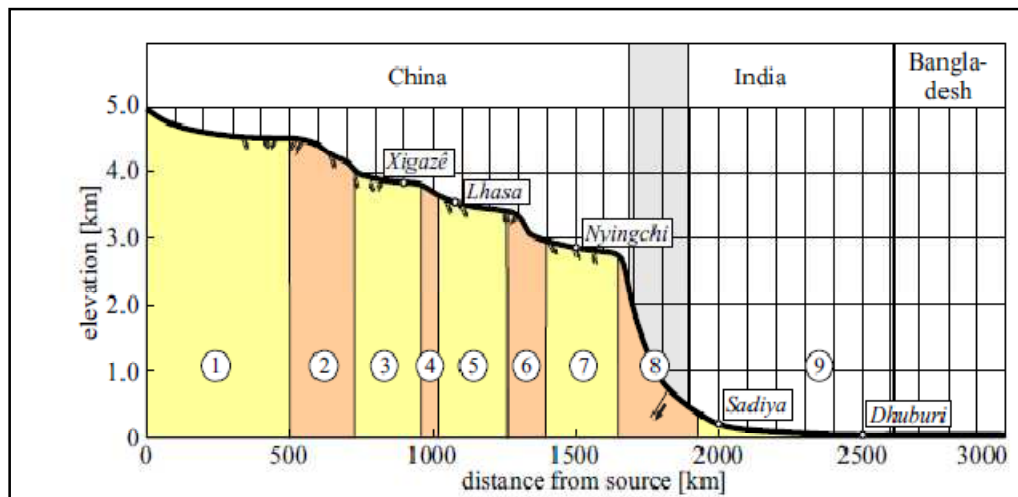


Figure 1.2: Longitudinal profile of the Brahmaputra River (Source: Zhang, 1998)

It springs at an altitude of 5100 m from the Chemayungdung glacier near mount Kailas in the Himalayas. It flows for about 1400 km in an easterly direction across

the Tibetan plateau, which is bordered by the Himalayas in the south and the Gandise Mountains in the north, while it descends to 3000 m. In this reach the river is known as the Tsang Po or Yarlung Zangbo (Jiang) River. Not far from Nyingchi at mount Namche Barwa the river enters one of the world's largest canyons; meanwhile rapidly descending. At an altitude of 200 m above sea level it leaves the Himalayan range as the Dihang River. The canyon is the main access route for the moist air currents from the Indian Ocean as a result of which the annual average precipitation varies on the Tibetan plateau from 200 mm at the western end to 900 mm at the eastern end. It was not before 1880 that the connection between the Yarlung Zangbo and the Brahmaputra was finally confirmed by the exploration of Pandit Kishen Singh (Montgomerie, 1885) and still, its narrow canyon through the eastern part of the Himalayas remains one of world's least explored regions (Bian, 1998; National Geographic, 1999).

The Dihang River joins with the Lohit River and Dibang River at west of the town of Sadiya in the Indian province Assam, after which it flows west through the plains of the Indian province Assam as the Brahmaputra River.

As the Brahmaputra River reaches the ninety degrees east meridian it makes a sharp left turn, goes south and enters Bangladesh with the name of Jamuna. The total length of the river from its source in southwestern Tibet to the mouth in the Bay of Bengal is about 2,850 km (including Padma and Meghna up to the mouth). The Jamuna enters Bangladesh east of Bhabanipur (India) and northeast of Kurigram district. Originally, the Jamuna (Brahmaputra) flowed southeast across Mymensing district where it received the Surma River and united with the Meghna, as shown in Rennell's Atlas (1785). By the beginning of the 19th century its bed had risen due to tectonic movement of the Madhupur Tract and it found an outlet farther west along its present course. It has four major tributaries: the Dudhkumar, Dharla, Teesta and the Baral-Gumani-Hurasagar system. The first three rivers are flashy in nature, rising from the steep catchment on the southern side of the Himalayas. The main distributaries of the Jamuna River are the Old Brahmaputra River, which leaves the

left bank of the Brahmaputra River 20 km north of Bahadurabad, and the New Dhaleswari River just south of the Bangabandhu Bridge (Figure 1.3).

The combined delta of Brahmaputra River and Ganges River (59,000 km²) is twice as large as the second largest delta in the world (the one of the Niger River). Their combined average discharge (32,000 m³/s) ranks third after the Congo River and the Amazon River, while the combined drainage area of the Ganges River (1,100,000 km²) and Brahmaputra River (924,000 km²) ranks only ninth. The river serves as an important inland waterway on both the Tibetan plateau and the Indian and Bangladeshi plains.

Catchment Characteristics

The Brahmaputra-Jamuna drains the northern and eastern slopes of the Himalayas, and has a catchment area of 5, 83,000 sq.km. 50.5 percent of which lie in China, 33.6 percent in India, 8.1 percent in Bangladesh and 7.8 percent in Bhutan. The catchment area of Jamuna River in Bangladesh is about 47,000 sq. km. The average annual discharge is about 19,200 m³/sec, which is nearly twice that of the Ganges. The Brahmaputra River is characterized by high intensity flood flows during the monsoon season, June through September. There is considerable variation in the spatio-temporal distribution of rainfall with marked seasonality.

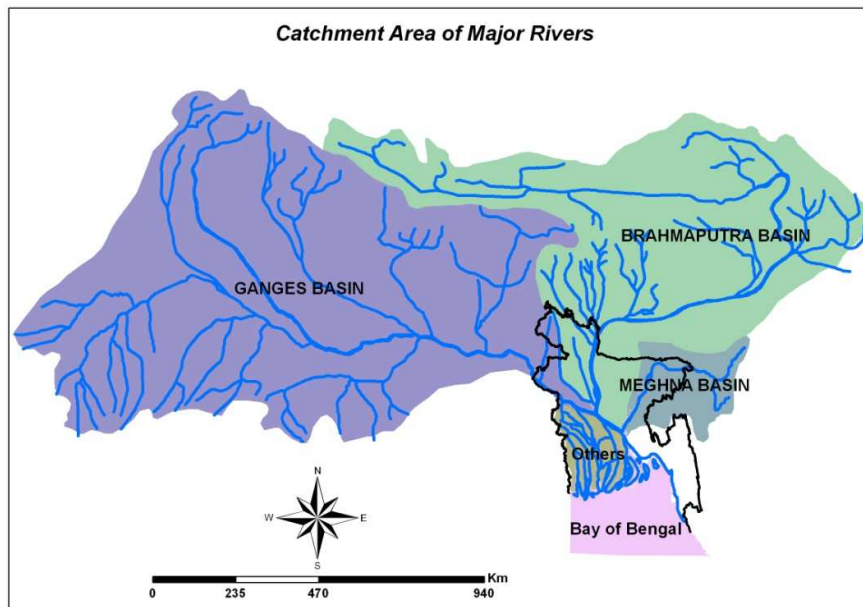


Figure 1.4: Catchment Area of Major Rivers (Source: CEGIS, 2011)

Precipitation varies from as low as 120 cm in parts of Nagaland to above 600 cm in the southern slopes of the Himalayas. In Bangladesh territory rainfall varies from 280 cm at Kurigram to 180 cm at Ganges-Brahmaputra confluence (FAP2). Monsoon rains from June to September accounts for 60-70% of the annual rainfall. These rains that contribute a large portion of the runoff in the Brahmaputra and its tributaries are primarily controlled by the position of a belt of depressions called the monsoon trough extending from northwest India to the head of the Bay of Bengal.

Deforestation in the Jamuna watershed has resulted in increased siltation levels, flash floods, and soil erosion. Occasionally, massive flooding causes huge losses to crops, life and property. Periodic flooding is a natural phenomenon which is ecologically important because it helps maintain the lowland grasslands and associated wildlife. Periodic floods also deposit fresh alluvium replenishing the fertile soil of the Jamuna River Valley. (Ref: IWM, Monitoring of Hydraulic and Morphological conditions of Jamuna River for the safety of Bangabandhu Bridge).

1.3 Background of the study

The Jamuna River in Bangladesh is a braided sand-bed river characterised by substantial planform changes during individual floods. The Jamuna is a braided stream characterised by a network of interlacing channels with numerous sandbars enclosed in between them. The sandbars, known in the Bengali as chars do not, however, occupy a permanent position. The river deposits them in one year very often to destroy and redeposit them in the next rainy season. The average discharge during flood amounts is about 60,000 m³/s, which combined with the flooding caused by the other large rivers, results in an inundation of 20–30% of the country. However, in 1987 and 1988 extreme floods occurred which led to the flooding of 40% and 60% of the country, respectively (Thorne and Russel, 1993). The peak discharge of 1988 flood was more than 90,000 m³/s and it coincided with the flood peak of the Ganges River (Thorne et al., 1993). These floods cause more damage to property of individuals, to infrastructural works, and to society as a whole, thereby retarding (or even stopping) the socio-economic development of the rural areas.

For this reason a number of internationally funded projects - jointly known as the Flood Action Plan (FAP) for Bangladesh - were started in 1990/1991 to investigate the problems associated with the flooding and to find ways to solve them.

Erosion of river bank in the Jamuna River is one of the major problems in Bangladesh. Thousands of people become homeless every year and they lose their homestead and croplands. Mosques, schools, hospitals and other infrastructures are

damaged due to erosion into the mighty Jamuna River shown in (Table 1.1 and 1.2). (Uddin & Rahman, 2011)

Table 1.1: Losses of livelihoods

Sl. No.	Item	Shuvogacha (%)	Sirajganj (%)	Betil-Enayetpur (%)	Randhunibari (%)
1.	Homestead	100	100	100	100
2.	Houses	100	100	100	100
3.	Cultivable land	90	84	87	100
4.	Pond	35	32	13	10
5.	Trees	90	72	67	70
6.	Factories (loom)	-	-	-	50

(Source: Uddin & Rahman, 2011)

Table 1.2: Losses of cultivated land

Sl. No.	Cultivated Land (ha)	Shuvogacha N=20	Sirajganj N=25	Betil-Enayetpur N=15	Randhunibari N=10
		(%)	(%)	(%)	(%)
1.	0-2	70	60	53	80
2.	2-4	25	28	33	20
3.	4-6	5	12	13	-
4.	6>	-	4	-	-

(Source: Uddin & Rahman, 2011)

The active bed of this river, which consists of multiple branches of up to 2 km wide during low flow, is between 5 and 17 km wide. Bank erosion may attain a rate of several hundreds of meters per year and the locations of maximum erosion shift rapidly over the years (Coleman, 1969; Klaassen and Masselink, 1992). Local erosion may result in scour holes of up to 40 m deep.

It is reported that one kilometer of right bank has already shifted towards westward direction since 1830 at Sirajganj town. To protect this town a massive hard point named Sirajganj hardpoint was constructed in 1998 under FAP 1 (FAP 1, 1994).

Without this hard point Sirajganj town would be washed out several years back. As Hard point is a local erosion-resistant feature constructed on a river bank or projecting out into the river. So, this hard point plays a vital role for the existence of Sirajganj town. Erosion is being continued just upstream of the Sirajganj town due to morphological change. Shuvogacha under Kazipur Upazila of Sirajganj district is one of the erosion prone areas along the right bank of the Jamuna River.

The morphology of Jamuna River is affected by the construction of one of the national assets of Bangladesh, the Bangabandhu Bridge with river training works as a part of bridge construction in 1998 on Jamuna River. Number of river training works (guide bunds and hard points) was constructed in addition with this 4.8km long road bridge, by constricting the river width from 10 km to 4.8 km. This Bridge connects Bhuapur on the Jamuna River's east bank to Sirajganj on its west bank (IWM, 2011). The river training works include two guide bunds, one on each side of the river. The guide bunds supplement the hard points at Sirajganj and Bhuapur. The intensity of channel shifting has been increased due to regulation of river width at Sirajganj–Bhuiyapur section from 11 km to 4.8 km. Planform analysis shows that the major channel has been stressed to migrate (315 m/year) eastwards. The Jamuna River is adjusted to a new morphology after construction of the Bangabandhu Bridge. A big permanent char is formed downstream of the Bangabandhu Bridge. But a branch channel is flowing in between bank line and the char. A lot of erosion affected people living near the bank line and on the adjacent char (Uddin and Rahman, 2011). Efficient and potentially affordable solutions to the problem of bank erosion have been developed and tested under the FAP (Flood Action Plan) 21/22 “Bank Protection and River Training/ Active Flood Plain Management (AFMP) Pilot Project”. The FAP 21 component dealt with structures to stabilize banks, where as FAP 22 component dealt more generally with measures and strategies to train the river channels and, at the same time, to increase or to maintain the hydraulic efficiency of the river in transporting water and sediments in combination with an optimum use of the flood plains (Rahman and Osman, 2009). For this purpose some test structures (groynes and revetments) were designed and constructed along the braided Jamuna River, and their performance was monitored.

Considering the dynamic situations prevail in the Jamuna River a Morphodynamic study has an utmost necessity to identify the morphological changes of the river.

1.4 Scope of mathematical modeling

River sedimentation and morphological processes are among the most complex and least understood phenomena in nature. Due to the fact that they intimately affect on our living conditions, scientists and engineers have been looking for better tools to improve our understanding and enhance the quality of our lives ever since the beginning of human civilization. In early times, the research methodologies were primarily based on field observation and physical modeling. However, it is neither practical, nor possible to measure all river processes continuously and simultaneously. Field data represents very closely the physical reality of the existing processes in the river. Whatever the detail and frequency of surveys, the representation will always be discrete in space and time, especially during the monsoon period when the rate of change of bed level is high; the bathymetry would in general not be expected to be in equilibrium with local flow conditions. In this case measurement of, say, sediment concentrations at certain location would depend of course on local flow conditions, but also on conditions upstream and on the flow history. Field surveys with the purpose of understanding the process would then include very large amount of information. To collect the data and analyze it would be a very costly and time-consuming task. In that respect mathematical modeling is an alternate tool to understanding the detail physical processes in the nature.

Mathematical modeling has been introduced as a tool to interpret the information provided by the field data in an integrated way. The mathematical models enable interpolation and extrapolation in space and time based on the observations from the field and on the understanding of the physical processes and their interaction to the extent that this has been incorporated in the model. (Ali, 2004)

Various 1-D, 2-D and 3-D hydrodynamic and sediment modules are in use in water engineering sector. Some of the widely used models are briefly summarized:

HEC model Series, including HEC-UNET, HEC-6, and HEC-RAS, is a set of one-dimensional models of river hydrodynamics and sediment transport provided by the U.S. Army Corps of Engineers.

MIKE model series together comprises a very extensive set of finite difference models in one-, two- and three dimensions. Most of the MIKE models (MIKE-11, MIKE-12, and MIKE-3) use a rectangular, potentially nested, grid. Modules exist to cover hydrodynamics, sediment transport, water quality, and wave generation/transformation. MIKE-21C is a newer one which uses curvilinear grid. Finite element version (MIKE-FM) is also in ongoing processes.

CH2D/CH3D is two- and three-dimensional finite difference models of hydrodynamics, salinity, and sediment transport. The models use a curvilinear orthogonal grid. It can be used together with CE-QUAL-ICM to model water quality. CH2D/CH3D are developed and maintained by the U.S. Army Corps of Engineers. However, the software is not freely available to users outside the U.S. Army Corps of Engineers. Model development and application are possible through a cooperative agreement with the Waterways Experiment Station or other branches within the Corps.

ADCIRC is a two- and three- dimensional finite element hydrodynamics model using an irregular grid and provided by the U.S. Army Corps of Engineers. ADCIRC is supported by the SMS preprocessing and display suite.

GEMSS consists of a three- dimensional finite difference hydrodynamic, water quality, and sediment transport model, with a curvilinear orthogonal grid. The model uses the same basic hydrodynamic model (GLLVHT) as CE-QUAL-W2. The model is developed by J.D. Edinger Associates. Model development and application are possible only through a cooperative agreement with the developers.

RMA model series, together with the SED-2D model, is a set of one-, two-, and three-dimensional models of hydrodynamics, sediment transport and water quality. The RMA models are finite element models. This model can be run with 1-D

elements, has significant computational efficiency. It has the capability of addressing certain control structures, but not all the structures envisioned for the ponds. The models are in the public domain. RMA is supported by the SMS preprocessing and display suite.

TELEMAC model series comprises a set of two- and three-dimensional finite element models of hydrodynamics, with modeling of salinity provided by WQ-2D and WQ-3D, and sediment transport by SUBIEF. The models use irregular triangular grids. TELEMAC and the associated models are commercially available from H.R. Wallingford, U.K.

SMS is a comprehensive environment for one-, two- and three-dimensional hydrodynamic modeling. SMS is used as a pre- and post-processor for surface water modeling, analysis and design. It includes tools for managing, editing and visualizing geometric and hydraulic data and creating, editing and formatting mesh/grid for use in numerical analysis.

SOBEK is a powerful modeling framework for flood forecasting, modeling of drainage systems, control of irrigation systems, sewer overflow design, river morphology, salt intrusion and surface water quality. The components within the SOBEK modeling framework simulate the complex flows and the water related processes in almost any system. The components represent phenomena and physical processes in an accurate way in one dimensional (1D) network systems and on two dimensional (2D) horizontal grids. It is the ideal tool for guiding the designer in making optimum use of resources.

The Delft3D modeling system, developed by Delft Hydraulics (www.wldelft.nl), is capable of simulating hydrodynamic processes due to waves, tides, rivers, winds and coastal currents. Hydrodynamic flow is simulated with the FLOW module (WL Delft Hydraulics, 2001), which solves the unsteady shallow water equations in two (depth-averaged) or three dimensions. It has been applied to model conditions of flow, sediment transport and morphological developments in the present study due to its highly flexible tool for various applications. The Delft3D can be run in Cartesian

(equidistant or stretched) or curvilinear coordinates; all necessary grid generation software for creating curvilinear grids is included with the Delft3D package.

As mathematical models have their limitations, they cannot stand alone. Results should be assessed critically against field/laboratory data to assure that misleading conclusions are not drawn from a poorly designed and calibrated mathematical model.

1.5 Objectives of the study

Based on the above study an attempt has been made to simulate the bed level changes of the river Jamuna by using the hydrodynamic and morphological model. The key features, to which this study limits itself, are as follows:

1. To apply Delft3D-flow, in order to carry out simulations of flows, sediment transports, morphological developments for the selected reach of Jamuna River.
2. To obtain the bed level changes of the selected reach of Jamuna River.
3. To calibrate and validate the model with the field observation data.
4. To compare the results with other model output.

The main outcome of the present study is to understand the hydrodynamic and morphological changes of the selected reach of the Jamuna river with the aid of Delft3D-FLOW hydrodynamic module where the sediment version of DELFT3D-FLOW dynamically updates the elevation of the bed at each computational time-step. The following processes will be simulated after several runs using two or more years of consecutive hydrographs:

1. Erosion and deposition in main channels at the monsoon period of the year
2. Possible bed level changes with time
3. Sediment transport variation with respect to depth average velocity.

1.6 Organization of the report

The first chapter of the study gives a brief presentation of the hydrodynamic and morphological processes of the overall river system of Bangladesh. It emphasizes the need of scope of mathematical modeling tools for analyzing the phenomenon and the background of the present study. It also includes the objectives of the present study.

The second chapter contains a description of the available information sources that have been used for this research, short account of previous studies and literature available in the domain in question. Also a short description about the Jamuna river of its course and features etc are also discussed.

The third chapter presents the basic theory and equations used to model the hydrodynamic and morphological changes of the river and also the step by step processes that have been done during this study means the methodology has been presented shortly. The calibration and validation processes using different parameters have been shown in this chapter.

The fourth chapter comprises a brief description of the models developed under this study. The generation of grid, land boundaries, bathymetries and also the set-up of Flow module is discussed briefly in this chapter.

The fifth chapter presents an analysis and interpretation of the output from the mathematical modeling and its application to the engineering interventions. Mainly the results include the comparison of the observed and simulated bed levels, analysis of the selected river reach, sediment transport rate at various periods of the year etc. Also the sensitivity analysis of the model has been included in this chapter.

Finally the study ends in chapter six by drawing conclusion and recommendation for the future study. This chapter contains a summary of the overall results of this research, including comments about the modeling process, and gives recommendations for the control and improvement of the conditions in Jamuna River, and to recover the sediment transport balance in the area so as to control the erosion/accretion problem.

CHAPTER 2

LITERATURE REVIEW

2.1 General

The mighty rivers, the Ganges, the Jamuna and the Meghna and their distributaries and tributaries flowing through Bangladesh are heavily charged with sediment and major part of Bangladesh is formed from sediment deposited by them. The erosion and deposition have complicated variations over time and space due to the abrupt changes of flow and sedimentation.

The Brahmaputra, one of the largest braided rivers in the world, originates from the Himalayas and enters Bangladesh at Kurigram as Jamuna. Though the history of Jamuna is not more than 250 years, it shows very severe changes in its course due to anthropogenic influences. Various previous studies have been reviewed in this chapter. Previous studies on the river Jamuna using mathematical model, review of characteristics of Jamuna River by different researchers are also presented.

A well-controlled system of physical and hydraulic features is maintained in water and sediment transport processes. The inter relationship between the attributes and their details in this organized system are highly complex and it is hard to visualize many of them simultaneously. However these interrelationships from the typical characteristics of rivers and some knowledge of the basic types of rivers are necessary before complex relationships can be understood.

2.2 Channel patterns

The pattern of a river is described as the appearance of a reach in a plan view. Observing plan views of most of the major rivers, they can be classified broadly into three major patterns- a) straight channel, b) meandering channel and c) braided channel (Leopold and Wolmen, 1957). Figure 2.1 shows the illustrations of the basic type of rivers. Although these three types represent the major divisions, it should be realized that a continuous gradation exists between one type and another.

2.2.1 Straight channel

A straight channel is one that does not follow a sinuous course. Straight channels are rare in nature (Leopold and Wolman, 1957). A stream may have moderately straight banks but the thalweg or path of greatest depths along the Channel is usually sinuous. Straight channels with prismatic cross-section are not typical in nature. It is only feasible for artificial channel.

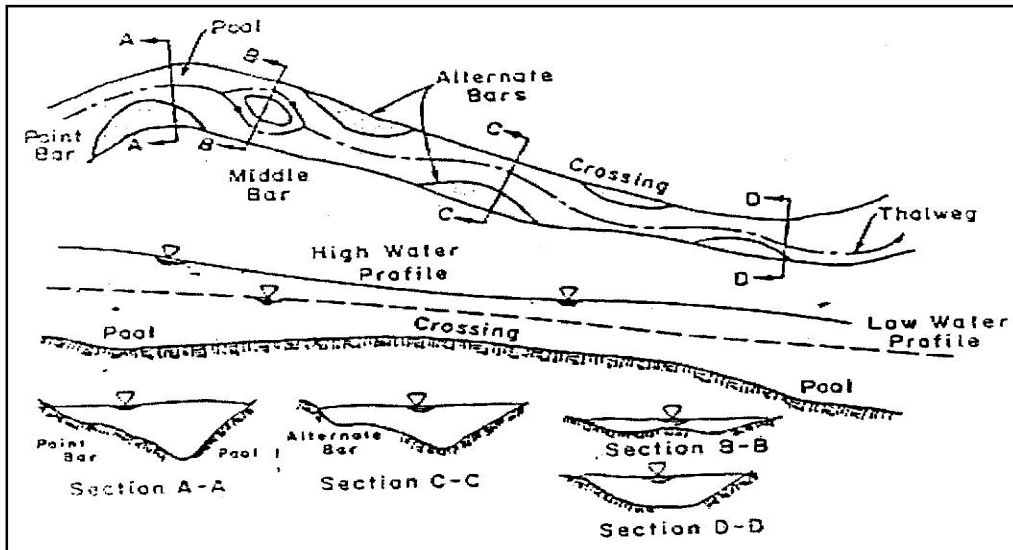


Figure 2.1: Channel patterns (Source: Schumm, 1977)

To differentiate between straight and meandering channels and sinuosity of a river, the relation between thalweg and length to down valley distance is most frequently used. The broad range of sinuosity for different types of rivers varies from 1 to 3. Sinuosity of 1.5 is taken as the division between meandering and straight channels by (Leopold et al, 1964). A series of shallow crossings and deep pools is formed along the channels in a straight channel with a sinuous thalweg developed between alternate bars (Figure 2.1).

Depending on the regime of the river, the erodibility of the banks, a straight channel can remain as such, if a river is dredged as a straight channel. Seldom only part of a river is straight, typically as stretch of a few miles in between two meander bend.

2.2.2 Meandering river

A meandering channel is one that consists of alternating bends, creating an S-shape to the top-view of the river. In particular, Lane (1957) showed that a meandering channel is one where channel alignment consists mainly of distinct bends, the shape of which have not been established principally by the varying nature of the topography through which the channel flows.

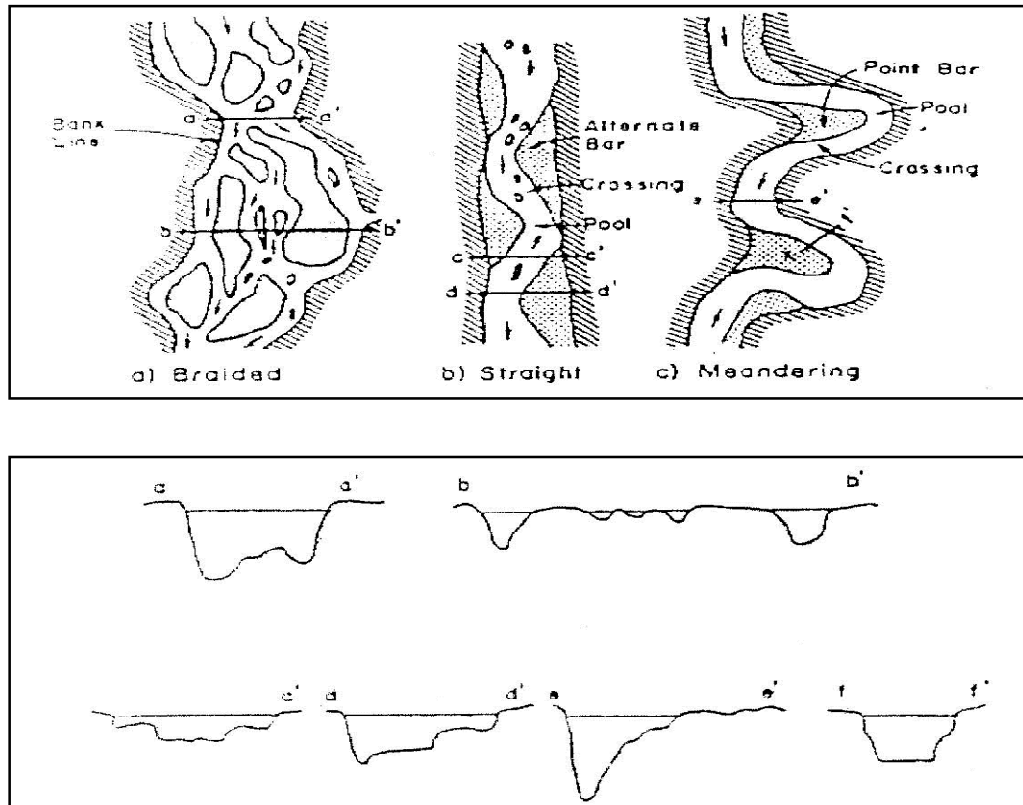


Figure 2.2.: Various features of channels (Source: Schumm, 1977)

Rivers carry the products of erosion as well as water, and in meanders, some sediment is transported by scour and fill. Scour takes place on the outer banks of the bends and deposition on the inner banks (Friedkin 1945, Sundborg 1956, Leopold & Wolman 1960, Leopold, Wolman & Miller 1964, Allen 1965). The meandering river contains a sequence of deep pools in the bends and shallow crossings in the short straight reach connecting the bends. The thalweg flows from a pool through a

crossing to the next pool forming the typical S-curve of a single meander loop at higher stages.

In the severe case, the changing of the flow causes chute channels to develop across the point bar at high stages (Figure 2.2).

2.2.3 Braided channel

A braided river is one with generally wide and poorly delineated unstable banks, and is depicted by a steep, shallow route with multiple channel divisions around alluvial islands (Figure 2.2). Leopold and Wolmen (1957) studied braiding in a laboratory flume. They deduced that braiding is one of many patterns that can maintain quasi-equilibrium among the variables of discharge, sediment load and transporting ability. The two primary reason that may be accountable for the braiding is stated by Lane (1957) as: (1) overloading, that is the channel may be full with more sediment than it can transport consequently accumulating part of the load, deposition occurs, the bed aggrades and the slope of the channel increases in an effort to maintain a graded condition and (2) steep slopes, which generate high velocity, multiple channels develop resulting the overall channel system to widen with rapidly forming bars and islands. The multiple channels are generally unstable and change position with both time and stage. The planform properties of braided rivers have received considerable attention, especially of their braiding intensity (Brice, 1964; Howard et al., 1970; Englund & Skovgaard, 1973; Rust, 1978; Hong & Davies, 1979; Mosley, 1981; Richards, 1985; Fujita, 1989; Friend & Sinha, 1993; Robertson-Rntoul & Richards, 1993; Islam, 2006). Usage of a suitable braiding parameter is an important measure towards better interpretation of braided river (Rust, 1978; Islam, 2006).

2.3 Factors influencing river geometry

Factors governing the geometry and roughness of an alluvial river are numerous and interconnected. Their characteristic is such that it is difficult to single out and study the function of a specific variable. Assessing the consequence of average velocity by increasing channel depth will affect other correlated variables as well. Again, not

only will the velocity respond to change in depth, but also the form of bed roughness, the position and shape of alternate, middle and point bars, the shape of cross-section, the magnitude of sediment discharge and so on. Therefore, the study of the mechanics of flow in alluvial channels and the response of channel geometry is incessant. Variables influencing the geometry of alluvial rivers are numerous and some of the important ones according to Simons (1971) are – Velocity, Depth, Slope, Density of water, apparent dynamic viscosity of the water sediment mixture, acceleration due to gravity, grain size of the bed materials, size distribution of bed materials, density of sediment, shape factor of the reach of the stream, shape factor of the cross-section of the stream, seepage force in the bed of the streams, concentration of the bed material discharge. Simons and Richardsen (1962) has described the role of the variables on resistance and bed form. Simons (1971) also partially explained their significance on the channel geometry. Leopold and Maddock (1953) and Wolman (1955) formalized a set of relations, to relate the downstream changes in flow properties (width, mean depth, mean velocity, slope and friction) to mean discharge. According to Knighton (1987) and Rhoads (1991), the dominant flow controls channel dimensions.

2.4 Sediment transport

Sediment transport is the movement of solid particles, typically due to a combination of the force of gravity acting on the sediment, and/or the movement of the fluid in which the sediment is entrained. An understanding of sediment transport is typically used in natural systems, where the particles are clastic rocks (sand, gravel, boulders, etc.), mud, or clay; the fluid is air, water, or ice; and the force of gravity acts to move the particles due to the sloping surface on which they are resting. Sediment transport due to fluid motion occurs in rivers, the oceans, lakes, seas, and other bodies of water, due to currents and tides; in glaciers as they flow, and on terrestrial surfaces under the influence of wind. Fluvial sedimentologists have carried out numerous studies to estimate quantitative hydrodynamics of ancient fluvial systems, particularly, their morphology and hydrology (Gardner, 1983; Casshyap and Khan,

1982; Tewari, 1993; Kale et al, 2004; Schumm, 1968; Bridge, 1978; Allen, 1984; Yen et al, 1992).

Sediment transport on the continental shelf depends on surface-wave conditions, bottom-boundary- layer currents, fluid stratification, and bed characteristics, including grain size, density, porosity, and surface roughness. In general, sediment transport rates and depths of bed reworking are greatest when large, long-period waves occur simultaneously with strong, persistent currents.

The sediments entrained in a flow can be transported

1. along the bed as bed load
2. in the form of sliding and rolling grains, or in suspension as suspended load advected by the main flow and
3. some sediment materials may also come from the upstream reaches and be carried downstream in the form of wash load.

A short description of these three types of load is discussed below.

Bed load moves by rolling, sliding, and hopping (or saltating) over the bed, and moves at a small fraction of the fluid flow velocity. Bed load is generally thought to constitute 5-10% of the total sediment load in a stream, making it less important in terms of mass balance. Several studies also proceeded to provide theoretical and semi-empirical relationships for the bed load transport rate. Einstein (1950) used a statistical description of the near-bed sediment motions and related the bed load transport rate to the probability of a particle being eroded from the bed, it relate to the flow intensity. Bagnold (1966) introduced equations giving the bed load, suspended load and total load transport rates as functions of the stream power for steady flows using considerations of energy balance and mechanical equilibrium.

Suspended load is the portion of the sediment that is carried by a fluid flow which settles slowly enough such that it almost never touches the bed. It is maintained in suspension by the turbulence in the flowing water and consists of particles generally of the fine sand, silt and clay size. Bagnold (1956) defines the suspended sediment

transport as the sediment transport in which the excess weight of the particles is supported by random successions of upward impulses imported by turbulent eddies.

Wash load is the portion of sediment that is carried by a fluid flow, usually in a river; such that it always remains close the free surface (near the top of the flow in a river). It is in near-permanent suspension and is transported without deposition, essentially passing straight through the stream.

2.5 Morphology of a river system

Aggradation (i.e. rising of the river bed by deposition) occurs in a river if the amount of sediment coming into a given reach of a stream is greater than the amount of sediment going out of the reach. Part of the sediment load must be deposited and hence, the bed level must rise (Ranga Raju, 1980). In alluvial channels or streams bed aggradation evolves primarily from the passage of flood events. The bed profile consequently reduces the section factor of the channel. Sediment deposition along streams or in reservoirs is a complex and troublesome process. It creates a variety of problems such as, rising of river beds and increasing flood heights, meandering and over flow along the banks, chocking up of navigation and irrigation canals and depletion of the capacity of storage reservoir (Hossain, 1997). Alves and Cardoso (1999) investigated of the effect of overloading on bed forms, resistance to flow, sediment transport rate and average bed profile of aggrading by overload. Numerous researchers have reported the aggradation and degradation phenomenon of alluvial-channels beds up to till date (Vries, 1973; Jain, 1981; Jaramillo, 1983; Mosconi, 1988).

Bed degradation (i.e. lowering of the bed by scouring) occurs when the amount of sediment coming into a given reach of a river is less than the amount of sediment going out of it (Ranga Raju, 1980). The excess sediment required to satisfy the capacity of the river will come from erosion of the bed and there will be lowering of the bed level, which will result in shifting of thalweg line of the river. If the banks are erodible material can be picked up from the banks and widening of the river will also result. Hence the whole process of aggradation and degradation of rivers have

potential effects on various hydraulic and geometric features of rivers such as cross-sectional area, section factor, shifting of thalweg line etc. Pioneering experimental work was only carried out in the seventies and eighties, namely by Soni (1975) and Mehta (1980).

2.6 Previous researches on Jamuna River

A large amount of data on the Bengal rivers has been obtained by international research in particular during the River Survey Project (1996), also indicated as FAP24. The data set contains daily water level records, regular cross-section surveys, and several special bathymetric and hydrodynamic surveys at a number of interesting locations. The following subsections describe the river characteristics on the scale of the river. Some characteristics of the river on the channel scale, such as observations on bed forms, sediment transport and individual plan form changes (Jagers, 2003).

The average annual flood of the Jamuna River is about $60,000 \text{ m}^3/\text{s}$, and the discharge during low flow lies between $4,000$ and $12,000 \text{ m}^3/\text{s}$; the water level slope gradually decreases from 10 cm/km at the Indian border to 6 cm/km near the confluence with the Ganges River with a mean of 7 cm/km . The slopes of the other major Bengal Rivers are even smaller (Ganges River 5.5 cm/km , Padma River 4 cm/km , and Upper Meghna River 2 cm/km and decreasing) in agreement with the observation that braided rivers have a steeper gradient than meandering rivers (Leopold and Wolman, 1957). The Jamuna River is up to 20 m deep in the large channels, and local scour holes may reach depths of up to 45 m . Depth-averaged velocities of 3 m/s are commonly observed during flood (FAP24, 1994). The major part of the discharge of the Jamuna River results from snow melt, but rainfall in Assam and in the northern part of Bangladesh contributes significantly.

The water level rises rather abruptly during April–June, fluctuates slightly during the next three months, and falls rapidly during October–November. Several discharge peaks can often be observed due to the dependence on rainfall and the distribution of the tributaries along the river in Assam and Tibet (Jagers, 2003).

The relative timing of the floods of the Jamuna and Ganges Rivers at their confluence has significant influence on the extent of the flooding and the local morphological changes. For instance the extreme flooding of 1988 was partly caused by the concurrence of the flood peaks of the Jamuna and Ganges Rivers (Thorne et al., 1993). The river has a total annual sediment flow of about 650 million tons. According to an extensive sampling carried out by (FAP 1, 1991), bank material seems to be quite uniform and consists of fine sand. The little variation in bank material composition in downstream direction is due to old clayey deposits.

Generally the peak discharge occurs between July and September and the lowest discharge in February-March of the year. The discharge of the Jamuna River shows significant seasonal variation with snowmelt in the Himalayas accounting for the majority of flow, whilst rainfall in Assam and Bangladesh contributes significantly. 1988 and 1998 hydrological events are extreme flood events for Jamuna whereas 1995 event is a moderate flood event for Jamuna. (IWM Report, 2011)

Although most of the flood plain sediments along the Jamuna River have been deposited by other rivers (before the major diversion early in the 19th century), their composition is similar to the sediment transported by the Jamuna River today. It mainly consists of fine sands and a generally small percentage of silt/clay which is characteristic for the very young and unweathered sedimentary rocks that make up the drainage basin of the Brahmaputra River (Jagers, 2003).

Table 2.1: Grain size (mm) of bed material collected in 1993-1994

River	Gauging Station	D ₁₆	D ₃₅	D ₅₀	D ₈₄	D ₉₀
Jamuna	Bahadurabad	0.13	0.16	0.22	0.29	0.34
Ganges	Hardinge Bridge	0.10	0.12	0.15	0.18	0.21
Padma	Baruria	0.10	0.12	0.14	0.18	0.22

(Source: FAP24 (1996))

The banks are in general made of 85% sand and 15% silt (diameter less than 0.063 mm) except for localised deposits that contain up to 55% silt and 35% clay. The sand fraction consists of 44% quartz, 18% rock fragments, 18% mica, 12% heavy minerals

and 8% feldspar (River Survey Project, 1996). The bed material fines in downstream direction from 0.25 mm near the Indian border to 0.16 mm at the confluence with the Ganges River which transports a slightly finer load (Table 2.1).

The major part of the downstream fining is probably the result of abrasion of the relatively soft mica particles of which a large amount originates from the Tista River (FAP24, 1996). Borings done within the framework of the River Survey Project have indicated that at least down to 40 m the sediments are similar to the sediments typical of the present-day Jamuna River. The sediment in the Old Brahmaputra River, however, is in general finer than the sediment in the Jamuna River near its off take (D_{50} is 0.16 mm); downstream of Mymensingh the river crosses a coarse reach in which the mean diameter increases up to 0.25 mm.

The combined Bengal Basin Rivers transport 13 million tons of sediment a day during flood conditions, and a total of approximately 1 milliard tons per year. Each year the floods inundate vast areas of Bangladesh, leaving behind about the half of this volume of sediment. The lightest sediment particles - clay and fine silt - are deposited on the flood plains as a thin layer of an average about 1 cm thick; the coarser materials - fine sands and silts - are predominantly deposited as crevasse splays adjacent to the river channel forming natural levees.

This sedimentation compensates the high subsidence rate of Bangladesh, thereby keeping the river courses and the Bengal coastline relatively stable. The development of the Bengal Delta over the last 18000 yrs is sketched in Figure 2.3. During this period, the Brahmaputra River has switched its course several times between its present course and the pre-1800 course.

According to Allison (1998), 21% of the annual sediment budget (mostly sand and silt) is deposited at the river mouth, thereby enlarging the sub aerial delta with an average of 4–7 km² of new land over the last 150–200 years. Another 12.5% (mud) is deposited further seaward as a subaqueous mud delta. Whereas the delta extends in the eastern part, the shoreline and shallow offshore areas of the western front are in a net erosional state (Allison, 1998). Net sediment transport along the coast is in

westward direction for about 100 km, from where the sediment is transported via the ‘Swatch of No Ground’ (a large submarine canyon) to the Bengal fan in the deeper parts of the Indian Ocean (Coleman, 1969; Kuehl et al., 1989; Goodbred and Kuehl, 2000b).

The levees consist almost entirely of overlapping crevasse-splay deposits of fine sands (up to 3 m thick) interlaced with thin layers of silt and clay. The fine sand crevasse-splays are deposited during flood when water and sediment leaves the main channel via overbank flow. Coleman (1969) observed that there is a slight change in the type of overbank flow along the Jamuna River from well separated channelised flows in the upstream area to more closely spaced broader flows in the downstream area. As the flood recedes a thin layer of silt and clay is left behind. Quite often, local rice farmers rapidly cultivate this bare land, and within a year the crevasse splays are hard to detect on aerial photographs because of cultural modification.

The high sediment load of the Jamuna River not only leaves its traces on the flood plain, but it also causes the rapid plan form changes of the river.

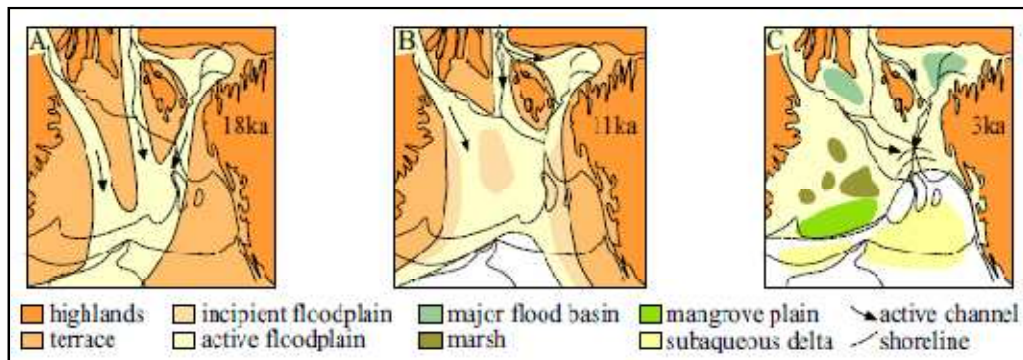


Figure 2.3: Development of the Bengal Delta (Source: Goodbred & Kuehl, 2000b).

Sedimentation does not only occur outside the rivers on the flood plain, but also inside the channels. The backwater effect of flood of the Jamuna River causes sedimentation in the Ganges River just upstream of their confluence (Fergusson, 1863) during the first month of the floods. The Ganges River normally reaches its maximum discharge at the end of August or the beginning of September after the

main peak of the Jamuna River; its flood clears out most of the deposited sediments. When the third flood peak of the Jamuna River is low or late, deposition can be expected in the lower reaches of the Jamuna River near Aricha (Coleman, 1969)

Tracking plan form changes in detail for a dynamic river like the Jamuna River is a challenging task. In the above figure the flow is shown from top to bottom. Hatched areas indicate missing data (Figure 2.4). The size of the Jamuna River and the extent of the surrounding flood plain make field surveys very time consuming. Therefore, whenever a field survey is carried out, only a limited area is covered. The development of remote sensing techniques has, on the other hand, made it possible to obtain relatively detailed data by means of contemporary remote sensing satellite systems because of the size of this river. Based on different combinations of signal strengths over the detection bands, different types of land use can be detected. The main branches of the all available years is shown on the left hand side of the figure. Some lines are regularly revisited; in particular the northwest-southeast line at northing 790 is remarkable. At that location the main branches of 1973, 1978 and 1980 (flowing out to the southeast) are in almost perfect alignment with the main branches of 1994, 1995 and 1996 (coming in from the northwest). The underlying cause may be related to tectonic influence; there are more of such indications as (Mosselman et al., 1995) showed. At other locations the main channel seems to be able to shift its direction but not its location (for instance at the Jamuna Bridge site). For further analysis of the plan form changes, (EGIS, 1997) digitized the channel centerlines from satellite images for 13 years between 1973 and 1995; the result of 1995 is shown on the right hand side in (Figure 2.5). They have distinguished one main branch (in general the widest) and several secondary branches. An overlay of these locations generally referred to as stable or nodal points of the braided plan form are sometimes characterized by a different composition of the bank material resulting in smaller erodibility. Although the migration rate may be reduced locally, these 'stable points' have shown to be transient on longer time scales. Satellite imaging systems are very useful for quickly determining land use and channel plan form over vast areas, but accurate elevation data are less easily although very time consuming,

often still the best source for elevation data. Remote sensing methods for obtaining elevation data are quick and efficient (Klees et al., 1997 a, b).

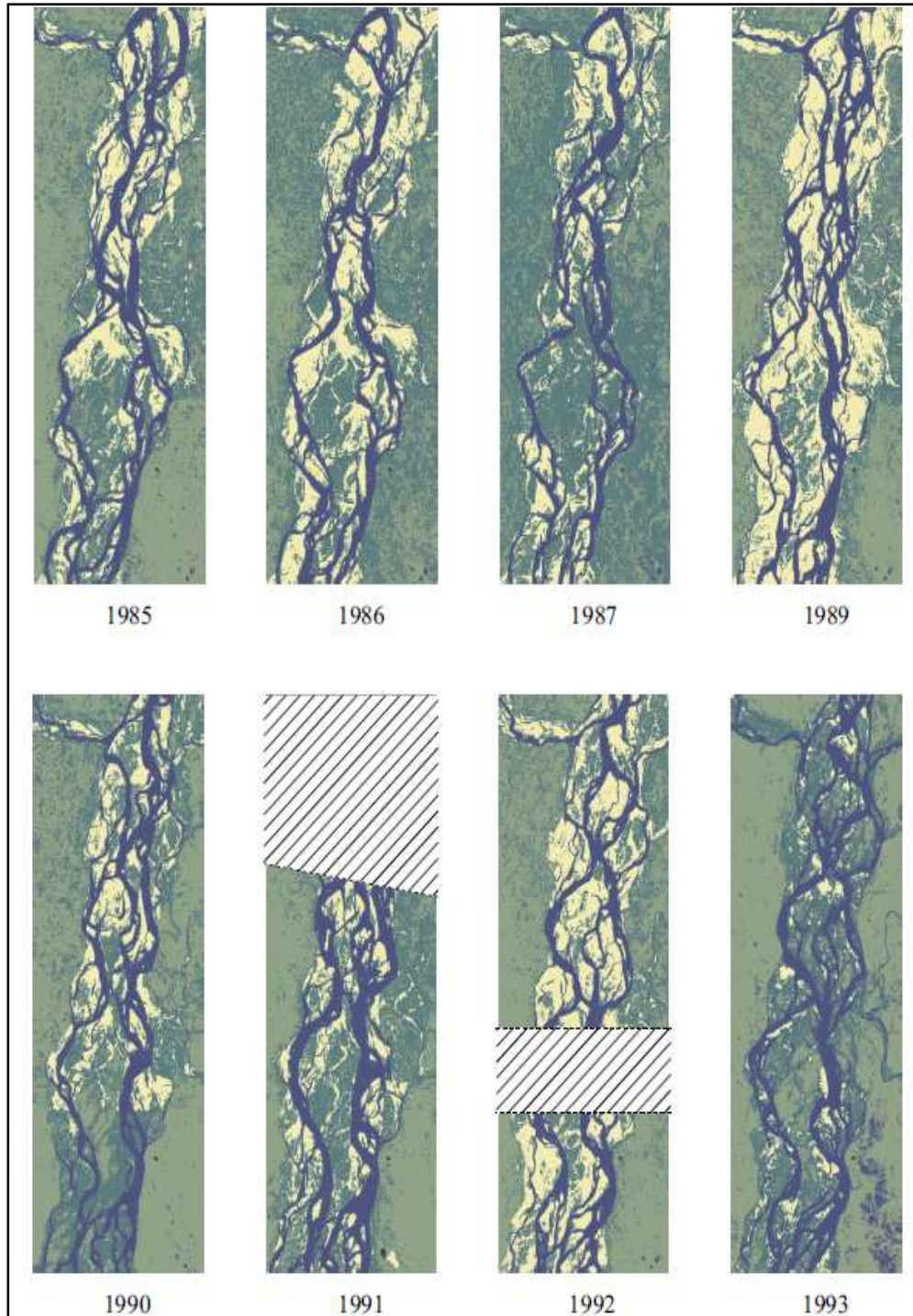


Figure 2.4: Low-stage plan forms of the Jamuna River (Source: Jagers, 2003)

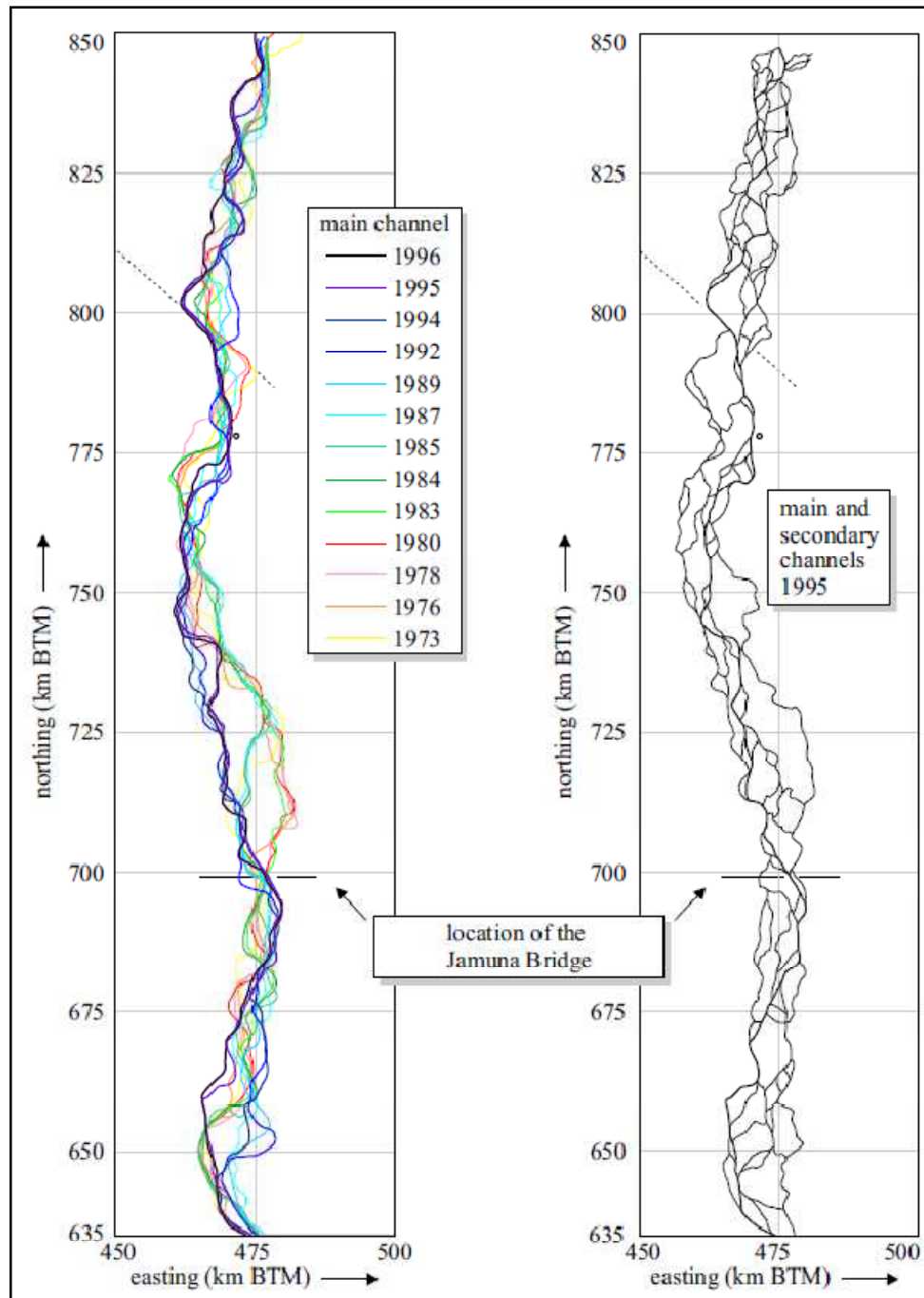


Figure 2.5: Movement of the main channel for the period 1973-1995 and plan form in 1995 (Source: EGIS).

A completely different way of obtaining elevation data has been used by (EGIS, 1997). Based on satellite images, they distinguished three types of land use: water,

sand, and other land. Sand pixels correspond in the densely populated Bangladesh to recently deposited (low lying) sand flats. The average elevation of sand covered areas was - based on elevation data obtained from cross-section surveys at several locations along the Jamuna River - determined to be 3.5 ± 1.0 m above SLW.

For the other land areas the elevation was correlated to the uninterrupted period that the area had been classified as ‘other land’ immediately preceding the date at which the latest satellite images and elevation data were obtained. They found the following relation between the average elevation in meters above SLW and the land age in years $elevation = 5.6 - 1.9e^{-age/3}$, which is also plotted in (Figure 2.6). This relation predicted three quarters of the calibration set within 1 m of the measured height. Using this relation a DEM (digital elevation model) was created for the flood plains in 1994 from which subsequently the plan forms at various characteristic discharges were determined (Figure 2.7).

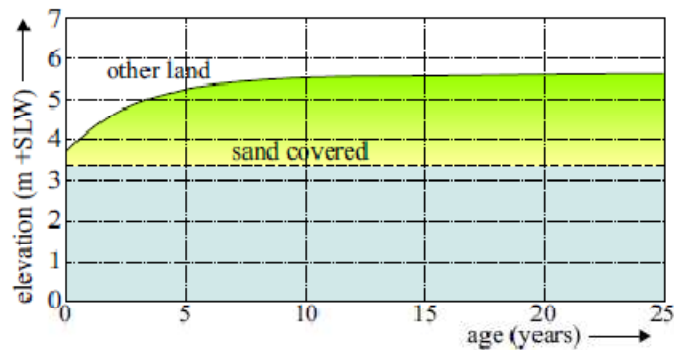


Figure 2.6: Relation between the elevation and the age of the land along the Jamuna River (Source: EGIS, 1997)

The plan forms have been constructed by EGIS (1997) using low-stage satellite images and field data by the River Survey Project (1996). Wash load does not play a role in the reshaping of the bed and deposits of the sediment can only be found in stagnant areas within the channel system.

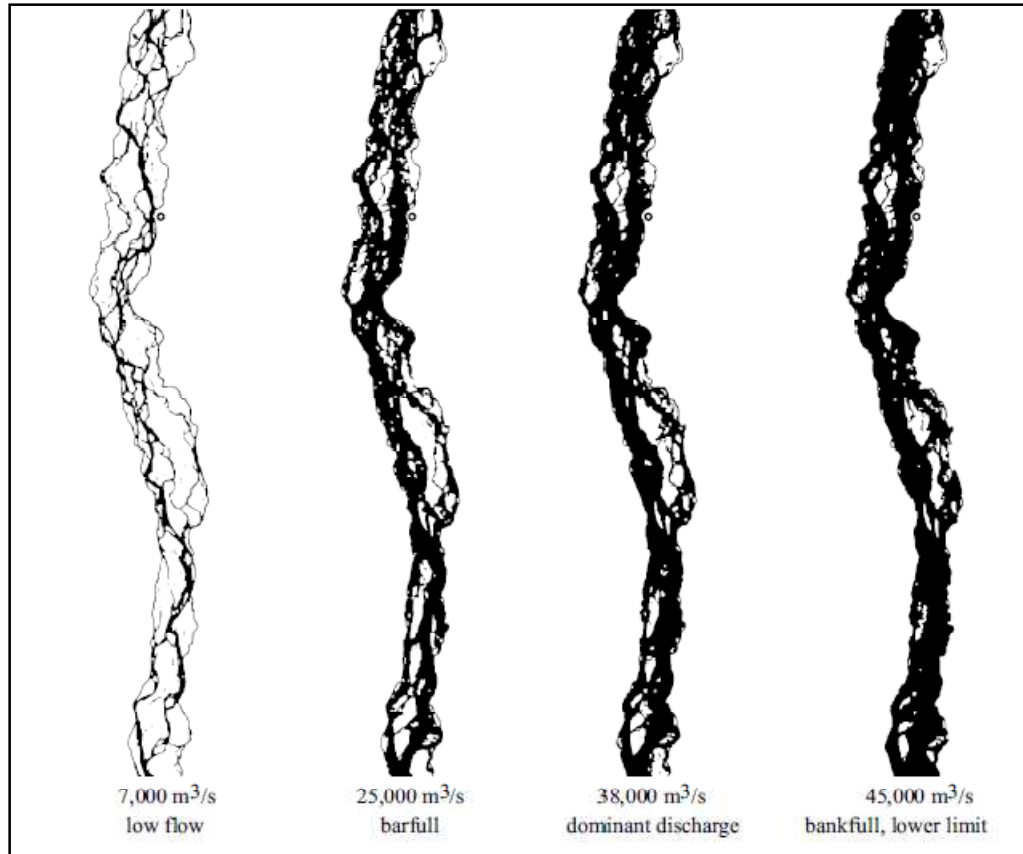


Figure 2.7: Plan forms of low flow, bar full, dominant and minimum bank full as defined by FAP1 and FAP24 for the Jamuna River at the beginning of 1994. (Source: EGIS).

For the Jamuna River the wash load consists of silt particles finer than $50\ \mu\text{m}$, settling at velocities less than $0.4\ \text{m/s}$, which in general only occur in the wake of bars and on the flood plain. Wash load does, therefore, not significantly contribute to the short-term morphological activity, but consolidated, erosion resistant deposits may influence the plan form on longer time scales. It also plays an important role in the build-up of the flood plain. These finest particles may in general not be ignored in estuarine environments because flocculation and, thus, the settling velocity increase if the salinity increases (Winterwerp, 1999). Silt transport in rivers is generally capacity limited, that is, the transport capacity for silt is so large that the sediment transport rate depends mainly on the upstream availability.

2.7 Previous studies on different rivers

Numerous studies have done on the hydro-morphological aspects such as hydraulic geometry, erosion/deposition and bed level variations in many rivers in Bangladesh. Most of these studies were carried out in the major rivers like the Ganges, the Brahmaputra, the Meghna and the Teesta River.

2.7.1 Studies in Bangladesh

Ali et al. (2002) investigated the effect of the changes in the planform and bed topography of the Jamuna River in the form of a stability analysis by perturbation technique. A two-dimensional model is developed and applied to the Jamuna River which accesses flow and sediment transport in an alluvial river with erodible and non-erodible banks. The proposed model is used to analyze both the meandering and braided patterns of the river. The results from the analyses of the Jamuna River show that instability always exists in the Jamuna River under maximum instability conditions because of its very low aspect ratio (1/1000) and more than three braids.

The observation of Bristow (1987) from satellite images suggested that the yearly volume of erosion and deposition in the Jamuna is the function of the high discharge and the duration of discharge. Bristow subdivided identified depositional areas from satellite images into four categories: addition to bars, lateral accretion to the bank, new mid channel bars and channel abandonment. Each types of deposition results into the other types of erosion, say for example abandonment of an old channel is the subsequent result of the formation of a new channel. Formation of a new medial bar results in the widening of a channel by bank or bar erosion.

The riverbed erosion and deposition in the Jamuna River was first studied by Coleman (1969). He found that due to high sediment load the erosion – deposition in the riverbed is extremely high and the processes are very complicated. His study was mainly based on the shifting of the thalweg, which is always associated with erosion and deposition in the riverbed, by comparing cross-sectional profiles measured

several times in a year at a certain section of the river, and by comparing each cross-section measured in two successive lean seasons at different locations in the river.

Hossain (1989) studied the erosion – deposition pattern, shifting characteristics and rate of change of cross-section and thalweg movement, including sediment transport of the Ganges. He found that the net deposition in the Ganges up to Brahmaputra confluence was approximately $4.26 \times 10^8 \text{ m}^3$ during 1967-68 to 1979-80 which corresponds to about 4.30 cm sediment deposition each year.

Hossain and Alam (1988) performed a quantitative evaluation of sediment transport rates in the Jamuna River and for that a comparative treatment of the applicability of few well known formulae were made. They showed that total suspended sediment discharge at Nakfatarchar was in between 439 million tons to 575 million tons and 94 percent of the flow occurs in the monsoon. They also found that sediment discharge may satisfactorily be expressed as a function of water discharge and flow velocity.

Habibullah (1987) studied the channel changes of the Jamuna over the time. He found that the amount of bank line eroded is much higher than that accredited. He also showed that maximum amounts of bank line erosion and deposition are 348 m/year and 335 m/year respectively.

Klassen and Masselink (1992) studied the bank erosion rate of the curved channels in the Jamuna River by analyzing the satellite images from 1976 to 1987. As the Jamuna River is a braided river, the various braided channels having different discharges, width and radius of curvature are usually active in eroding the bank at different places. They found that in the Jamuna River the bank erosion is generally associated with the rotation and extension of bend rather than translation.

Mohammad A. H. Bhuiyan et al. (2010) evaluated the ongoing geoenvironmental impacts of Brahmaputra-Jamuna (BJ) River around the Jamuna Bridge (JB) site. Remote sensing and GIS techniques are adopted to evaluate the temporal and spatial geohazards. This study shows that the intensity of channel shifting has been

increased due to regulation of river width at Sirajganj–Bhuiyapur section from 11 km to 4.8 km. Planform analysis shows that the major channel has been stressed to migrate (315 m/year) eastwards.

Rahman (1978) had studied the erosion of the Padma River from Goalunda to confluence of Padma-Meghna near Chandpur. He produced some relationships between thalweg sinuosity with meander pattern.

Soni et al. (1980) conducted an experiment that covered a wide range of flow and sediment loading conditions. They observed that after a long time, the aggradation in downstream of the section of increased sediment supply was stopped once the hydraulic conditions became compatible with the increased sediment load.

Analyzing satellite images, Thorne et al. (1993) estimated the bank erosion rate of the right bank of the Jamuna River for the period of 1973-1992. They estimated bank erosion at an interval of 500 m apart and averaged the erosion rate for 10 km. The average bank erosion rate for the period 1973-1992 varies from 0 to 160 m/year and the average erosion rate is about 80 m/year. They found that for a shorter time-scale the bank erosion rate increases, and the average bank erosion rate is higher for a higher flood discharges. They also found that catastrophic events of bank erosion (> 350 m/year) generally occur for short duration, 2 to 4 years and this erosion took place at the outer bank of the curved channels.

Thorne and Osman (1988) attempted to predict the bank erosion rate for the right bank of the Jamuna River for different locations, extrapolating the previous results.

2.7.2 Studies around the world

Over the past decades several studies have been made to evaluate morphological changes of the major rivers in and outside of Bangladesh. Although the list provided is not exhaustive, yet it provides some information in this respect.

Jain (1989) proposed a guide for estimating river bed degradation. The rate and extent river bed degradation resulting from sediment interruption were determined by

means of computer based numerical experiment. He presented the results in the form of algebraic relations that can be easily applied by practicing Engineers to estimate the temporal and optimal river bed degradation during the preliminary phase of the engineering designs. The proposed relationship for the bed degradation has been verified with the field data of Missouri river.

Jaramillo and Jain (1984) performed investigations on the aggradation and degradation of alluvial channel bed and introduced a one-dimensional nonlinear parabolic model for non-equilibrium processes in the alluvial rivers. Their model can be used as a tool for predicting aggradation-degradation processes in alluvial rivers.

Ramez et al. (2002) carried out a study on influence of sediment transport on the computation of water in the river Rhone. They showed that the increase of the head losses due to bed forms is interpreted in the U-curves (ratio of Strickler coefficients versus ratio of bottom shear stresses) and of S-curves (Strickler coefficient versus discharge). This effect is stronger at dominant discharge. It can lead to a rise of water level much higher than the final topographical change. For the presented example of a reach of River Rhône near Bourg lès Valence, this rise is estimated over 1 m for the dominant discharge of about 1200 m³/s.

Ranga-Raju (1980) did a study on the practical computation of degradation and aggradation on alluvial river based largely on the works carried out in India. He presented semi-empirical methods for computation of bed and water surface profiles for some of the commonly encountered cases of aggradation.

2.8. Mathematical modeling studies

Numerical hydrodynamic models of unsteady flow in rivers are widely used as an engineering tool in the design and planning of water resources projects. In recent years, several studies viz Master Plan Organization (MPO, 1987), Bangladesh Water Development Board (BWDB, 1987), used the hydrodynamic as well as morphological models of unsteady flow for computing flood flows and transport rates for the rivers in Bangladesh. Besides Bangladesh due to invent of high speed

computer nowadays, mathematical models are also extensively used for the simulation of the natural processes all over the world. There are several methods in numerical solutions i.e i) Method of Characteristics, ii) Finite Element Method, iii) Finite Difference Method etc. Some of them are summarized below:

2.8.1 Studies in Bangladesh

Feasibility study for the Gorai River Restoration Project (GRRP) for augmenting dry season flow through the Gorai off take had been taken-up by the Government of Bangladesh (GoB) in 1997. A two-dimensional morphological model had been developed for simulating the hydraulic and morphological processes in the Gorai off take to study the feasibility of undertaking Gorai river restoration work. A quasi-steady flow calculation was carried-out for the morphological calculation using MIKE-21C of DHI Water and Environment. A helical flow module was used to calculate the streamline curvature generated secondary flows. The sediment transport computed are composed of bed-load and suspended load. For the bed load calculation, the effects of the helical flow and bed slope were accounted through the direction of bed-shear stress and direction of the bed-slope. The model was calibrated and validated at the off take with extensive data collected for three consecutive monsoons from 1998 to 2000. Both Chezy's roughness (depth invariant) and depth variant roughness were used in the study.

Jagers (2003) has focused on Modelling techniques to predict plan form changes of braided rivers and their relation with state-of-the-art knowledge on the physical processes and the availability of model input data. Three Modelling techniques have been analysed with respect to their suitability for predicting plan form changes of braided rivers: a neural network, a cellular model (Murray and Paola, 1994) and an object-oriented approach (Klaassen et al., 1993). Two-dimensional depth-averaged morphological simulations of sharp bends have been carried out to improve the understanding of the processes involved. The results of those simulations indicate that cutoff formation of Jamuna is accelerated by a low water level downstream, a large (alluvial) roughness, a low threshold for sediment transport, and a small value for the exponent c of the Shields parameter q (or of the velocity u) in the sediment

transport relation if the average sediment transport rate remains constant. A simple model concept for simulating head ward erosion has been presented and tested. Finally, an algorithm for formation of new channels has been presented that can be implemented as a new module in the branches model.

Analysis of the processed data revealed that formation of bars caused channel bifurcation and created anabranches which together increased the total width of the Jamuna from 7 km to 12 km over the study period. The anabranches thus created either lost or gained with gradually. The one losing width ultimately becomes only a remnant allowing the bar to merge with the flood plain.

The channel developed an oscillatory nature which erosion at the bank and the bar developing a meander. He also revealed that the confluence has undergone an oscillation due to the movement of the Ganges and formation of bars in the Jamuna. This movement is estimated as 12 km within the study period.

Halcrow (2002) reviewed the morphological processes of the Jamuna River at Pabna Irrigation Rural Development Project (PIRDP). Halcrow proposed riverbank protection based on the morphological studies of the area. Three reaches of the bank had been identified as susceptible to different degrees of erosion, and then the sites were being prioritized to allow the introduction of a staged intervention program for protecting the vulnerable bank reaches. A 4 km reach of bank line within PIRDP showed immediate need for protection.

Houqe (1999) has studied the fluvial processes of the braided Jamuna in its 73.65 km reach including confluence with the Ganges using application of remote sensing and GIS. Using eleven sets of LANDSAT satellite images from 1973 to 1996, he studied the bank erosion, meander travel, bar formations of Jamuna River and migration of Jamuna-Ganges confluence.

In 2003, two models had been developed at IWM for finding a suitable location of ferry ghat for BIWTA (Bangladesh Inland Water Transport Authority). For these two models: one is a 30 km long and another one is a 200 km long reaches, where

Jamuna-Ganges confluence had been included for both to study the erosion-deposition pattern in the confluence region. The key features of the study were to find a sustainable channel, which should have the minimum navigational depth round the year. The short-model is used to evaluate the engineering interventions and the long-model is used to simulate long-term bed level changes along the navigational routes (BIWTA, 2003).

Two-dimensional model of Ganges River for Pakshey bridge project was developed in 1999 by IWM and DHI (Danish Hydraulics Institute). The simulation was developed using FESWMS-2DH model (version 3.0). FESWMS-2DH is an acronym for finite element surface water Modelling system for two-dimensional flow in a horizontal plane. It is a computer program to perform two-dimensional hydraulic Modelling of rivers, floodplains and highway crossings. Main objectives of the study were to find the impacts of the new bridge and river training works on the existing Hardinge Bridge, river training works and the downstream irrigation intake canal and also to evaluate the expected morphological changes in the river regime due to proposed bridge.

2-D hydraulic model and morpho-dynamic model are developed by IWM in 1998 under the Meghna Estuary Study. The Meghna Estuary Study has covered an area of the lower Meghna from Chandpur town up to the Bay of Bengal. The model has been developed using Mike-21. The dominant hydraulic and morphologic conditions and processes in the study area are studied through regional and detailed local 2-D models. To determine the dynamic behaviour of the entire estuary system, computations are carried out under different hydrodynamic conditions during low and monsoon seasons. Neap tide and spring tide, current velocity and sediment transport patterns and wave conditions are assessed in that study. The results of these computations give qualitative and quantitative information about the spatial and temporal variations of the water level, current velocity, discharge as well as sediment transport and the rate of sedimentation and erosion.

A morphological model of Jamuna River at Jamuna bridge site was developed in 1995. The model was carried out by IWM (Institute of Water Modelling) using

MIKE – 21C, which is a two-dimensional finite difference curvilinear grid model for simulating hydrodynamic and sediment transport in vertically homogeneous flow. The model covered a reach, extending 20 km upstream to 10 km downstream approximately from bridge site. Bathymetry and hydrological data of the year 1994 were used in the model. Simulation of the hydrodynamics for pre-bridge and post-bridge conditions was carried out for the entire monsoon period of 1994. Changes from pre- to post bridge conditions have been extracted. The morphological model was run for one and a half month. The results showed that water level had increased by 0.5m at the upstream of guide bund due to bridge construction.

BWDB (2011) initiated a project for protection of the left bank of the Padma River from erosion at Bhagyakul Bazar, Baghra Bazar and Kobutorkhola under Sreenagar Upazila of Munshigonj district. Institute of Water Modelling (IWM) carried out a study using Mathematical Modelling tool MIKE – 21C in 2011 to ascertain hydro-morphological design parameters of protection works of this project. The study provides the identification of erosion trend of the vulnerable areas, devising suitable options of river bank protection works, determination of maximum expected scour level around river bank protection works, assessment of morphological changes in the vicinity of the river bank protection works, assessment of river bank protection-induced morphological changes, providing outline design of river bank protection works, formulation of monitoring program for the river bank protection works.

2.8.2 Studies around the world

A hydrodynamic and sediment transport model was developed in support of a feasibility study for a port construction project in Dharma River, Orissa, India. The proposed port had to be at the mouth of the Dharma River in the Bay of Bengal. This would require development and maintenance of a 19 km long navigational channel, and also a dike to divert Dharma river flow into the navigation channel to minimize the maintenance dredging requirements. Tidal circulation and sediment transport were modeled using RMA2 and SED2D.

To study the meander migration and scour of the Roer River, a model had been developed by Delft hydraulics for the Dutch Water Board. The main goal of the project was to determine the migration velocity and migration development of the meander bends, and the depth and velocity of the bed erosion of the Roer at the location of tunnel. With the 1-D hydraulic and morphological model system SOBEK, calculations were carried out to determine the large-scale morphological development and the flood scour of the Roer at the tunnel location.

In order to demonstrate the impact of sediment supply on the morphology of Tenryuu River (Japan), downstream of the Akida dam, Delft Hydraulics developed a two-dimensional model using the Delft2D-River system. The activities included 2-D schematization, extending the model system with the 'Aishida' and Michiue sediment transport equations, hydraulic and morphological evolution of supplied sediment volume.

Two-dimensional model was developed to examine the morphological effects and changes in navigability of the Waal River due to lowering of groynes. This model was developed with the help of Delft2D-River packages.

Hayter and Mehta (1986) demonstrated cohesive sediment related problems in estuaries include shoaling in navigable waterways and water pollution. A two-dimensional, depth-averaged, finite element (FE) cohesive sediment transport model, CSTM-H, has been developed and may be used to assist in predicting the frequency and quantity of dredging required to maintain navigable depths and the fate of adsorbed pollutants. Algorithms which describe the processes of erosion, dispersive transport, deposition, bed formation and bed consolidation are incorporated in CSTM-H. The Galerkin weighted residual method is used to solve the advection-dispersion equation with appropriate source/sink terms at each time step for the nodal suspended sediment concentrations. The model yields stable and converging solutions. Partial verification was carried out against a series of erosion-deposition experiments in the laboratory using kaolinite and a natural mud as sediment.

Nguyen et al. (2009) have studied a two-phase numerical model for suspended-sediment transport in estuaries. They presented a full 2-D numerical model for sediment transport in open channels and estuaries using a two-phase (fluid–solid particle) approach. The physical concept and the mathematical background of the model have given and test-cases have been carried out to validate the proposed model. In order to illustrate its feasibility for a real estuary, the model has been applied to simulate the suspended-sediment transport and the formation of turbidity maximum in the Seine estuary. The numerical results show that the main characteristics of estuarine hydro-sediment dynamics in the Seine estuary are in fact reproduced by the proposed model. A qualitative agreement between the numerical results and the actual observations has been obtained and presented in this study.

Shimizu and Itakura (1989) applied a two-dimensional model in calculating the bed variation in alluvial channels. The model was applied to analyze the bed variations with or without meso-scale bed configuration such as alternating bars (pool and riffles) and braided bars, which can be observed even in straight channels.

Van Kessel (1999) carried out a number of tests on the performance of the non cohesive (sand) formulations in the sediment version of Delft3D-FLOW. These tests were carried out by Modelling a long (8km) straight flume with a movable sand bed. The roughness and slope of the flume were such that a constant flow depth and depth-averaged velocity were achieved along the length of the flume.

2.9 Summary

Several modeling studies have been conducted to till date to understand the behavior of the different type of rivers in Bangladesh as well as over the world. But most of these models are very expensive and some are very time consuming. On the other hand Delft3D flow (FLOW), morphology (MOR) and wave (WAVE) modules are available in open source and has proven its capabilities on many places around the world, like the Netherlands, USA, Hong Kong, Singapore, Australia, Venice, etc. (Delft3D Open Source Community). Delft3D is a powerful tool for the understanding and forecasting of river morph dynamic behavior, because it takes into

account the most relevant factors involved in this process (as input parameters) and gives a broad range of results (as output parameters) presented in an accessible manner. Jamuna is one of the largest rivers in Bangladesh. Every year the widening of the river, bank erosion, development of large bars and deposition in main navigational channels, are happened to be the major problems. On the basis of background of the study and the literature review the main focus of the study is to assess the morphology of the selected reach of the river by using the Delft3D numerical model.

CHAPTER 3

THEORY AND METHODOLOGY

3.1 General

Engineers have studied the subject of sediment transport for centuries. Different approaches have been used for the development of sediment transport functions or formulas. These formulas have been used for solving engineering and environmental problems. Results obtained from different approaches often differ drastically from each other and from observations in the field. Some of the basic concepts, their limits of application, and the interrelationships among them have become clear to us only in recent years. Many of the complex aspects of sediment transport are yet to be understood, and they remain among the challenging subjects for future studies.

The mechanics of sediment transport for cohesive and non cohesive materials are different. This chapter addresses non cohesive sediment transport only. This chapter starts with a review of the basic concepts and approaches used in the derivation of incipient motion criteria and sediment transport functions or formulas.

In Delft3D, the physical processes are modeled by a system of equations that consists of two hydrodynamic equations, the continuity equation and the momentum horizontal equations, and one transport equation for conservative constituents. In this study the governing equations that Delft3D uses to model the hydrodynamic and morphological changes of the river are described.

3.2 The basic equations of fluid dynamics

The basic equations of fluid flow, encode the familiar laws of mechanics:

- conservation of mass (the continuity equation)
- conservation of momentum

At the level of “fluid elements”, in any domain, the flow equations must be solved subject to a set of conditions that act at the domain boundary.

3.2.1 The Continuum Hypothesis - Fluid Elements

At a microscopic scale, fluid comprises individual molecules and its physical properties (density, velocity, etc.) are violently non-uniform. However, the phenomena studied in fluid dynamics are macroscopic, so instead of taking this molecular detail into account, the fluid is treated as a continuum by viewing it at a coarse enough scale that any “small” fluid element actually still contains very many molecules.

3.2.2 The Continuity Equation

A volume V is considered bounded by a surface S that is fixed in space. This mass inside it is given by $\int_V \rho dV$, so the rate of decrease of mass in –

$$\dot{V} = -\frac{d}{dt} \int_V \rho dV = -\int_V \frac{\partial \rho}{\partial t} dV \quad \dots \dots \dots (3.1)$$

If mass is conserved, Eqn. 1 must equal the total rate of mass flux out of V . The rate of outward mass flux across any small element dS of S is $\rho v \cdot dS$, where the magnitude of dS is equal to the element’s area. Integrating over the whole surface, the rate of mass flux out of –

$$\dot{V} = \int_S \rho v \cdot dS = \int_V \nabla \cdot (\rho v) dV \quad \dots \dots \dots (3.2)$$

The integrand $\nabla \cdot (\rho v)$ on the RHS is expressed in Cartesian coordinates $x = (x, y, z)$, $v = (u, v, w)$ as –

$$\nabla \cdot (\rho v) = \frac{\partial(\rho u)}{\partial x} + \frac{\partial(\rho v)}{\partial y} + \frac{\partial(\rho w)}{\partial z} \quad \dots \dots \dots (3.3)$$

Figure 3.1 shows clearly that gradients in the flow field are required for non-zero net flux. For mass to be conserved everywhere, Equation 3.1 and 3.2 must be equal for any volume V and so the continuity equation –

$$\frac{\partial \rho}{\partial t} + \nabla \cdot (\rho v) = 0 \quad \dots \dots \dots (3.4)$$

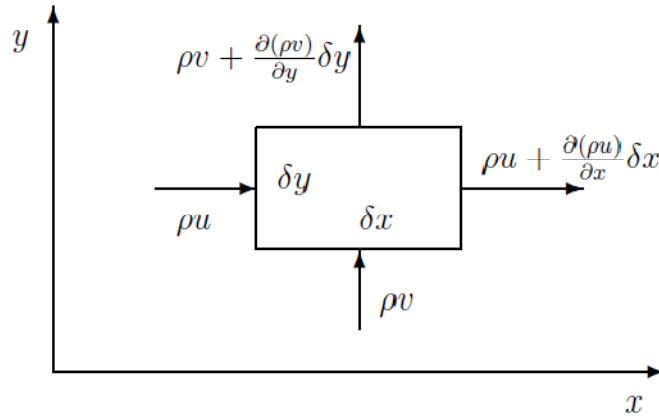


Figure 3.1: Mass fluxes entering and leaving an element.

The Material Derivative

For any physical quantity $f = f(x, t)$ (density, temperature, each velocity component, etc.), the material (or substantive) derivative becomes –

$$\begin{aligned} \frac{Df}{Dt} &= \frac{d}{dt} f(x(t), y(t), z(t), t) = \frac{\partial f}{\partial t} + \frac{dx}{dt} \frac{\partial f}{\partial x} + \frac{dy}{dt} \frac{\partial f}{\partial y} + \frac{dz}{dt} \frac{\partial f}{\partial z} = \frac{\partial f}{\partial t} + u \frac{\partial f}{\partial x} + \\ v \frac{\partial f}{\partial y} + w \frac{\partial f}{\partial z} &= \frac{\partial f}{\partial t} + v \cdot \nabla f \quad \dots \dots \dots \end{aligned}$$

(3.5)

Equation 3.5 conveys the intuitively obvious fact that, even in a time-independent flow field ($\frac{\partial f}{\partial t} = 0$ everywhere), any given element can suffer changes in $f(v \cdot \nabla f)$ as it moves from place to place.

The continuity equation can also be written in the form –

$$\frac{D\rho}{Dt} + \rho \nabla \cdot v = 0 \quad \dots \dots \dots (3.6)$$

If the fluid is incompressible, $\rho = \text{constant}$, independent of space and time, so that $\frac{D\rho}{Dt} = 0$.

The continuity equation then reduces to

$$\nabla \cdot v = 0 \quad \dots \dots \dots (3.7)$$

which in Cartesian coordinates is

$$\frac{\partial u}{\partial x} + \frac{\partial v}{\partial y} + \frac{\partial w}{\partial z} = 0 \quad \dots \dots \dots (3.8)$$

The Delft3D-flow module similarly performs the hydrodynamic computations by solving the Navier Stokes' equations for shallow water in two (depth-averaged) or three dimensions, under the hydrostatics pressure assumption, which neglects the vertical acceleration due to buoyancy effects or changes in bottom topography (Lesser et al. 2004).

The depth-averaged continuity equation is given by (Lesser et al. 2004):

$$\frac{\partial \zeta}{\partial t} + \frac{\partial [HU]}{\partial x} + \frac{\partial [HV]}{\partial y} = S \quad \dots \dots \dots (3.9)$$

Where, S represents the contribution of the discharge of water, ζ stands for the water level and H is the water depth.

3.2.3 Conservation of Momentum

The Cauchy Equations

A volume V bounded by a material surface S that moves with the flow, always containing the same material elements. Its momentum is $\int_V dV \rho v$, so the rate of change of momentum = $\frac{d}{dt} \int_V dV \rho v = \int_V dV \rho \frac{Dv}{Dt}$ (3.10)

Stress tensor $[\pi]$, defined so the force exerted per unit area across a surface element $dS \equiv \hat{n}dS$ (by the fluid on the side to which \hat{n} points on the fluid on the other side) is $f = [\pi] \cdot \hat{n}$.

$$\text{Total force (body + surface)} = \int_V dV \rho g + \int_S [\pi] \cdot dS$$

$$= \int_V dV(\rho g + \nabla \cdot [\pi]) \quad \dots \dots \dots (3.11)$$

By Newton's second law, Eqns. 3.10 and 3.11 must be equal for any V, so the Cauchy equation –

$$\rho \frac{Dv}{Dt} = \rho g + \nabla \cdot [\pi] \quad \dots \dots \dots (3.12)$$

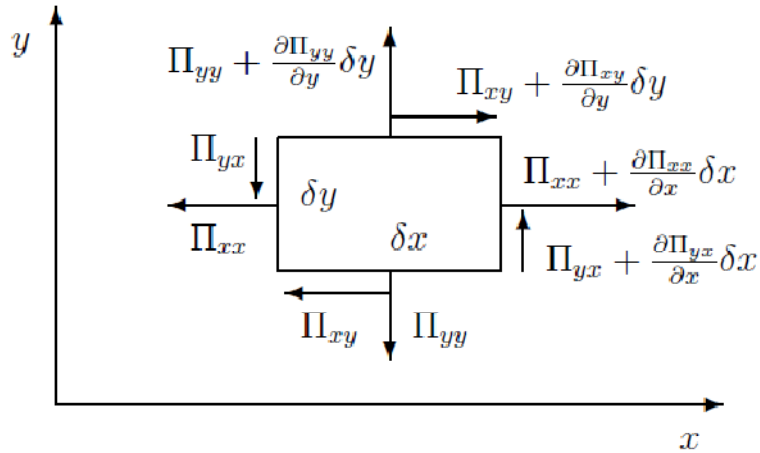


Figure 3.2: Surface stresses on a fluid element in 2 dimensions.

π_{ij} is the force per unit area in the “i” direction across a plane with normal in the “j” direction. As can be seen from (Figure 3.2), gradients in the stress tensor are needed for there to be a net force on any element (consistent with the surface integral of $[\pi] \cdot \hat{n}$ equating to a volume integral of $\nabla \cdot [\pi]$). It is possible to show that the stress tensor is symmetric, i.e.

$$\pi_{xy} = \pi_{yz}, \pi_{zx} = \pi_{xz}, \pi_{yz} = \pi_{zy} \quad \dots \dots \dots (3.13)$$

Otherwise any small fluid element would suffer infinite angular acceleration.

Constitutive Relations

The surface stresses $[\pi]$ on any element arise from a combination of pressure p and viscous friction, as prescribed by the constitutive relations

$$\pi_{xx} = -p + \lambda \nabla \cdot v + 2\mu \frac{\partial u}{\partial x}, \quad \pi_{xy} = \mu \left(\frac{\partial v}{\partial y} + \frac{\partial u}{\partial x} \right) \quad \dots \dots \dots (3.14)$$

$$\pi_{yy} = -p + \lambda \nabla \cdot v + 2\mu \frac{\partial v}{\partial y}, \quad \pi_{yz} = \mu \left(\frac{\partial v}{\partial z} + \frac{\partial w}{\partial y} \right) \quad \dots \dots \dots (3.15)$$

$$\pi_{zz} = -p + \lambda \nabla \cdot v + 2\mu \frac{\partial w}{\partial z}, \quad \pi_{xz} = \mu \left(\frac{\partial u}{\partial z} + \frac{\partial w}{\partial x} \right) \quad \dots \dots \dots (3.16)$$

μ and λ are the coefficients of dynamic and bulk viscosity respectively.

Incompressible Navier-Stokes Equations

For incompressible flow, the constitutive relations reduce to –

$$\pi_{ij} = -p \delta_{ij} + \mu \left(\frac{\partial u_i}{\partial x_j} + \frac{\partial u_j}{\partial x_i} \right) \quad \dots \dots \dots (3.17)$$

where $v = (u_1, u_2, u_3)$, $x = (x_1, x_2, x_3)$ and defined –

$$\delta_{ij} = 1 \text{ if } i = j \text{ and } \delta_{ij} = 0 \text{ if } i \neq j$$

Inserting Eqn. 3.17 into Eqn. 3.12, assuming constant μ , and utilising again the incompressibility condition 7, the incompressible Navier–Stokes (N–S) equations –

$$\text{Continuity: } 0 = \frac{\partial u}{\partial x} + \frac{\partial v}{\partial y} + \frac{\partial w}{\partial z}$$

$$\text{Momentum, x: } \rho \frac{Du}{Dt} = \rho g_x - \frac{\partial p}{\partial x} + \mu \left(\frac{\partial^2 u}{\partial x^2} + \frac{\partial^2 u}{\partial y^2} + \frac{\partial^2 u}{\partial z^2} \right)$$

$$\text{Momentum, y: } \rho \frac{Dv}{Dt} = \rho g_y - \frac{\partial p}{\partial y} + \mu \left(\frac{\partial^2 v}{\partial x^2} + \frac{\partial^2 v}{\partial y^2} + \frac{\partial^2 v}{\partial z^2} \right)$$

$$\text{Momentum, } z: \rho \frac{Dw}{Dt} = \rho g z - \frac{\partial p}{\partial z} + \mu \left(\frac{\partial^2 w}{\partial x^2} + \frac{\partial^2 w}{\partial y^2} + \frac{\partial^2 w}{\partial z^2} \right) \quad \dots \dots \dots (3.18)$$

Or, in compact notation

$$\text{Continuity: } \nabla \cdot v = 0 \quad \dots \dots \dots (3.19)$$

$$\text{Momentum: } \rho \frac{Dv}{Dt} = \rho g - \nabla p + \mu \Delta v \quad \dots \dots \dots (3.20)$$

In which Δ is the Laplacian operator. For uniform ρ , the gravitational force is exactly balanced by a pressure gradient $\nabla p_0 = g$ that does not interact with any flow, defining $P = p - p_0$ gives –

$$\rho \frac{Dv}{Dt} = -\nabla P + \mu \Delta v \quad \dots \dots \dots (3.21)$$

Similar equation is followed by Delft3D

The momentum equation in ξ and η direction are –

$$\begin{aligned} \frac{\partial u}{\partial t} + \frac{u}{\sqrt{G_{\xi\xi}}} \frac{\partial u}{\partial \xi} + \frac{v}{\sqrt{G_{\eta\eta}}} \frac{\partial u}{\partial \eta} + \frac{w}{d+\zeta} \frac{\partial u}{\partial \sigma} - \frac{v^2}{\sqrt{G_{\xi\xi}}\sqrt{G_{\eta\eta}}} \frac{\partial \sqrt{G_{\eta\eta}}}{\partial \xi} + \frac{uv}{\sqrt{G_{\xi\xi}}\sqrt{G_{\eta\eta}}} \frac{\partial \sqrt{G_{\xi\xi}}}{\partial \eta} - \\ f v = - \frac{1}{\rho_0 \sqrt{G_{\xi\xi}}} P_{\xi} + F_{\xi} + \frac{1}{(d+\zeta)^2} \frac{\partial}{\partial \sigma} \left(\nu_v \frac{\partial u}{\partial \sigma} \right) + M_{\xi} \\ \frac{\partial v}{\partial t} + \frac{u}{\sqrt{G_{\xi\xi}}} \frac{\partial v}{\partial \xi} + \frac{v}{\sqrt{G_{\eta\eta}}} \frac{\partial v}{\partial \eta} + \frac{w}{d+\zeta} \frac{\partial v}{\partial \sigma} - \frac{u^2}{\sqrt{G_{\xi\xi}}\sqrt{G_{\eta\eta}}} \frac{\partial \sqrt{G_{\xi\xi}}}{\partial \eta} + \frac{uv}{\sqrt{G_{\xi\xi}}\sqrt{G_{\eta\eta}}} \frac{\partial \sqrt{G_{\eta\eta}}}{\partial \xi} + f u = \\ - \frac{1}{\rho_0 \sqrt{G_{\eta\eta}}} P_{\eta} + F_{\eta} + \frac{1}{(d+\zeta)^2} \frac{\partial}{\partial \sigma} \left(\nu_v \frac{\partial v}{\partial \sigma} \right) + M_{\eta} \quad \dots \dots \dots (3.22) \end{aligned}$$

Where ν_v represents the vertical eddy viscosity coefficient. Density variations are neglected, except in the baroclinic pressure terms, P_{ξ} and P_{η} represent the pressure gradients. The forces F_{ξ} and F_{η} in the momentum equations represent the unbalance of horizontal Reynold's stresses. M_{ξ} and M_{η} represent the contributions due to external sources or sinks of momentum (external forces by hydraulic structures, discharge or withdrawal of water, wave stresses, etc.).

3.3 Advection-Diffusion Equation

Delft3D calculates the transport of sediment by solving the three-dimensional advection-diffusion equation for suspended particles (equation 3.3) (Deltares 2009). In which, the flow velocities and eddy diffusivities are calculated from the hydrodynamic equations 3.8 and 3.20. In addition, the program is able to adjust the density of water in relation to temperature and salinity (Deltares 2009) and differentiates the settling velocities and sediment fluxes between cohesive and non-cohesive particles.

$$\frac{\partial c}{\partial t} + \frac{\partial U c}{\partial x} + \frac{\partial V c}{\partial y} + \frac{\partial (w-w_s)c}{\partial \sigma} - \frac{\partial}{\partial x} \left(\varepsilon_{s,x} \frac{\partial c}{\partial x} \right) - \frac{\partial}{\partial y} \left(\varepsilon_{s,y} \frac{\partial c}{\partial y} \right) - \frac{\partial}{\partial \sigma} \left(\varepsilon_{s,z} \frac{\partial c}{\partial \sigma} \right) = 0$$

... .. (3.23)

Where,

C = Depth averaged suspended sediment concentration [kg m⁻³]

U, V = Flow velocity components in the x- and y- direction [m s⁻¹]

w_s = Settling velocity [m s⁻¹]

ε_{s,x,y,z} = Eddy diffusivities in three directions [m² s⁻¹]

(w – w_s)= “assumption that the settling velocity with respect to the flowing water is the same that in stagnant water” (Ribberink 2010).

The settling velocity for cohesive and non-cohesive sediment is calculated in relation to the concentration (Deltares 2009). In high concentrations, the presence of other particles reduces the settling velocity of a single particle.

3.4 Settling Velocity

The settling velocity of non-cohesive sediments can be modeled by the Van Rijn (1993) formulation, which depends upon a representative sediment diameter, D_s. The formulation is of relative importance for this study as the model is calibrated for the Van Rijn’ 84 equation, which in Delft3D, requires the settling velocity as an input value.

$$w_s = w_{s,0} = \begin{cases} \frac{(s-1)gD_s^2}{18\nu}; & \text{when } 65 \mu\text{m} < D_s \leq 100 \mu\text{m} \\ \frac{10\nu}{D_s} \left[\left(1 + \frac{0.01(s-1)gD_s^3}{\nu^2} \right) - 1 \right]; & \text{when } 100 \mu\text{m} < D_s \leq 1000 \mu\text{m} \\ 1.1[(s-1)gD_s]; & \text{when } D_s > 1000 \mu\text{m} \end{cases}$$

(3.24)

And

$$D_s = \begin{cases} 0.64D_{50}; & \text{for } T \leq 1 \\ D_{50}(1 + 0.015(T - 25)); & \text{for } 1 \leq T \leq 25 \\ D_{50}; & \text{for } 25 \leq T \end{cases} \quad \dots \dots \dots (3.25)$$

s = relative density ρ_s/ρ_w of the suspended sediment fraction

D_s = representative diameter of sediment fraction [m]

D_{50} = median grain size of bed material [m]

ν = kinematic viscosity coefficient of water [$\text{m}^2 \text{s}^{-1}$]

T = non-dimensional bed shear stress

3.5 Deposition and Erodibility on Delft3D

The model quantifies the sediment entering the flow due to an upward diffusion (erosion) and the sediment dropping out of the water column due to the settling velocity of particles (deposition). The sediment fluxes between the bed and flow are based on modeled approximations by sink and source terms acting on a layer above the reference height a developed by van Rijn (1993), named in Delft3D as the kmx layer (Figure 3.3). The concentration approximation follows a standard Rouse profile from the reference height a, to the centre of the kmx layer (Deltares 2009). Shortly, the deposition and erosion flux through the kmx layer can be expressed as follows:

Deposition flux: $D = w_s c_{kmx}$ (3.26)

Erosion flux: $E \approx \varepsilon_s \left(\frac{c_a - c_{kmx}}{\Delta z} \right)$ (3.27)

Where,

w_s = settling velocity [m s^{-1}]

ε_s = sediment diffusion coefficient evaluated at the kmx layer.

c_{kmx} = sediment concentration at the kmx layer [kg l^{-1}]

Δz = difference in elevation between the kmx layer and the van Rijn's reference height a [m]

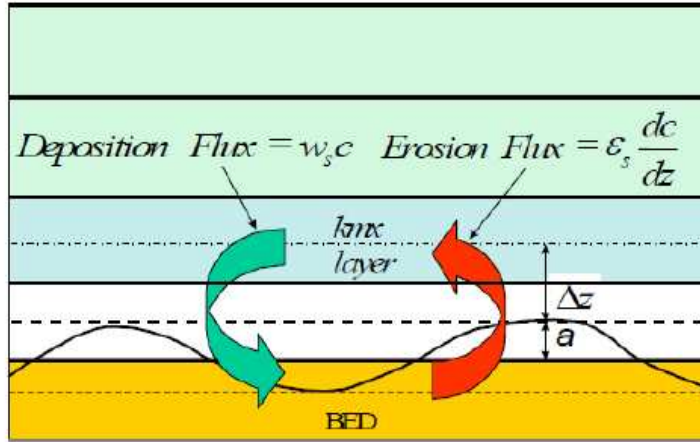


Figure 3.3: Schematization of flux on the kmx layer (Deltares 2009)

Each half time-step the source and sink terms model the quantity of sediment entering the flow due to upward diffusion from the reference level and the quantity of sediment dropping out of the flow due to sediment settling. A sink term is solved implicitly in the advection diffusion equation, whereas a source term is solved explicitly. The required sink and source terms for the kmx layer are calculated as follows.

Erosive flux due to upward diffusion

$$E^{(l)} = \varepsilon_s^{(l)} \frac{\partial c^{(l)}}{\partial z} \dots \dots \dots (3.28)$$

where $\varepsilon_s^{(l)}$ and $\frac{\partial c^{(l)}}{\partial z}$ are evaluated at the bottom of the kmx layer.

The erosion flux is split in a source and sink term:

$$E^{(l)} \approx \frac{\alpha_2^{(l)} \varepsilon_s^{(l)} c_a^{(l)}}{\Delta z} - \frac{\alpha_2^{(l)} \varepsilon_s^{(l)} c_{kmx}^{(l)}}{\Delta z} \dots \dots \dots (3.29)$$

$\alpha_2^{(l)}$ correction factor for sediment concentration

$\varepsilon_s^{(l)}$ sediment diffusion coefficient evaluated at the bottom of the kmx cell of sediment fraction (l)

$c_a^{(l)}$ reference concentration of sediment fraction(l)

$c_{kmx}^{(l)}$ average concentration of the kmx cell of sediment fraction (l)

Δz difference in elevation between the centre of the kmx cell and Van Rijn's reference height

$$Source_{erosion}^{(l)} = \frac{\alpha_2^{(l)} \varepsilon_s^{(l)} c_a^{(l)}}{\Delta z} \dots \dots \dots (3.30)$$

$$Sink_{erosion}^{(l)} = \frac{\alpha_2^{(l)} \varepsilon_s^{(l)} c_{kmx}^{(l)}}{\Delta z} \dots \dots \dots (3.31)$$

Deposition flux due to sediment settling

The deposition flux is approximated by:

$$D^{(l)} \approx \alpha_1^{(l)} c_{kmx}^{(l)} w_s^{(l)} \dots \dots \dots (3.32)$$

This results in a simple deposition sink term:

$$Sink_{deposition}^{(l)} = \alpha_1^{(l)} c_{kmx}^{(l)} w_s^{(l)} \dots \dots \dots (3.33)$$

The total source and sink terms is given by:

$$Source^{(l)} = \alpha_2^{(l)} c_a^{(l)} \left(\frac{\varepsilon_s^{(l)}}{\Delta z} \right) \dots \dots \dots (3.34)$$

$$Sink^{(l)} = \left[\alpha_2^{(l)} \left(\frac{\varepsilon_s^{(l)}}{\Delta z} \right) + \alpha_1^{(l)} w_s^{(l)} \right] c_{kmx}^{(l)} \quad \dots \dots \dots (3.35)$$

where $w_s^{(l)}$ and $c_{kmx}^{(l)}$ are evaluated at the bottom of the kmx layer

These source and sink terms are both guaranteed to be positive.

Regarding the calculation of the sediment transport, Delft3D allows the combined use of cohesive and non-cohesive sediment. By default, the formulations of Van Rijn are applied for the suspended and bed load transport of non-cohesive sediment, which is the case of the sandy sediment in the area of the selected reach. If desired, it is possible to use other sediment transport formulae for non-cohesive sediment; however it has been decided to stick to Van Rijn's approach, because it is the most used in other studies involving Delft3D, hence the most experienced and functional.

Due to the fact that sand transport models are often based on semi-empirical equilibrium transport formulae that relate sediment fluxes to physical properties, such as velocity, depth and grain size, it is crucial to perform sensitivity analysis of the formulae used.

Pinto et al. (2006) compared four sediment transport formulations considering only the tidal current only: Ackers and White (1973); Engelund and Hansen (1967); van Rijn (1984 a,b,c) and Karim and Kennedy (1990). The authors concluded that the van Rijn formula is the most sensitive to basic physical properties. Hence, it should only be used when physical properties are known with precision.

3.6 Sediment Transport

3.6.1 Suspended and Bed Load Transport

The bed evolution is based on the sediment continuity (Equation 3.28), where the first term expresses the changes in bed level in time (Tonnon et al. 2007) and the second and third terms are the sediment fluxes (bed and suspended load) in the x-

and y- directions, respectively. The equation states that the bed level evolution in time is depended on the suspended and bed load gradients in the x and y directions.

$$\frac{\partial z_b}{\partial t} + \frac{\partial(S_{b,x}+S_{s,x})}{\partial x} + \frac{\partial(S_{b,y}+S_{s,y})}{\partial y} = 0 \quad \dots \dots (3.36)$$

Where,

$S_{b,x,y}$ = bed-load transport in x- and y-direction [$\text{kg m}^{-1} \text{s}^{-1}$]

$S_{s,x,y}$ = sediment-load transport in x- and y-direction [$\text{kg m}^{-1} \text{s}^{-1}$]

z_b = bed level [m]

The suspended and bed load transport are computed by standard sediment transport formulations (Van Rijn (1993), Engelund-Hansen (1967), Bijker (1971), Soulsby, etc), which subsequently are corrected for bed-slope effects, upwind bed compositions and sediment availability (Deltares 2009). The Van Rijn’ 84 formulation is able to calculate the suspended and bed load transport separately and distinguishes between the transport modes according to the reference height. Above the reference height the concentration is catalogued as suspended load and below as bed load. In river systems, as the particles are bigger, the settling velocity of particles is higher than in other aquatic systems, the latter can be confirmed with the aid of the Rouse Number P, which is a non-dimensional number that defines the transport mode of the sediment. (Equation 3.29)

$$P = \frac{w_s}{ku_*} \quad \begin{array}{l} P > 2.5 \text{ Bed Load} \\ 0.8 < P < 1.2 \text{ Suspended Load} \\ P < 0.8 \text{ Wash Load} \end{array} \quad \dots \dots (3.37)$$

Where,

u_* = Critical shear velocity [m s^{-1}]

k = von karman constant, typically 0.40

w_s = Settling velocity, (0.1 m/s, calibrated Delft3D model) [m s^{-1}]

According to the Van Rijn' 84 formulation (Deltares 2009), the critical shear velocity u^* is determined by:

$$u_* = q \sqrt{\frac{f_{cb}}{8}} \quad \dots \dots \dots (3.38)$$

where,

q = Depth average velocity, 1 m s^{-1}

f_{cb} = friction factor expressed as (Deltares 2009)

$$f_{cb} = \frac{0.24}{\left[\log_{10}\left(\frac{12H}{3D_{90}}\right)\right]^2} \quad \dots \dots \dots (3.39)$$

with H = water depth

and $D_{90} = 1.5D_{50}$

3.6.2 Bed Load Transport: Van Rijn' 84

For simulation without waves, the magnitude of the bed load transport is calculated according to Van Rijn' 84 equation, for which the model is calibrated:

$$S_b = \begin{cases} 0.053 \sqrt{(s-1)gD_{50}^3} D_*^{-0.3} T^{2.1}, & \text{for } T < 3.0 \\ 0.1 \sqrt{(s-1)gD_{50}^3} D_*^{-0.3} T^{1.5}, & \text{for } T \geq 3.0 \end{cases} \quad \dots \dots \dots (3.40)$$

Where, S_b is the bed load transport rate [$\text{kg m}^{-1} \text{ s}^{-1}$] and D_* and T are the shear velocity, non-dimensional particle size and the non-dimensional bed-shear stress respectively (Van Rijn' 84), with –

D_* Non-dimensional particle size:

$$D_* = D_{50} \left[\frac{(s-1)g}{v^2} \right]^{\frac{1}{3}} \quad \dots \dots \dots (3.41)$$

T Non-dimensional bed-shear stress:

$$T = \frac{\mu_c \tau_{bc} - \tau_{cr}}{\tau_{cr}} \quad \dots \dots \dots (3.42)$$

In which, the critical bed shear stress τ_{cr} is written based on the Shields parameter which is defined as a function of the non-dimensional particle parameter D_* :

$$\tau_{cr} = (\rho_s - \rho)gD_{50}\theta_{cr}$$

$$\theta_{cr} = \begin{cases} 0.24D_*^{-1}, & \text{for } 1 < D_* < 4 \\ 0.14D_*^{-0.64}, & \text{for } 4 < D_* < 10 \\ 0.04D_*^{-0.1}, & \text{for } 10 < D_* < 20 \\ 0.013D_*^{-1}, & \text{for } 20 < D_* < 150 \\ 0.055, & D_* > 150 \end{cases} \quad \dots \dots \dots (3.43)$$

Where, the formulas to calculate the bed shear stress are:

$$\tau_{bc} = \frac{1}{8}\rho_w f_{cb} q^2 \quad \dots \dots \dots (3.44)$$

Where μ_c is the reference level, for which the given calibrated model assumes a value of 0.3 m and in which the Chézy coefficient C' is expressed as a function of the grain size D_{90} , interpreted in Delft3D as $1.5D_{50}$. The equation is written as:

$$\mu_c = \left(\frac{18 \log\left(\frac{12H}{\xi_c}\right)}{C'} \right)^2 \quad \dots \dots \dots (3.45)$$

$$f_{cb} = \frac{0.24}{\left[\log_{10}\left(\frac{12h}{3D_{90}}\right) \right]^2} \quad \dots \dots \dots (3.46)$$

$$C' = 18 \log\left(\frac{12h}{3D_{90}}\right) \quad \dots \dots \dots (3.47)$$

The 2D-Chézy coefficient C can be determined with the following formulations:

Chezy formulation: $C = \text{Chezy coefficient} \left[m^{1/2}/s \right]$

Manning formulation: $C = \frac{\sqrt[6]{h}}{n}$

White Colebrook's formulation: $C = 18 \log_{10} \left(\frac{12h}{k_s} \right)$

Where,

h = total water depth [m]

n = Manning coefficient $\left[m^{1/3}/s \right]$

k_s = Nikuradse roughness length [m]

The general Modelling approach in Delft3D is that hydrodynamic flow is calculated on a boundary fitted grid to which bathymetry, initial conditions and boundary conditions are applied. Sediment transports are calculated following the flow and wave field, according to the applied sediment transport formula.

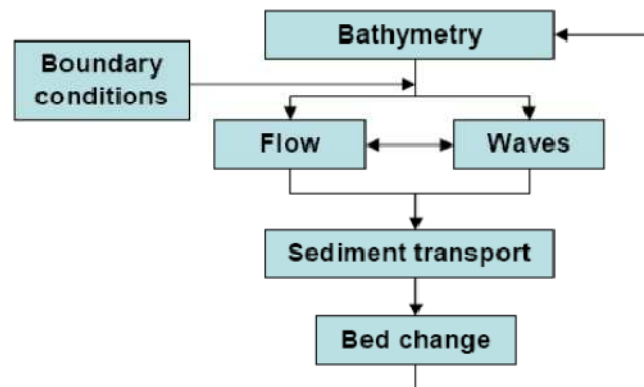


Figure 3.4: Schematic overview Delft3D calculation steps (Source:Roelvink, 2006)

Variations in sediment transports in their turn determine the morphological development of the model. The processes of flow, waves, sediment transport and morphological updating are all executed at each time step according to the 'online' approach (Roelvink, 2006, Figure 3.4).

3.7 Methodological Steps

At first the study area has been defined using a satellite image of Pre monsoon 2010. Then the boundaries of the study areas are defined by using the data of left and right

bank of Jamuna for April 2010 of the selected 50 km reach. The land boundary is obtained from GIS and the bathymetry is obtained using the Delft3D- QUICKIN module. The bathymetry is interpolated to the grid nodes by triangulation interpolation method. Once the grid is generated, various parameters such as boundary conditions, roughness, eddy viscosity, initial conditions, time step, sediment characteristics etc are assigned using the Flow module of Delft. Flow GUI saves all the files required to run different modules of Delft3D.

3.8 Profile of the study area

The study reach is selected within the district of Sirajganj and Tangail from E463400 m to E486500 m and N680000 m to N730000 m (BTM coordinate) and covers about 50 km reach of the Jamuna River (30km upstream and 20km downstream of The Bangabandhu Multi-purpose Bridge). Kazipur is situated at the right side at the upstream end and Chauhali is situated at the downstream end of the study reach. Balkuchi and Sirajganj on the right bank and Gopalpur and Bhuapur on the left bank are other important places to be considered along the study reach. The location of the study area is shown in Figure 3.5.

There are number of river training and bank protection works on the both bank of the river in the study area. These are comprised of the Bangabandhu Multi-purpose Bridge river training works (RTW) and BWDB bank protection works.

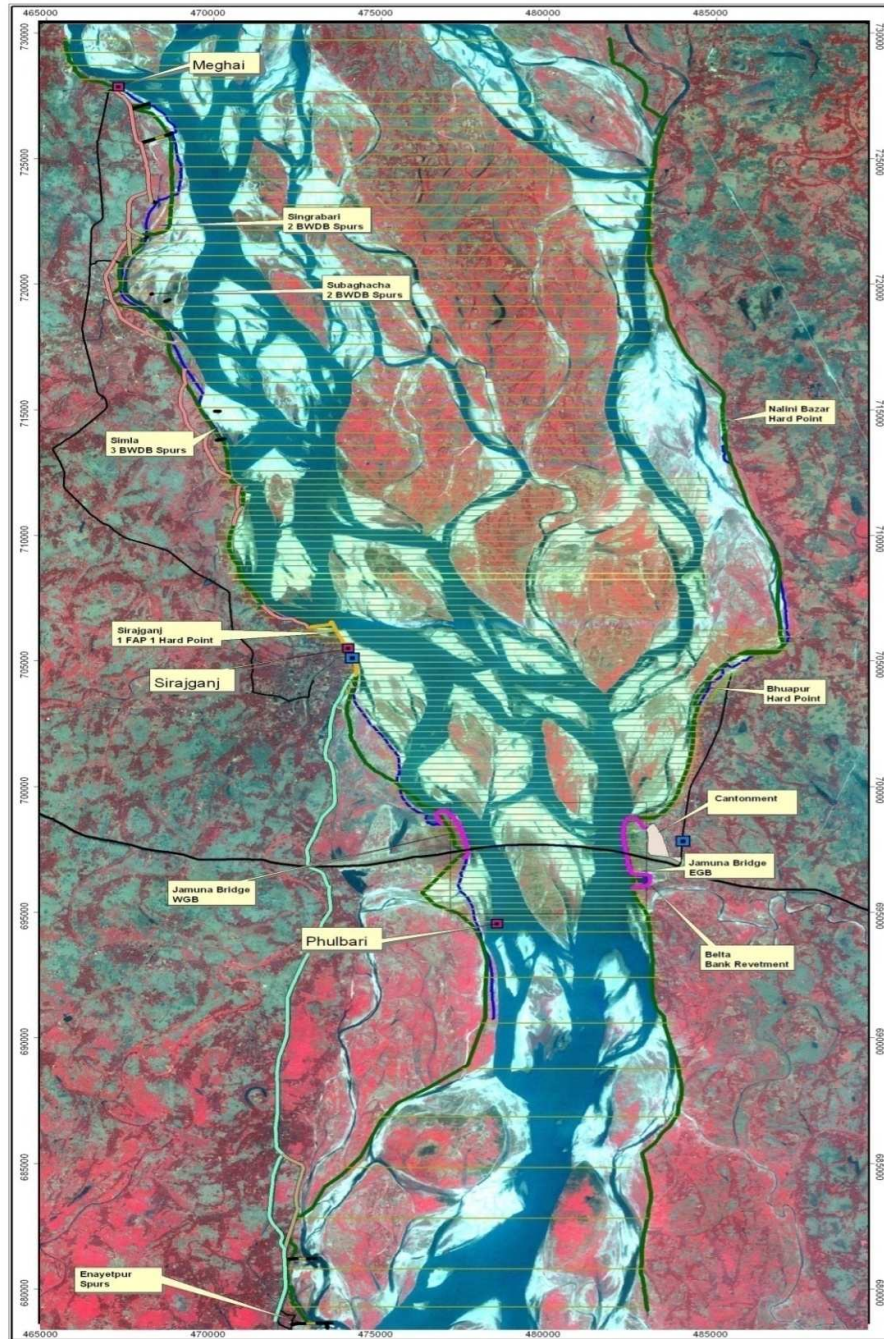


Figure 3.5: Study Area on the Jamuna River (Source: IWM, 2010)

The river reach is characterized by well defined braiding nature, meta-stable islands, nodes, sandbars, shifting ana-branches and rigorous bank erosion. Geomorphologically, the eastern bank is bounded with the lateral extension of Madhupur

Tract and the west bank is the Barind Tract, which is composed of silty clay. Topographically, the study area is part of alluvial plains (low land) formed by the sediments of river and its tributaries and distributaries. The study area belongs to region: floodplains and sub-region: Jamuna floodplain. The sub-region can be again subdivided into the Bangali-Karatoya floodplain, Jamuna-Dhaleshwari floodplain, anddiyaras and chars (Source: Banglapedia). The soil and topography of chars and diyaras vary considerably. Some of the largest ones have point bars. The elevation between the lowest and highest points of these accretions may be as much as 5 m.

3.9 Data Collection and Analysis

In order to determine the trend of the critical hydro-morphological conditions of the Jamuna River Historical as well as most recent hydro-morphological data (pre-monsoon 2011) have been Collected by IWM covering the distance between Kazipur situated at the upstream end and Chauhali situated at the downstream 50 km reach of Jamuna River incorporating all infrastructures including guide bunds and adjacent hard points of Bangabandhu Bridge.

The secondary data for the present study has been collected from Bangladesh Water Development Board (BWDB) and IWM. A number of reconnaissance surveys in pre monsoon 2011 were done by IWM survey team. The survey concluded cross-section, bank line and water level. The water level data of 2010 has been collected from BWDB.

3.9.1 Satellite Image Data

Satellite images for the Jamuna River have been collected from Institute of Water Modelling (IWM). The image is needed to extract the actual bank line of selected is for assessment of bank line shifting and also in generating computational grid of the model.

3.9.2 Description of the selected stations

For Monitoring of Hydraulic and Morphological Conditions of Jamuna River for the Safety of Bangabandhu Bridge as well as hydro-morphological forecasts of the river at the critical locations within the bridge area for monsoon 2011, IWM collected data during December 2010 - January 2011 for the stated 50 km reach from Kazipara to Chauhali. Cross Sectional data of the particular reach have been collected at an interval of 500 m for the first 10 km, then reduced to 250 m for 11 to 35 km and again increased at an interval of 500m for 35 to 50 km.

3.10 Approach and methodology followed during data collection

3.10.1 Coordinate System

The position (x,y) of the data points has been received from the GPS is in Bangladesh Transverse Mercator (BTM).

3.10.2 Bench Mark

For connecting water level gauges in the study area the existing and temporary Bench Marks (TBM) established by different organizations have been used.

3.10.3 Bathymetric Survey

In the flowing region of the river the bathymetric survey has been conducted by the survey boat. Digital echo sounder and the DGPS have been used to measure the water depths and positions of the vessels successively. Staff gauges were used to record the Simultaneous water levels relative to the datum (mPWD) with a known gauge zero level at upstream and downstream of the survey reach.

3.10.4 Char Survey

Conventional optical levels (fly leveling) has been used in surveying the dry area.

3.10.5 Bankline (Alignment) Survey

The alignment survey has been carried out by ProXR GPS (DGPS). At selected time intervals the GPS position (northing & easting) of the alignment of the bank line is continuously stored in the data logger.

3.10.6 Water Level Gauging

Water level gauges were established along the right bank of the Jamuna to conduct the bathymetry survey. Daily 3 hourly water levels have been recorded from 06:00 hour to 18:00 hour. The gauges have been connected to the PWD datum from the known reference BM/TBM by direct fly leveling.



Figure 3.6: Water level gauge on the River Jamuna

The river bank alignment has been surveyed for a total length of 67 km on both the right and left banks. Easting, northing and the length are contained in the alignment data.

A standard quality control procedure was maintained for all survey and data collections.

3.11 Data Analysis

For understanding the morphological condition of the Brahmaputra Jamuna River, two years cross-sectional data are taken. Also to know the long term morphological

behavior of Brahmaputra Jamuna River flexible integrated Modeling suite Delft3D software, which simulates two-dimensional (in either the horizontal or a vertical plane) and three-dimensional flow is used. Delft3D consists of a number of well-tested and validated programs, which are linked and integrated with one-another. The GUI allows visualizing model input, reference data and simulation results as time series and animations of two and three-dimensional data sets. It is a well proven tool for hydrological and morphological model calculation. Additional pre and post processing tools (such as the QUICKIN tool, a powerful editor of grid related data is used to simulate the water level of the Sirajgonj station for all the time steps entered on the Flow GUI and also shows the simulated bed level changes after 1 to 2 years for the every cross sections.

In case of second objective, the two years cross-sectional data 2010-2011 are used. The observed bed levels are extracted from the cross-sections of the bathymetry data given by IWM by using of the Arc GIS Software which have been used to compare with the simulated results.

To calibrate the model data of water level versus time for the months of monsoon (1-4-2010 to 30-7-2010) are inserted in table A.1. From table A.1 a graph is plotted showing a better result for calibration. And for validate the model data of water level versus date and time for another two months of monsoon (27-4-2011 to 27-6-2011) are inserted in table A.2. From table A.2 a graph is plotted showing a better result for validation.

For the last objective, the comparison of the simulated result that is the model output of Delft3D model, with the output of Mike 21 has been done. In these case the observed data of 2011 has been used.

3.12 Mathematical Modeling

3.12.1 Grid Generation

Steady hydrodynamic module is the foundation of all models. Grid generated under this model is used for rest of the models. Grid generation is the most important task in any model application.

In this study the curvilinear grid has been used that are created, modified and visualized by Delft3D-RGFGRID module. Curvilinear grids are applied in finite difference models to provide a high grid resolution in the area of interest and a low resolution elsewhere, thus saving computational effort.

The generated grid points in M-direction and in N-direction are 299 and 146 respectively. The size of individual grid is (124 X 171) m². Bathymetry of the grid was to be assigned. Before any further development, mesh quality has been checked to obtain a suitable and accurate solution. Various criteria has been checked, these include: orthogonality, aspect ratio, courant number, grid smoothness and resolution to minimize truncation errors in the finite difference scheme.

3.12.2 Bathymetry Generation

The study area was developed with good quality grids and then surveyed bathymetric data were interpolated into those mesh nodes Normally bathymetric survey has been carried out in the flowing part of the river The survey boat moved across the river approximately in straight lines following pre-set transect lines, measured the water depths and the corresponding positions. The depth schematization may be uniform or non-uniform across the model area. A non uniform (space-varying) bathymetry is given in an attribute file. Bathymetry has been developed under known parameter settings.

3.12.3 Sensitivity Analysis

Different parameter mainly the eddy viscosity and manning's roughness coefficient has been tested with entering different values as input for checking the sensitivity of the model.

3.12.4 Calibration and Validation of the Model

During model development, many uncertainties exists related to input as model geometry, boundary conditions, roughness, eddy viscosity etc. which can have momentous impact on model solutions. Once geometry and boundary conditions have been obtained with reasonable accuracy from the field, it is common practice to set them out of preview of the calibration process. Validation is a multi-step process of model adjustments and comparisons, leavened with careful consideration of both the model and the data. During validation, a new set of observed data have been incorporated to justify whether the calibrated parameters produces satisfactory result for a new condition.

3.12.4.1 Hydrodynamic Calibration

For hydrodynamic calibration, mostly roughness and eddy viscosity are the parameters to play with to obtain an adequate match with the observed field conditions. For the present study, the water levels at Sirajgonj station located 30 m upstream of Kazipur were compared with the simulated water levels of the model for the same location. Due to lack of data of the dry season the calibration was undertaken only for the wet season for 2 months (20 April 2010 to 28 June2010). The roughness parameter (Manning's n) was adjusted to get the best result.

3.12.4.2 Hydrodynamic Validation

The computed water surface elevations by the model were validated with observed water surface elevations at Sirajgonj station for the months of 3 April 2011 to 14 August 2011. Good agreement between the observed and simulated water levels indicates satisfactory performance of the model. During the calibration and

validation process, the model showed good agreement with observed data for wet periods. Therefore the model was capable to simulate different conditions and scenarios used in the present study.

During the calibration and validation process, the model showed good agreement with the observed data for the monsoon periods. For the lack of data for dry season it was not possible to calibrate and validate for dry seasons.

3.12.5 Simulation of the Model

When satisfactory results are obtained in calibration and validation, the model was considered ready for simulation and various analyses. First the model was run for the base period of year 2010. The model was simulated for the two consecutive years 2011 and 2012 to predict the hydraulic and morphologic responses of the river. The analysis was carried out for the river profile as well as for the selected cross sections.

3.13 Summary

This chapter comprehensively reviews and evaluates basic approaches and theories used in the determination of non cohesive sediment transport rate. The step by step methods conducted in this study is also discussed. Delft 3D models the hydrodynamics processes according to the continuity and momentum equation, whereas, the transport of sediment is modeled by the three-dimensional advection-diffusion equation. The settling velocity for non-cohesive sediment is modeled in Delft 3D according to the Van Rijn' 93 formulation, which depends upon the sediment concentration and the representative sediment diameter D_s , function of the median grain size D_{50} . The model quantifies the amount of sediment entering the water column due to an upward diffusion (erosion) and a downward settling velocity (deposition) passing through the *kmx layer*.

In this study, the Van Rijn' 84 equation for bed load transport is utilized. The formula is commonly used for situations without waves and calculates the bed load transport rate according to the non-dimensional particle size.

CHAPTER 4

MODEL SETUP

4.1 General

The study of natural river changes and the interference of man in natural water bodies is a difficult but important activity, as increasing and shifting populations place more demands on the natural sources of fresh water. Although the basic mechanical principles for these studies are well established, a complete analytical solution is not known but for the most basic cases. The complexities of the flow movement and its interaction with its boundaries, which are themselves deformable, have precluded the development of closed form solutions to the governing equations that describe the mechanical behavior of fluid and solid-fluid mixtures. As a result, alternative techniques have been developed to provide quantitative predictions of these phenomena as an aid to engineering projects and river restoration efforts. Modelling is one such technique. There are two types of models: mathematical models and physical models (sometimes also called scale models).

Numerical modeling has become very popular in the past few decades, mainly due to the increasing availability of more powerful and affordable computing platforms. Much progress has been made, particularly in the fields of sediment transport, water quality, and multidimensional fluid flow and turbulence. Graphical user interfaces, automatic grid generators, geographic information systems, and improved data collection techniques (such as LiDAR, Light Distancing and Ranging) promise to further expedite the use of numerical models as a popular tool for solving river engineering problems.

4.2 Numerical Model

The problem at hand cannot be solved directly for the prototype in numerical models. The process from prototype data to the modeling and to final interpretation of the results (i.e., the modeling cycle) is complex and prone to many errors. Careful

engineering judgment must be exercised at every step. The modeling cycle is schematically represented in (Figure 4.2).

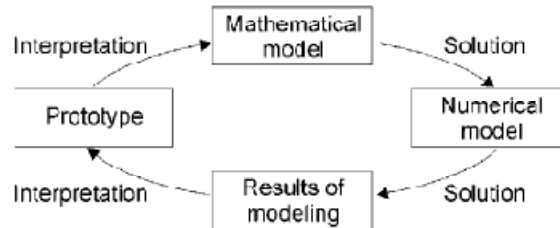


Figure 4.1: Computer Modeling cycle from prototype to the Modeling results

The prototype is the reality to be studied. It is defined by data and by knowledge. The data represents boundary conditions, such as bathymetry, water discharges, sediment particle size distributions, vegetation types, etc. The knowledge contains the physical processes that are known to determine the system's behavior, such as flow turbulence, sediment transport mechanisms, mixing processes, etc. Understanding the prototype and data collection constitute the first step of the cycle.

In the first interpretation step, all the relevant physical processes that were identified in the prototype are translated into governing equations that are compiled into the mathematical model. A mathematical model, therefore, constitutes the first approximation to the problem. It is the prerequisite for a numerical model.

Next, a solution step is required to solve the mathematical model. The numerical model embodies the numerical techniques used to solve the set of governing equations that forms the mathematical model.

Another solution step involves the solution of the numerical model in a computer and provides the results of modeling. This step embodies further approximations and simplifications, such as those associated with unknown boundary conditions, imprecise bathymetry, unknown water and or sediment discharges, friction factors, etc.

Finally, the data needs to be interpreted and placed in the appropriate prototype context. This last step closes the modeling cycle and ultimately provides the answer to the problem that drives the modeling efforts.

4.3 Description of the model used in this study

Delft3D is a software developed by WL | Delft Hydraulics, which provides a multidisciplinary approach and numerical Modeling for coastal, river and estuarine areas. It simulates in two (either in the horizontal or a vertical plane) and three-dimensions the time and space variations of six phenomena and their interconnections: flows, sediment transports, waves, water quality, morphological developments and ecology; and it is capable of handling the interactions between those processes. To achieve this, Delft3D consists of several modules, grouped around a mutual interface, which are linked and capable to interact among them. However, the modules can also run independently of one-another. These modules which are used in this study are:

Hydrodynamics module (FLOW)

This module basically simulates non-steady flows in relatively shallow water. It incorporates the effects of tides, winds, air pressure, density (due to salinity and temperature) differences, waves, turbulence and drying and flooding of tidal flats. The output of the module is used in all the other modules of Delft3D.

Sediment transport module (SED)

This module simulates the transport, erosion and settling of cohesive and non-cohesive, organic or inorganic, suspended or bed sediments.

Morphodynamic module (MOR)

With the feedback of bottom changes to the hydrodynamic computation this module execute bottom changes due to sediment transport gradients and user defined, time dependent boundary conditions. Both wind and waves act as driving forces and a

number of transport formulae have been built in. An essential feature of this module is the dynamic feedback with the FLOW and WAVE modules, which allow the hydrodynamic flows and waves to adjust them to the local bathymetry and permits for forecasts on any time scale.

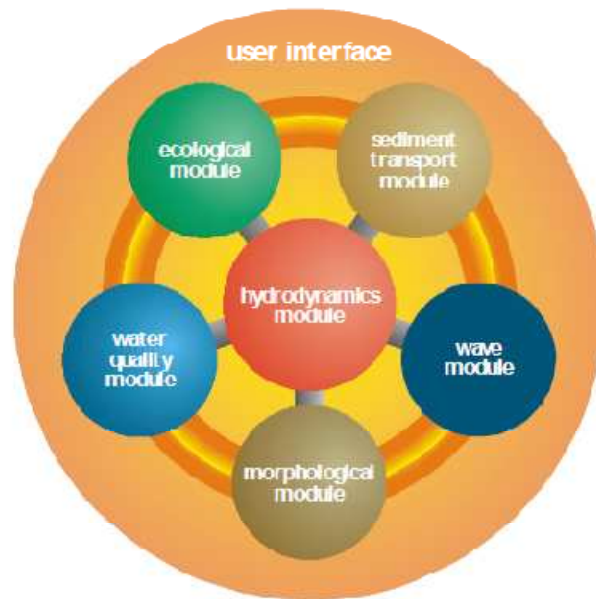


Figure 4.2: Interaction among the main Delft3D modules

Delft3D is integrated software, which implies that its aggregate performance is more comprehensive than that of the sum of its individual components. When simulating a water system, for instance, currents, morphology and water quality are accounted for by inter-related modules, allowing for continuous feedback between those phenomena, just as occurs in nature. A special Graphical User Interface (GUI) has been designed to allow the interaction between the user and the modules in a friendly manner preventing misinterpretations and/or lack of information. Also, the GUI is used for the data entry and management, visualization of model data and control of actual model runs, by a menu shell through which it is possible to access the various modules. Furthermore, there are a number of tools and utilities for pre and post-processing, from which the most used in this research are:

RGFGRID

RGFGRID is a graphical program for generation and manipulation of grids, allowing the generation of orthogonal, curvilinear grids of variable grid size for the computations. The variable grid sizes allow for a high resolution in the area of interest and a lower resolution far away at the model boundaries, thus saving computational effort. Furthermore, the grid lines may be curved to follow land boundaries and channels smoothly, avoiding the so-called stair-case boundaries that may induce artificial diffusion.

The grid-generator RGFGRID is designed so that grids can be created and modified with minimum effort, fulfilling the requirements of smoothness and orthogonality. Various grid manipulation options are provided in order to fine tune the grid. All operations are incorporated in a graphical interface, providing easy control of the grid generation process.

QUICKIN

QUICKIN is a graphical program for interpolation and modification of bathymetric data to the form accepted by the Delft3D modules. Often the depth samples (raw data) are originated from various sources, each of different date, quality and resolution. In order not to contaminate high quality samples with low quality samples, QUICKIN allows for subsequent loading of data sets.

The FLOW and WAVE modules use equations that in fact are averaged over the grid dimensions. Therefore, the best results are obtained if the model bathymetry approximates the real bathymetry in an averaged sense rather than in a local sense. Thus, if the sample resolution is higher than the grid resolution, an averaging method is required. On the other hand, if there are less sample points than grid points, a triangulation interpolation method is preferred. The various interpolation methods and step-by-step approach of generating an optimal model bathymetry are operated from a graphical user interface.

QUICKPLOT

QUICKPLOT is a post-processing program used to visualize the outcome of different simulation processes, with the possibility of a graphical and/or numerical representation of the results. QUICKPLOT allows uniform access to all types of data files produced by the Delft3D modules, to select and visualize computational results and measured data.

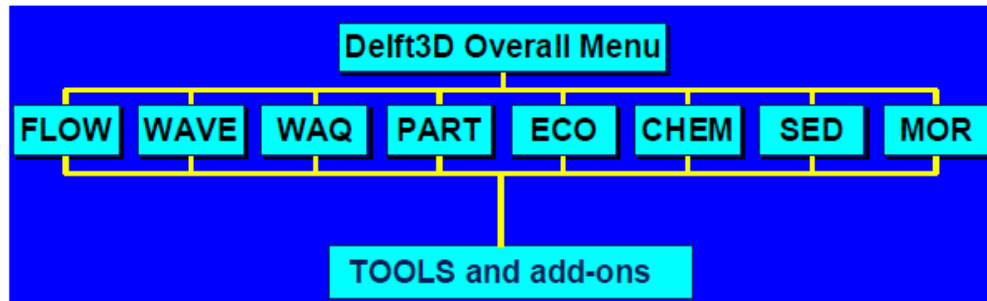


Figure 4.3: Structure of Delft3D

4.4 Modeling framework

For the objectives of this research, only the FLOW modules and MOR modules have been used. In fact, in this case the MOR module is not working as an independent unit, but as a morphology extension integrated to the FLOW module. Thus, the sediment transport option in FLOW allows the use of several of the existing functionalities in the MOR module has been used.

During the simulation, the FLOW module calculates non-steady flow and transport phenomena that result from tidal and meteorological forcing on a rectilinear or a curvilinear, boundary fitted grid (previously generated using RGFGRID). The hydrodynamic conditions (velocities, water elevations, density, salinity, vertical eddy viscosity and vertical eddy diffusivity) calculated in the FLOW module is used as input to the MOR modules.

The MOR module integrates the effects of waves, currents and sediment transport on morphological developments, which are used for the next simulation of the FLOW

modules. This is a cyclical routine that can be modeled as a hierarchical tree structure of processes, the process tree, in which time intervals for the elementary processes are defined. Processes may be executed a fixed number of times, for a given time span or until some condition is met. The link between the involved process modules (FLOW and MOR) occurs via a dynamic coupling. This allows a feedback between the processes which can affect water flow and sediment movement.

4.5 Space and time variation

Physical phenomena vary on space and time, therefore a dimensional description of the natural processes is required for an accurate representation of the reality. The numerical hydrodynamic modeling system FLOW solves the unsteady shallow water equations in two (depth-averaged) or in three dimensions. The system of equations consists of the horizontal equations of motion, the continuity equation, and the transport equations for conservative constituents.

In this case, to model the morphological conditions in Jamuna River, it has been decided to use a time dependent, two-dimensional approach, because the sediment transport, which is the process of interest for this study, can efficiently and accurately be modeled in 2D. Besides, 2D modeling requires less computational time, therefore allowing more test-runs for the calibration as well as for the representation of multiple scenarios.

Furthermore, the variation of time scales for the diverse natural processes (ranging from the order of hours or days in the hydrodynamic simulations, to the order of months and years in the morphological simulations) represents a difficulty for the integrated modeling of such processes. Long morphological simulations are achieved by using the morphological time scale factor that scales up the speed of the changes in the morphology to a rate that it begins to have a significant impact on the hydrodynamic flows. The implementation of the morphological time scale factor is achieved by simply multiplying the erosion and deposition fluxes from the bed to the flow and vice-versa by this scale factor, at each computational time-step. This allows

accelerated bed-level changes to be incorporated dynamically into the hydrodynamic flow calculations.

4.6 Model Set-Up

To set-up Delft3D, as for any numerical model, one of the most important factors is to analyze and prepare the input data, mainly physical conditions. This task demands reliable and enough data to obtain accurate results, and the process of transforming the available data to the input format required is time consuming. The various types of data and information needed to operate the model are entered through the user interface GUI, and are stored in several input files that can be modified manually by editing the files, or by means of the GUI.

Considering the information available, it has been decided to prepare three different basic set-ups for the Delft3D model, including:

- Set-up for April 2010: As initial set up to run the model
- Set-up of December 2010: For hydrodynamic calibration
- Set-up of September 2011: For hydrodynamic validation

Most complete available data (such as bathymetries) is for the year 2010, therefore the other basic set-ups are based on 2010 data when needed, as well as in some extrapolations of existing data. Moreover, Set-up 2010 includes all the information retrieve during the visit to Jamuna and is the source set-up for the Modeling of the final scenarios of this study. Based on these considerations, the set-up process is described in the following sections.

4.6.1 Land Boundaries

At the first step land boundaries are generated for the different set-ups. The land boundary represents the land-water marking, i.e. the boundary between land and water. Land boundaries are only useful visual indications, and have no influence in the computations of the model. (Figure 4.6.1)

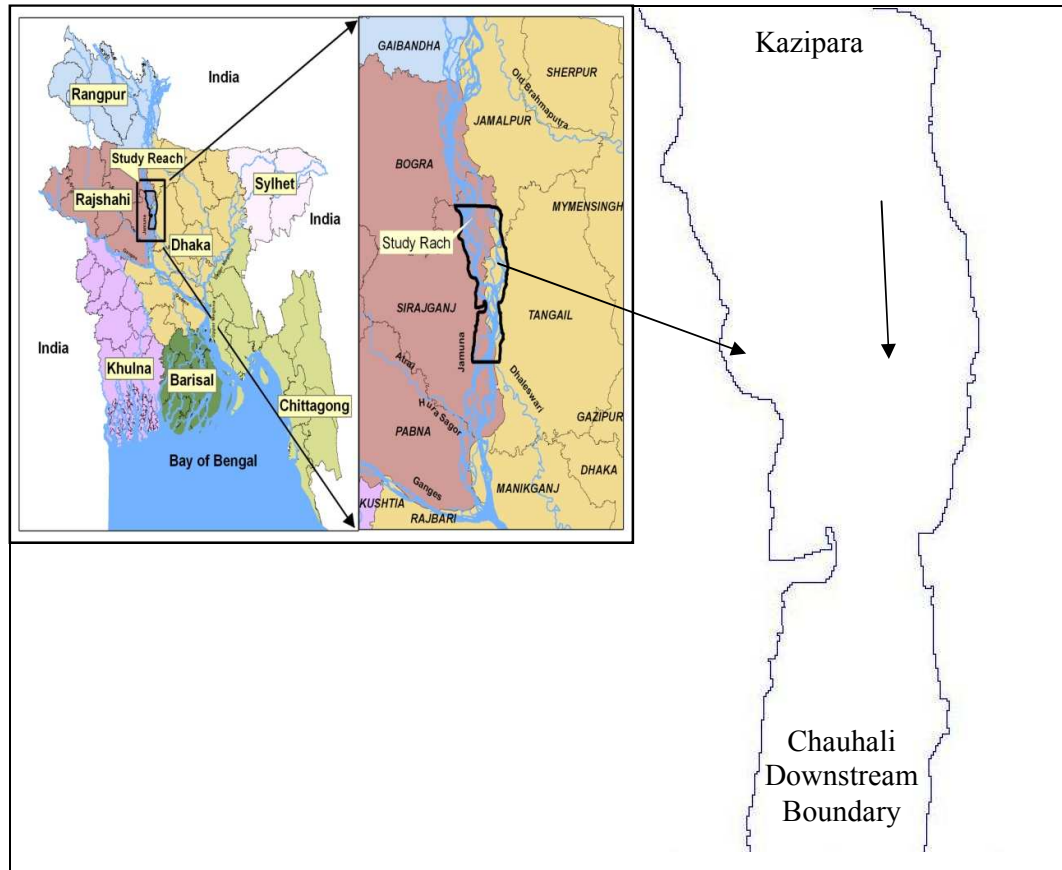


Figure 4.4: Land Boundary for selected reach of Jamuna River

4.6.2 Grid set up of the study reach

The grids were created that represent the area of study, and that provide the cells for the numerical computation. This process is done manually using the grid generator program RGFGRID, taking the land boundary as a reference to fit with the grid, and considering an area wide enough to avoid unreliable shadows and disturbed data in the grid open-boundaries, which can affect the area of study (Figure 4.6.2)

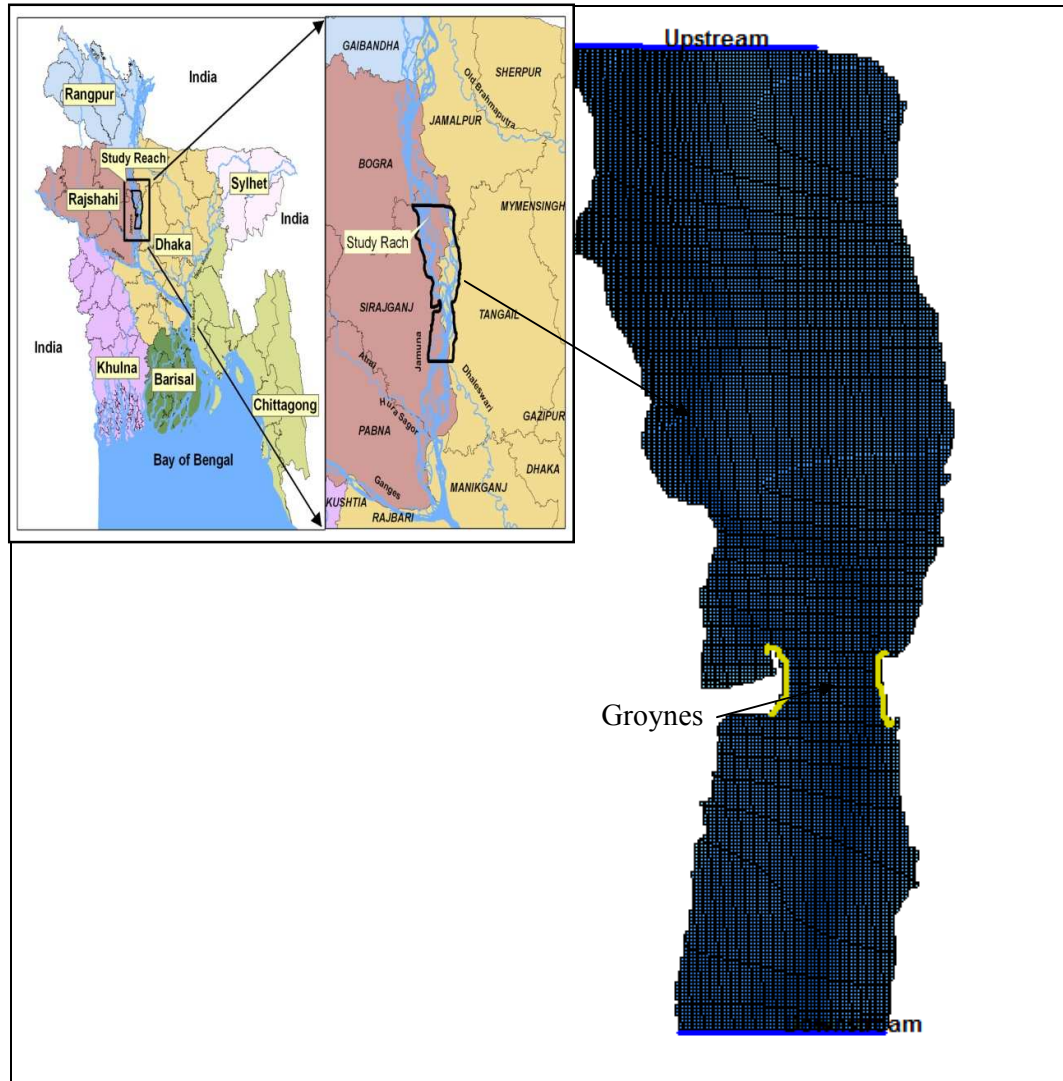


Figure 4.5: Flow grids for selected reach of Jamuna River

4.6.3 Refine Grid

An important task is to refine the grid in the areas of interest, such as the bridge location, hard points the eroded/accreted beaches and the surf zone (main area for long shore sediment transport), where it is essential to have more resolution and a finer computation. In (Figure 4.6.3), the refinement of the grid has been done near to the Sirajgonj and Bhuapur Hard points and also near the bridge location.

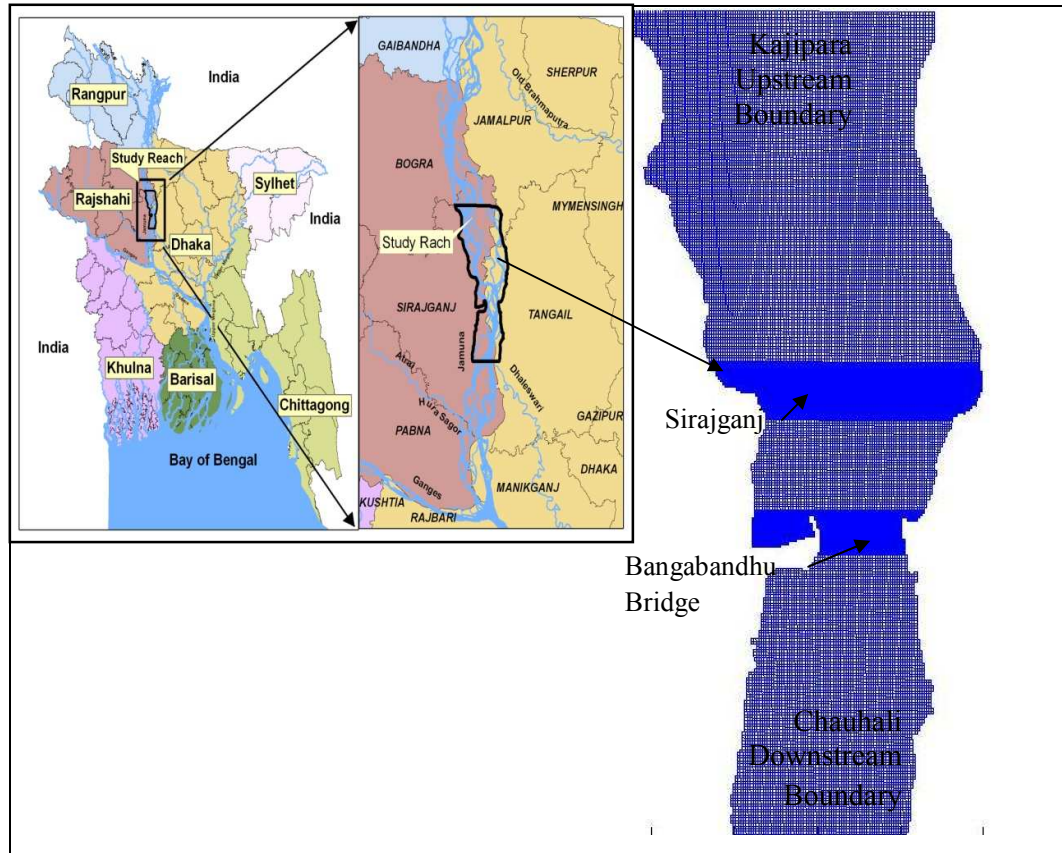


Figure 4.6: Grids Refinement for selected reach of Jamuna River

4.6.4 Orthogonalise Grid

Next the grid has been orthogonalised (cells as rectangular as possible) in order to fulfill the Delft3D computational requirement of orthogonality for the well functioning of the model. This has shown in (Figure 4.6.4), of the cosine values of grid corners. The cosine values should be close to zero. The error in the computed direction of the pressure term in Delft3D-FLOW is proportional to these values. In offshore areas the orthogonality should be less than 0.02. Near closed boundaries, higher values are sometimes acceptable. (Delft-RGFGRID - User Manual). In the study reach, it can be seen that the value in the inner model has been kept in range of 0 to 0.03, which is an acceptable limit for well functioning of the model.

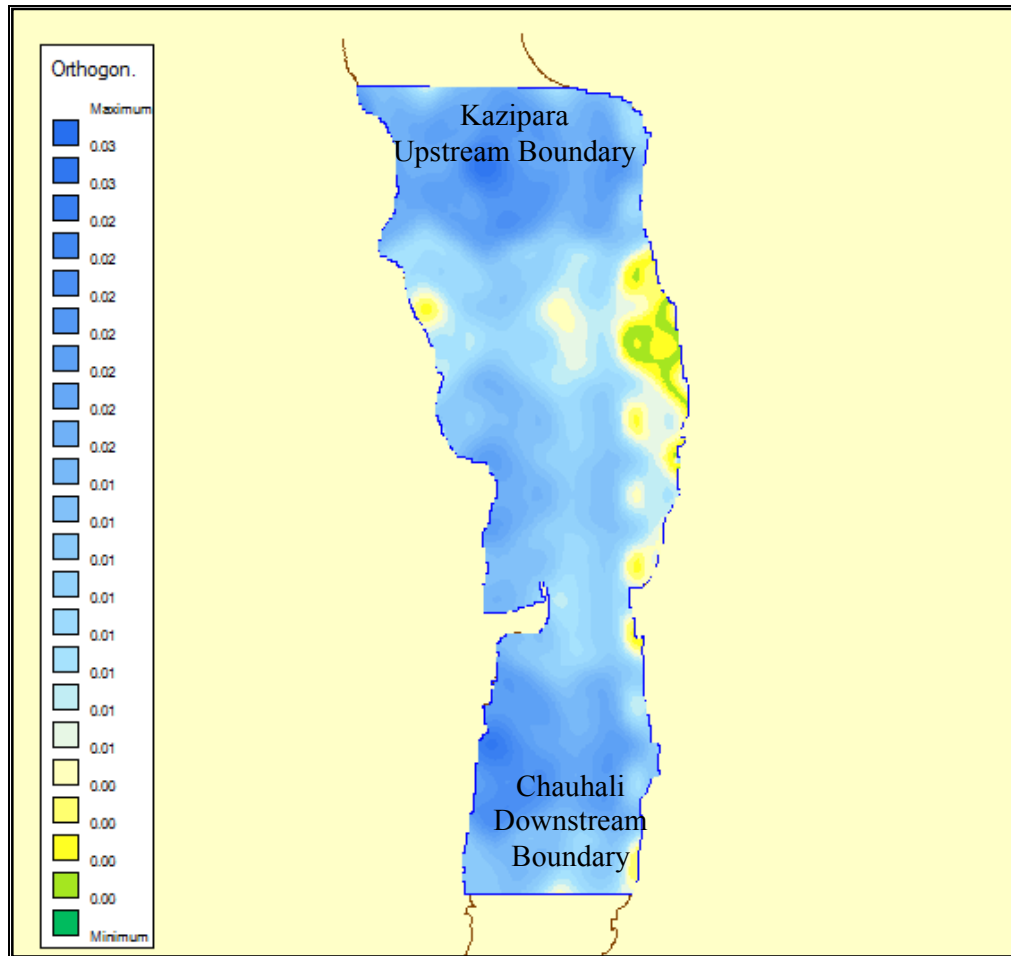


Figure 4.7: Orthogonality of grids for selected reach of Jamuna River

4.6.5 Grid Smoothness (Aspect Ratio)

The quality of a grid is to a large extent determined by its orthogonality and the rate with which certain properties change over the area to be modeled (smoothness). A measure for the grid smoothness is the aspect ratio of grid cells (ratio of the grid cell dimension in M- and N-direction) and the ratio of neighboring grid cell dimensions. Ratio of M-size/N-size, value ≥ 1 . Must be in the range [1,2] unless the flow is predominantly along one of the grid lines. In the modeled reach in (Figure 4.6.5), the value varied in the range [1 to 1.66], which is in the acceptance range of DELFT model.

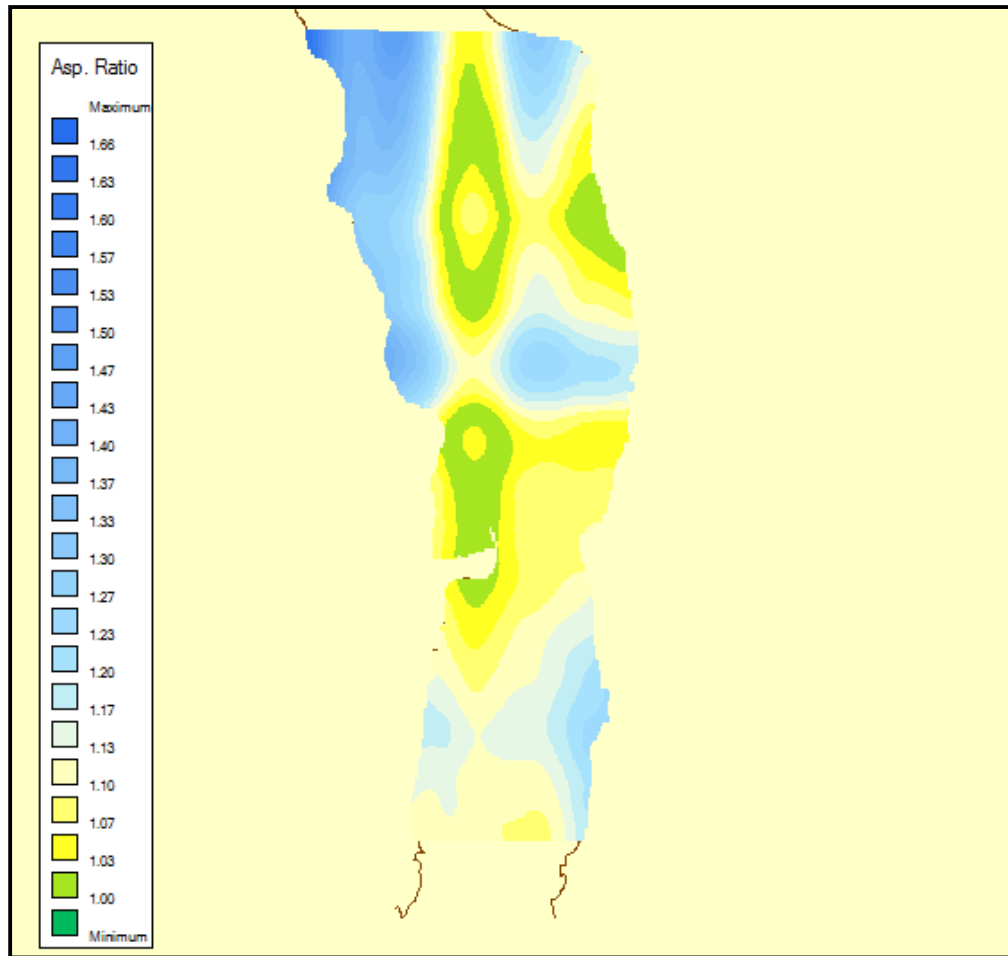


Figure 4.8: Aspect ratio of grids for selected reach of Jamuna River

4.6.6 Bathymetry Development

The developed bathymetry of the study area is shown in (Figure 4.6.5). Grid can be generated using the observed bathymetric points. But grid generated in this way would not give better quality model. Hence, the study area has been developed with good quality grids and then surveyed bathymetric data are interpolated into those mesh nodes. Normally triangular interpolation has been used but other methods are also available under Delft-Quickin program. Before the interpolation process to select the active interpolation area, a polygon has been generated. From the toolbar the edit option has been clicked then selected the polygon. Furthermore, the bathymetry has been smoothed by operating the depth smoothing option.

IWM lean period bathymetry data surveyed during April 2010 has been used to set-up the initial bathymetry of the model. The distribution of measured and interpolated bathymetries is shown in (Figure 4.6.5) and (Figure 4.6.6).

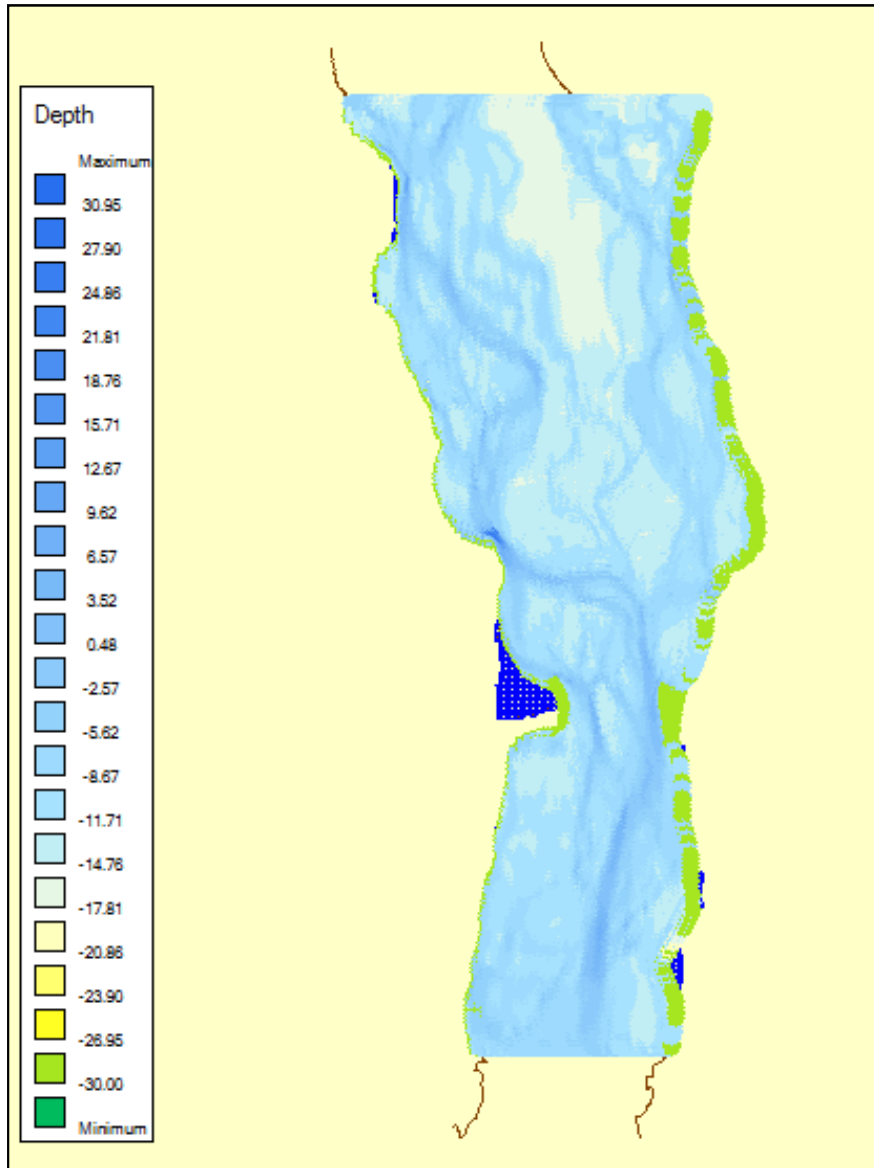


Figure 4.9: Measured Bathymetry used in the model

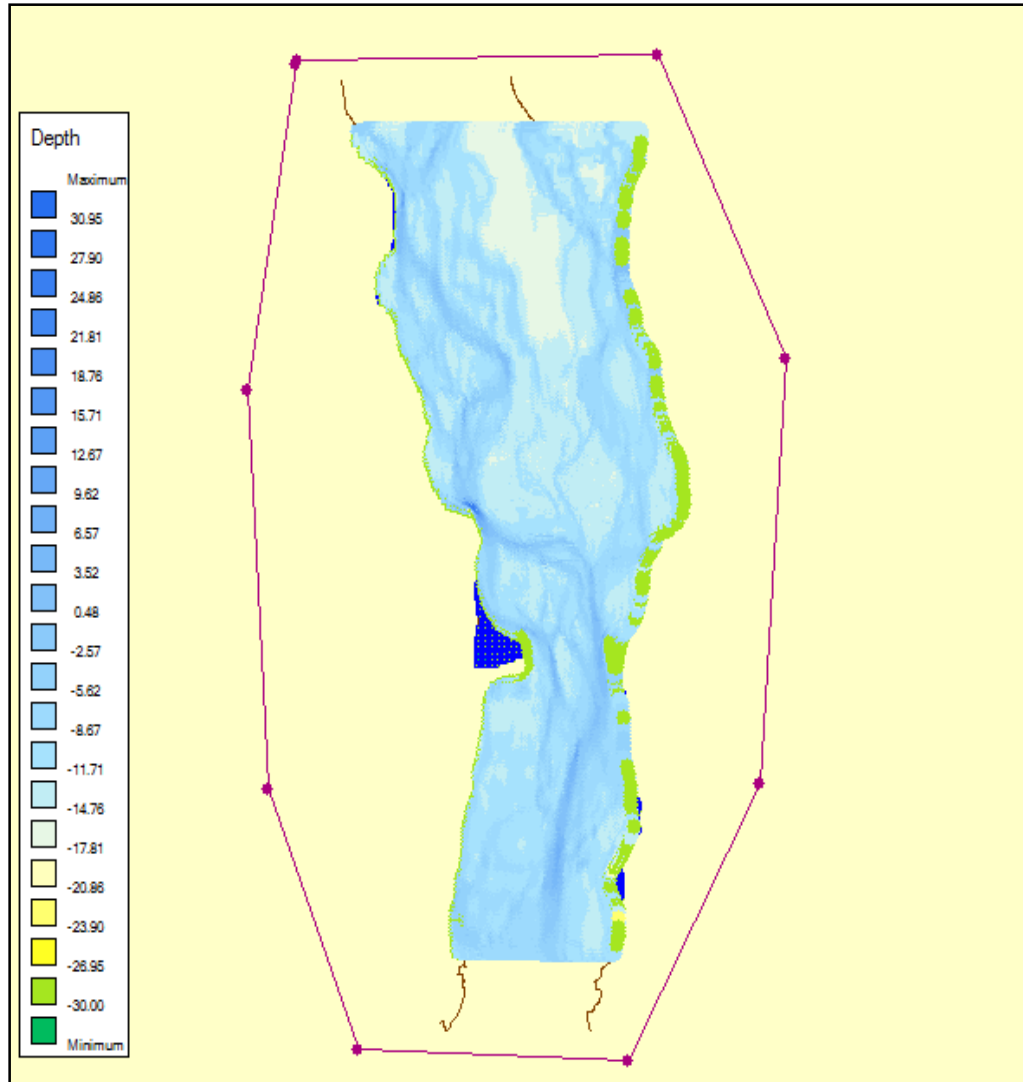


Figure 4.10: Interpolated Bathymetry used in the model

4.7 Flow Module Set-Up

Setting-up the FLOW model has been done through the user interface GUI of the FLOW module. In the first stage a description of the project and the selection of the grid file and the depth file (bathymetry) have been done. The location of the project (latitude and orientation) is also a requested data in order to consider the influence of the Coriolis force (for Jamuna: 24.39996 dec. deg N, 0 dec. deg W). Afterwards the following aspects have been taken into account.

4.7.1 Dry Points and Thin Dams

To represent structures that interfere and influence the hydrodynamic computations, FLOW comprises the concept of dry points and thin dams. The main difference between them is that dry points are grid cells that are permanently dry during a computation irrespective of the local water depth, whereas thin dams are infinitely thin objects that prohibit flow exchange between two adjacent computational cells without reducing the total wet surface and the volume of the model. The purpose of a thin dam is to represent small obstacles (e.g. breakwaters, dams) in the model, which have sub-grid dimensions, but large enough to influence the local flow pattern. In the present study groynes has been provided and constricted the area near the Bangabandhu Bridge. The model grid in the groins area has been refined previously in the Delft3D QUICKIN module to get better resolution. The disadvantage is that, every time the grid is modified, many other input files must be modified as well, such as depth files, observation points and cross sections. This is a weakness of Delft3D model, because requires a lot of efforts and is time consuming.

4.7.2 Time Frame

For the simulations with FLOW, the hydrodynamic simulation time has been set to 122 days with a time step of 1 minute. The time step is important because for explicit Modelling schemes such as Delft3D (where the unknown value of the dependent variable at one time level is expressed as an explicit function of the known values of the dependent variable at earlier time levels), the accuracy and numerical stability of the model depends on the Courant Number defined as:

$$Cr = c \frac{\Delta t}{\Delta x} \quad \dots \dots \dots (4.7.2)$$

Where,

c = celerity

Δt = simulation time step

Δx = grid size variation

In general, Delft3D model is stable for Courant Numbers of 20 or lower; nevertheless the model can work for higher Cr when, under the criteria of the researcher, results are accurate and the calibration and validation process is acceptable.

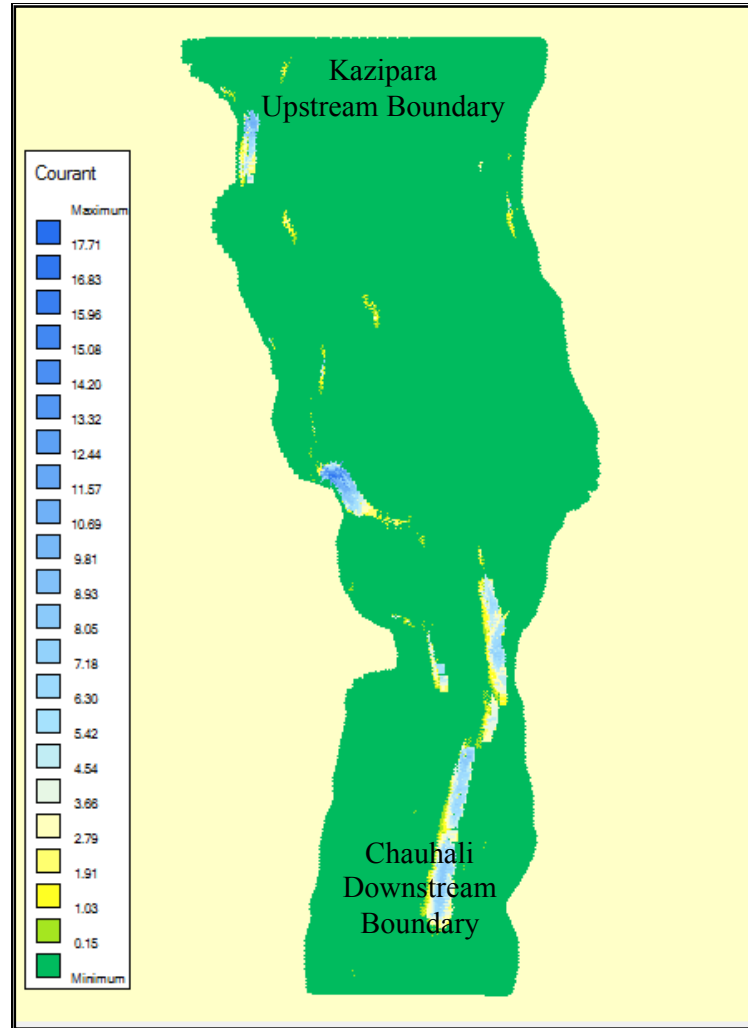


Figure 4.11: Courant Number variation as function of the grid size

4.7.3 Boundary Set Up

Boundaries are important as they define the input conditions to the Modelling process within the grid. For the FLOW grid, four boundaries have been defined. It consists of two open boundaries (Upstream and Downstream boundaries) and two

closed boundaries showing the bank lines. Normally total discharge is assigned at the upstream inflow boundary and water level at downstream boundary. The model of the Jamuna River had a total discharge boundary at the upstream Kazipura and a water level boundary at downstream at Chauhali.

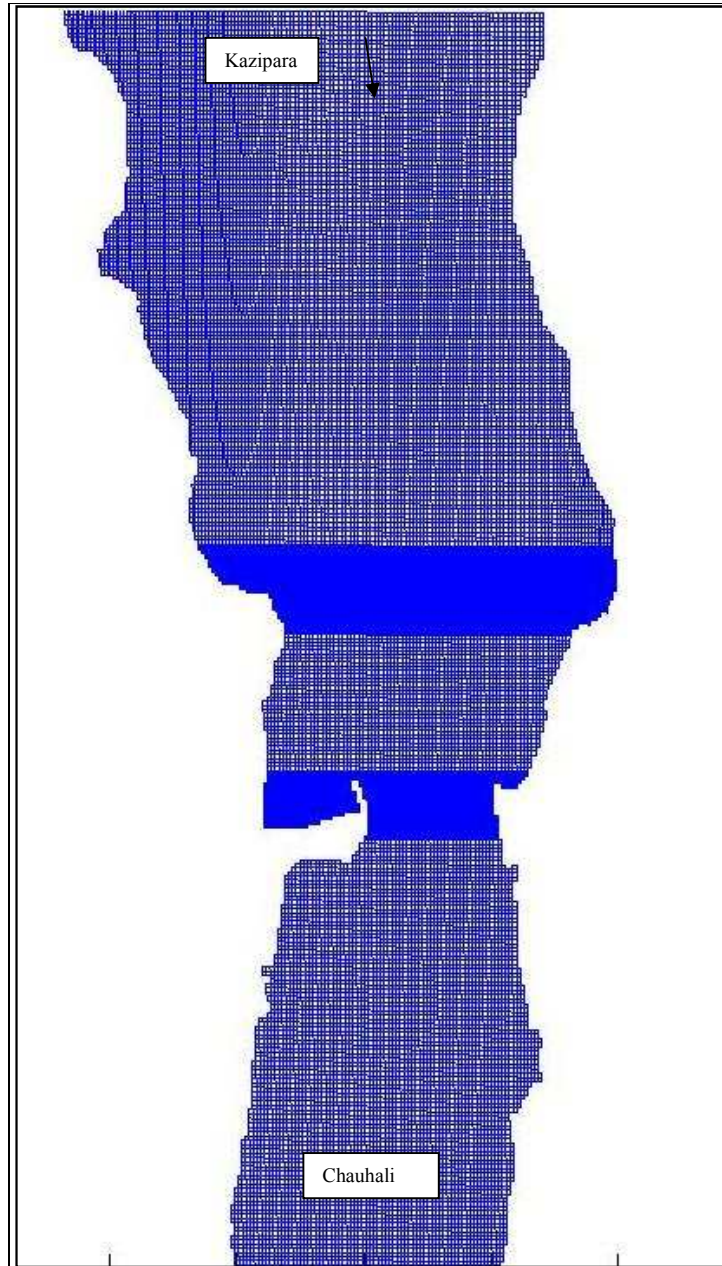


Figure 4.12: Flow Boundaries

In Delft3D, boundary conditions can be assigned to every node or in line of that boundary. The rating curve at Bahadurabad has been used to generate boundaries at upstream northern end. Interpolated water level from Shirajganj has been applied to downstream boundary. All the boundaries are applied for two distinct periods – for the month of April 2010 to June 2010 during calibration and for four distinct periods for the months of April 2011 to August 2011 during validation. The discharge and water level hydrographs of these periods as shown in Figure 4.7.3 and Figure 4.7.4 have been taken to apply into the model as boundary conditions and subsequent calibration and validation purposes.

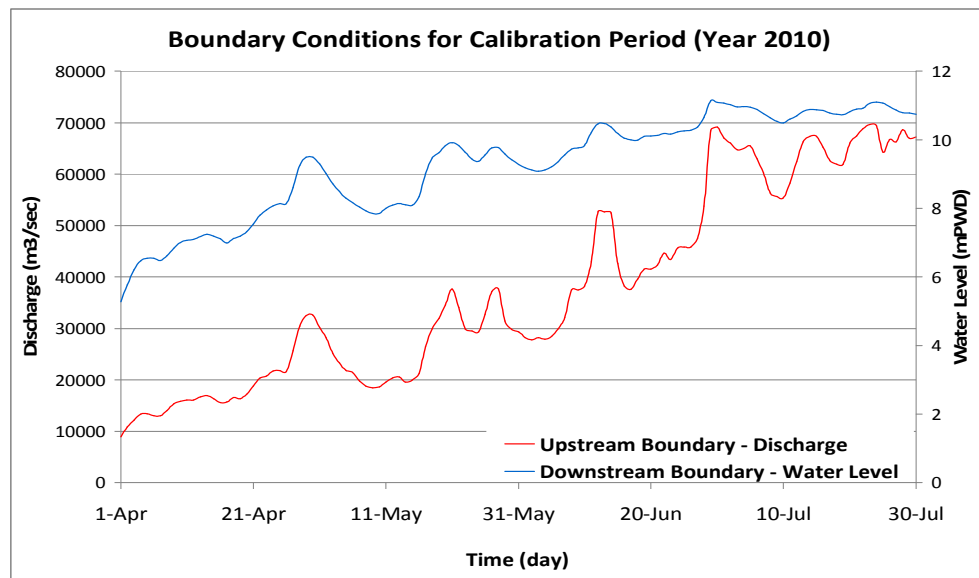


Figure 4.13: Time series hydrographs from April to July 2010 used in the model as Boundary Conditions for Calibration Period

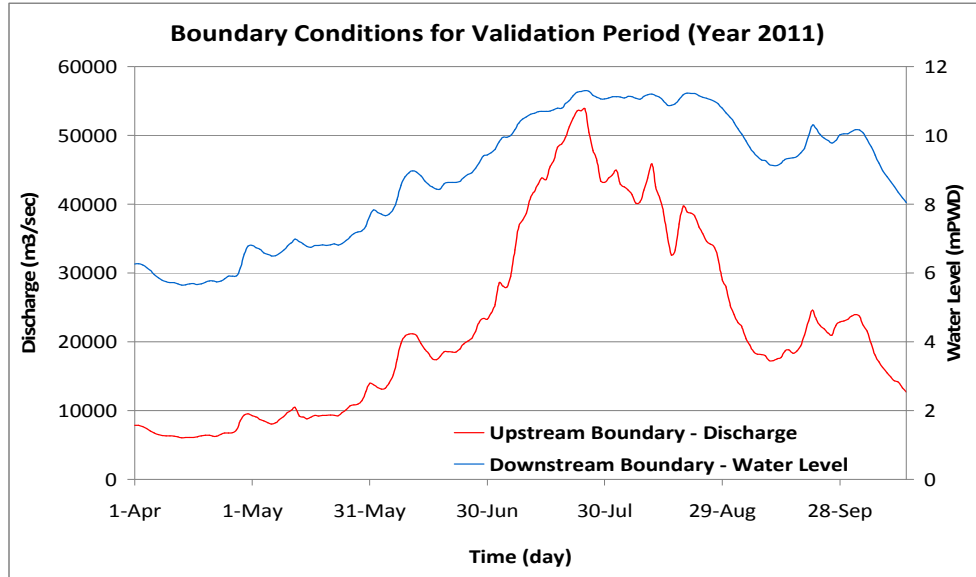


Figure 4.14: Time series hydrographs from April to October 2011 used in the model as Boundary Conditions for Validation Period

In the year 2010 the water level rises abruptly during April to July as well as the discharge also increased abruptly. Again in 2011 it can be observed from the hydrograph that the water level raised abruptly during April to June, fluctuated slightly during the next three months then slightly falls from the end of August almost to the mid of September then again slightly raises in the end of September. In case of discharge similarly abruptly discharge raised from April to July then slightly fluctuated downward for the next three months, and falls rapidly during the end of August to September. Several discharge peaks can often be observed due to the dependence on rainfall and the distribution of the tributaries along the river in Assam and Tibet.

4.7.4 Initial Conditions

Initial conditions, which state the hydrodynamic condition at the start of simulation, need to be defined for all models. Usually the time series boundary conditions at specified upstream and downstream ends are available from various sources. Other than these, discharge or water level data at all the other points at model are not

available. So, for defining the initial conditions at all the points at the model, it becomes essential to run a steady hydrodynamic model with a specified discharge and water level in defined upstream and downstream ends. The first steady run is a cold-start, used when initial water levels for nodes other than the downstream boundary are unknown. In cold start, initial downstream water surface elevation must be provided in such a manner that all the mesh nodes of the model remain submerged, otherwise the steady solution may diverge. For simplicity, the initial water level for the whole domain was assumed same as the downstream water level boundary condition, and accordingly velocity is assumed to be zero at all nodes. Downstream water surface elevation is decreased gradually towards desired water level boundary condition.

For the present study, as it has been intended to start simulation from 1st April 2010, the water level has been found 5.27 m is chosen as our desired downstream boundary. As such, 8944 m³/s inflow boundary discharge has been found respectively for the corresponding downstream 5.27 mPWD water level. Once the cold start solution is obtained, it is used as hot-start for other steady or unsteady models.

4.7.5 Parameters in Hydrodynamic Flow Module

Various inputs and parameters contribute in adjusting the solution technique of the hydrodynamic module of Delft3D. These are Eddy viscosity, bed resistance or roughness parameter etc.

Table: 4.1 Hydraulic Parameters used in model

Parameters	Values considered in the model
Roughness parameter (Manning's, n)	0.014 for char and 0.025 for channel
Horizontal Eddy Viscosity	1
Vertical Eddy Viscosity	1

The turbulence parameter coefficient of eddy viscosity is used for the distribution of flow by exchanging lateral momentum of flow. In Delft3D, the eddy viscosity has been specified 1 on the basis of several studies. (IWM, 2011)

Roughness parameter such as Manning's 'n' is an important parameter in hydrodynamic module since it provides some control over the fluid velocity magnitude and direction.

The Manning's 'n' is mainly a calibration parameter in the hydrodynamic module and was taken in the range of .014 to .025 m^{1/2}/s based on various conditions of the domain. Depth varying roughness has been used with the lower value of 0.025 where the bathymetry depth is more than or equal to 6 mPWD and .014 where the depth is below 6 mPWD (Mike 21C manual).

The morphological module is used to capture various morphological changes of the river. This module simulates various features based on the results obtained during hydrodynamic calculations. Various inputs and parameters associated with this module are sediment transport predictors, alluvial resistance, grain size of soil etc. Van Rijn formula was applied for Sediment transport prediction in this study. The grain size of Jamuna River was taken 200 µm, reference density for hindered settling 1600 kg/m³, Specific density 2650 kg/m³, Dry bed density 1600 kg/m³, also the initial bed layer thickness is taken uniform 5 m along the domain (IWM, 2011).

4.7.6. Morphological Updating

The elevation of the bed is dynamically updated at each computational time-step. At each time-step, the change in the mass of bed material that has occurred as a result of the sediment sink and source terms and transport gradients is calculated. This change in mass is then translated into a bed level change based on the dry bed densities of the various sediment fractions. Both the bed levels at the cell centers and cell interfaces are updated. A number of additional features have been included in the morphological updating routine in order to increase the flexibility.

4.7.7 Morphological “Switch”

To specify to update the calculated depths to the bed MorUpd (or equivalently BedUpd) flag in the morphology input file has been set. The use of MorUpd or BedUpd only affects the updating of the depth values (at ζ and velocity points); the amount of sediment available in the bed will still be updated.

Morphological data is quite important because it is the link between FLOW and MOR modules. In fact, the MOR module is indirectly defined within the FLOW input and therefore it is not necessary to go through an independent MOR set-up process. Under the morphological data, the morphological scale factor is defined; in this case the factor has been set to 8.25 for all the simulations which means that for a hydrodynamic simulation time of 121 days the morphological time is approximately equal to 1000 days (Approximately 33 months)

Under the numerical parameters, an important input is the smoothing time which is the time that the model takes to stabilize the processes after the initial conditions of the simulation. During this initial interval, the output of the model is inaccurate and does not reflect the reality, this is why a smoothing time is necessary. In this case it has been set to 60 minutes.

4.7.8 Monitoring Option

To monitor the evolution of the Modeling process it is possible to define observation points and cross sections in which Delft3D will calculate and store the different output variables. All the observation points and cross sections will be linked to an output file and the results can be graphically displayed using QUICKPLOT. (Figure 4.7.5)

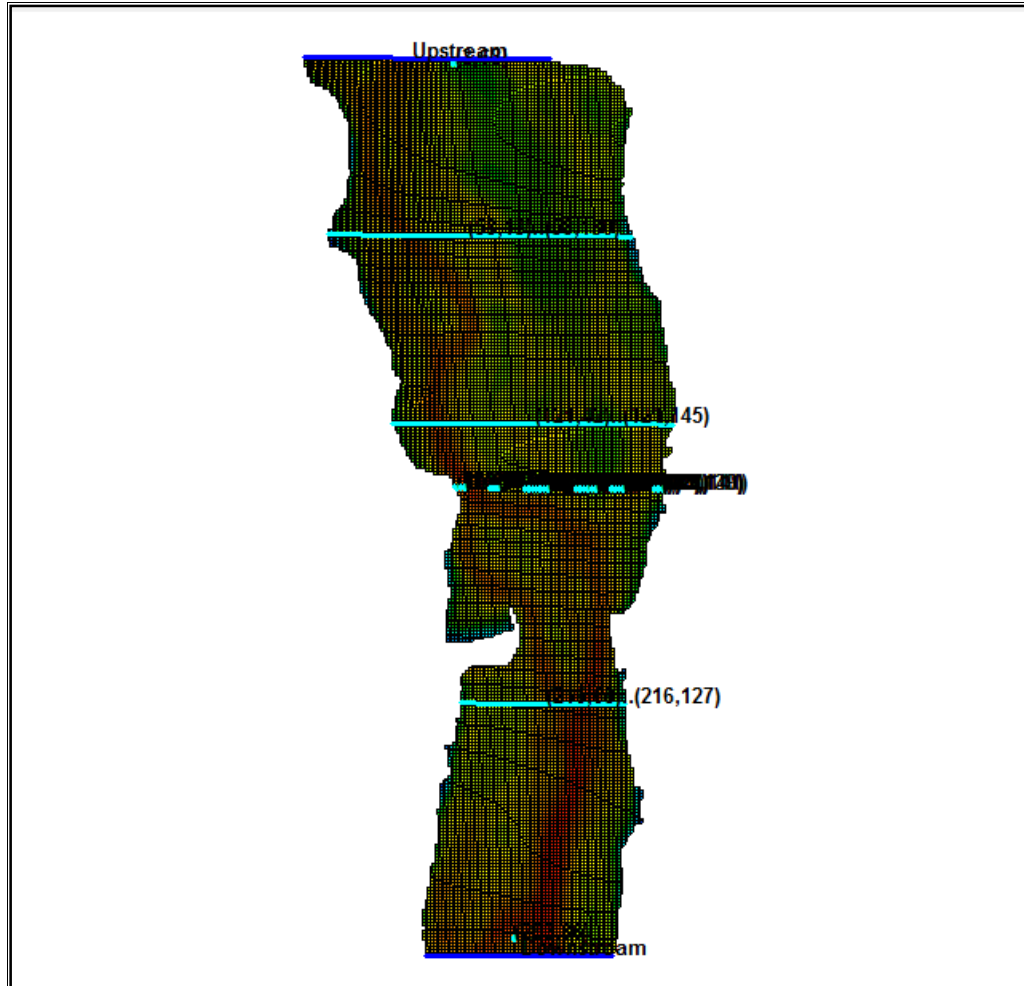


Figure 4.15: Observation points and cross sections

Observation points are used to monitor the time-dependent behavior of one or all computed quantities as a function of time at a specific location, e.g. water elevations, velocities, fluxes, and concentration of the constituents among others. Observation points represent an Eulerian viewpoint at the results. Observation points are located at cell centers, i.e. at water level points. In the present study several observation points has been selected near the Sirajgonj station for observing the value of the simulated water level.

Cross-sections are used to store the sum of computed fluxes (hydrodynamic), flux rates (hydrodynamic), fluxes of matter (if existing) and transport rates of matter (if

existing) sequentially in time at a prescribed interval. A cross-section is defined along a constant grid line and it must include at least two adjacent grid points. In the present study 5 cross-sections has been selected. The location of each cross section has been measured form upstream boundary.

4.8 Summary

Delft3D is a powerful tool for the understanding and forecasting of riverine and coastal morphodynamic behavior, because it takes into account the most relevant factors involved in this process (as input parameters) and gives a broad range of results (as output parameters) presented in an accessible manner, using graphs with the possibility to convert the results into text files. This allows the user to analyse oceanographic variables such as waves, hydrodynamic variables such as flows, morphologic variables such as sediment transport, and man-made variables such as dredging and dumping volumes. (Delft3D-FLOW_User_Manual).

RESULTS AND DISCUSSIONS

CHAPTER 5

5.1 General

This chapter presents the results of the hydrodynamic and morphological analysis of the particular reach of Jamuna River, selected as study area by means of Delft3D modeling. The simulation results of the mathematical modeling of this study area have been analyzed and also compared with the field measurements, which have assisted to acquire experience and knowledge regarding the changing nature of the Jamuna River.

The aim of this present study is to observe the morphological changes of the selected reach of the braided river Jamuna by using the Delft3D software and also to compare the results obtained from the simulation with the field observations. The simulated bed level changes compared with the field measurements, movement of bank line and channel shifting at vulnerable locations as well as the aggradations and degradation near chars and channels are some of the morphological events analyzed in this chapter.

Erosion or deposition at any nodes points to the bed level lowering or rising, respectively. However, it cannot automatically shift the bank-line when a bank node gets erosion/deposition for itself. So any lowering of nodes at the bank, indicate the bank at that location is vulnerable, which is supposed to produce bank erosion and subsequent bank-line shifting. In this model vulnerable banks are identified by taking several cross-sections at different locations of the model, where the bank nodes have undergone lowering of its bed elevations.

5.2 Model Calibration

5.2.1 Necessity of Model Calibration

Model calibration is the most important step in the overall model development. It is an iterative adjustment of the model parameters so that simulated and observed responses of the system match within the desired level of accuracy. In reality, all models require some degree of calibration to fine tune the predictive ability of the model. Without calibration it is not possible that any activities would produce satisfactory solutions for real world situations. In a hydrodynamic model, errors may occur in from four potential sources (Abramowitz and Stengun, 2003):

- (i) Random or systematic error in input data,
- (ii) Error due to incorrect parameter values and
- (iii) Error due to incomplete or incorrect model formulation.

Errors from source (iii) are minimized, during the calibration process whereas the mismatch between the simulated and observed outputs is due to all the four sources. Errors related to (i) and (ii) determine the minimum level of disagreement between the observed and simulated outputs. Hence, the objective of model calibration is to minimize the errors from source (iii) until they become insignificant compared to the errors from sources (i) and (ii). As far the fourth source is concerned, effort has to be made to determine that the state equation, initial condition and boundary condition have been specified correctly.

Usually parameters values are adjusted through ‘trial and error’ by running the model repeatedly. Sound understanding of physical process of the phenomenon and experience with similar real world systems can be of great help in determining the correct parameters values. For a large number of parameters, it is not realistic to try and adjust all the parameters one by one or in combination. A more sensible approach is to attempt a coarser simulation using only a few parameters whose values are least well known or to which the model shows maximum sensitivity (Abramowitz and Stengun, 2003).

5.2.2 Calibration Data

There are a number of uncertainties that exists related to input as model geometry, boundary conditions, roughness, eddy viscosity etc, which can have momentous impact on the model solutions. Once geometry and boundary conditions have been obtained with reasonable accuracy from the field, it is common practice to set them out of preview of the calibration process.



Figure 5.1: Comparison of simulated and measured water levels of Jamuna River for calibration at Sirajganj

Roughness and eddy viscosity are the parameters that have been used to play to obtain an adequate match with the observed field conditions in the present study. Manning's roughness coefficient has been adjusted after several trial of the model during calibration to $n = 0.014$, when water depth is lower than 6 m and $n = 0.025$, when water depth is higher than 6 m (Mike 21C manual). The value of eddy viscosity has been considered as 1.0 (IWM, 2011). Calibration of the model has been done using the set up of April 2010. For hydrodynamic calibration, computed water surface elevations have been compared with the observed water surface elevations at

Sirajganj station for the period of April to July, 2010. Calibration results showed that the computed values are within ± 0.6 m (Figure 5.1).

5.3 Model Verification

5.3.1 Necessity of Model Verification

Most real world models contain a large number of parameters; it is not always possible to produce a combination of parameters values which replicate the recorded data satisfactorily. However, this does not ensure an adequate model formulation or optimal parameter values. The calibration may have been achieved entirely by numerical curve fitting without considering whether the parameter values so obtained are physically reasonable. Moreover, it might be possible to achieve multiple calibrations or apparently equally satisfactory calibrations based on different combination of parameter values. It is therefore important to find out if a particular calibration is satisfactory or which of the several calibrations is the best one by testing (verifying) the model with a different set of data not used during calibration (Halim and Faisal, 1995).

According to Klemes (1986), a simulation model should be tested to show how well it can perform the task for which it is intended. Performance characteristics derived from the calibration data set are insufficient as evidence of satisfactory model operation. Thus the verified or validated data must not be the same as those used for calibration but must represent a situation similar to that to which the model will be applied operationally.

5.3.2 Verification Data

Once the model has been calibrated, the next step is to validate the model by comparing the outputs to historical data from the study area. Validation is a multi-step process of model adjustments and comparisons, leavened with careful consideration of both the model and the data. The computed water surface elevations by the model were validated with observed water surface elevations at Sirajganj station for the period of April to August, 2011.

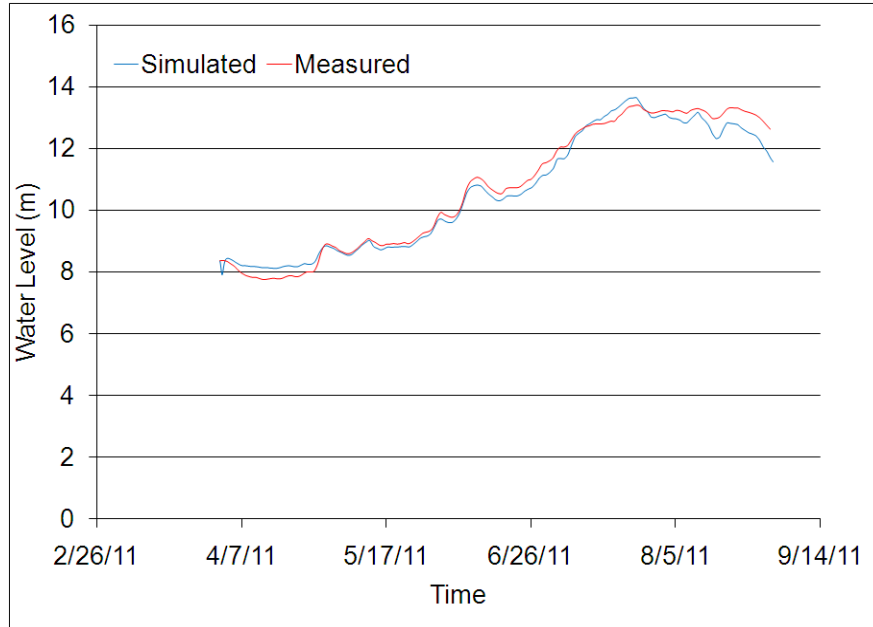


Figure 5.2: Comparison of simulated and measured water levels of Jamuna for validation at Sirajganj

During the calibration and validation process, the model has showed good agreement with the observed data for the monsoon periods. For the lack of data during dry season it has been not possible to calibrate and validate for dry seasons.

5.4 Simulation of the model

In this section Delft3D Flow module has been used for hydrodynamic and sediment transport modeling. From the previous article we can see that the results have shown satisfactory agreement during calibration and validation process. Hence the model was considered to be ready for simulation and various analyses. At the beginning the model had been run for the base period of year 2010. Initial bathymetry of April 2010 has been taken as base for simulation as shown in Figure 5.3. In this figure the x-coordinate indicates the easting values and the y-coordinate indicates the northing value of the selected sections of the study reach. Then to verify the result of the observed and simulated bathymetry several cross sections are compared. The observed and simulated bed levels at different cross-sections in December 2010 have

been compared. The result showed a very good agreement. The model was then simulated for predicting the hydraulic and morphologic responses of the river in the years of 2011 and 2012.

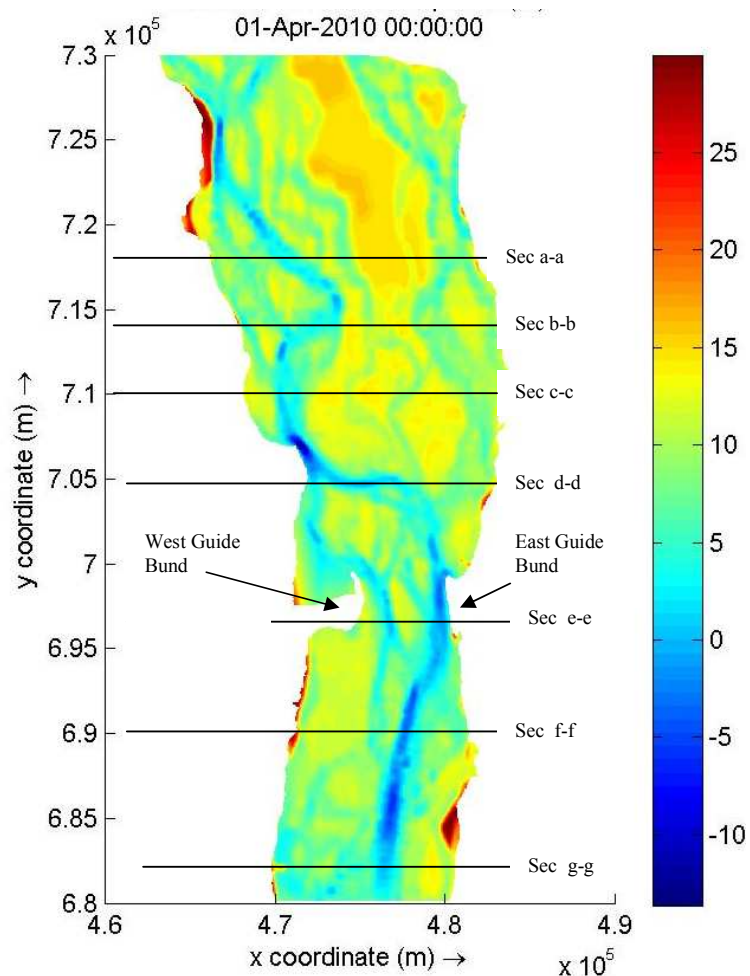


Figure 5.3: Cross Sections shown in Bathymetry of selected reach of the Jamuna River for comparison

5.4.1 Comparison of observed and simulated bed elevations

Sediment model simulated bathymetry of December 2010 is compared with the observed bathymetry in December 2010. Comparisons at different cross-sections are presented as the distance along cross-section versus bed elevations in mPWD

(Figure 5.4 to 5.10). From the results it is found that simulated bed elevations adequately matched with the measured bed elevations.

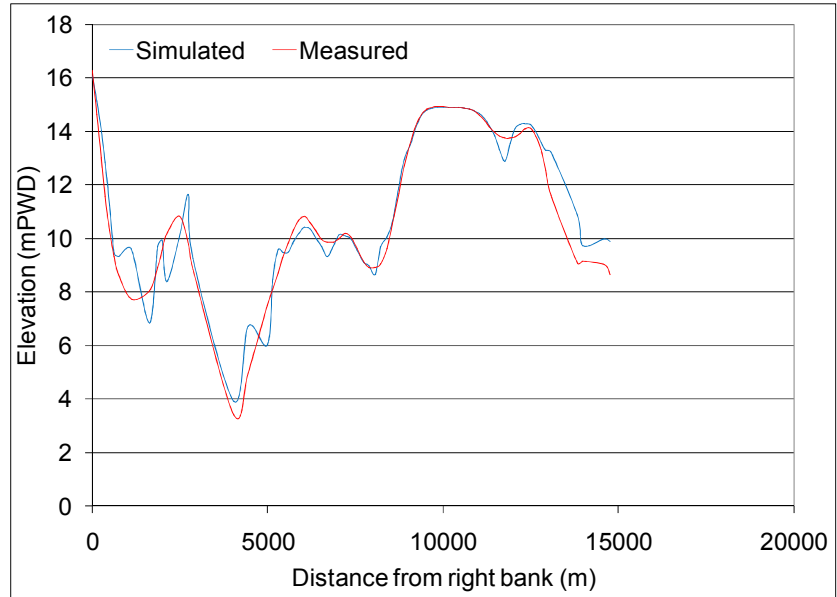


Figure 5.4: Comparison of Cross-Section at (Sec a-a)

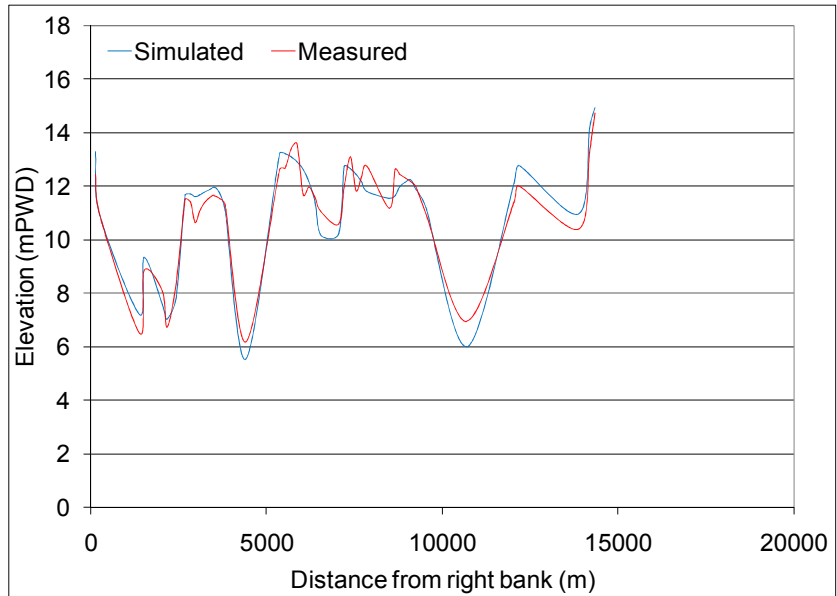


Figure 5.5: Comparison of Cross-Section at (Sec b-b)

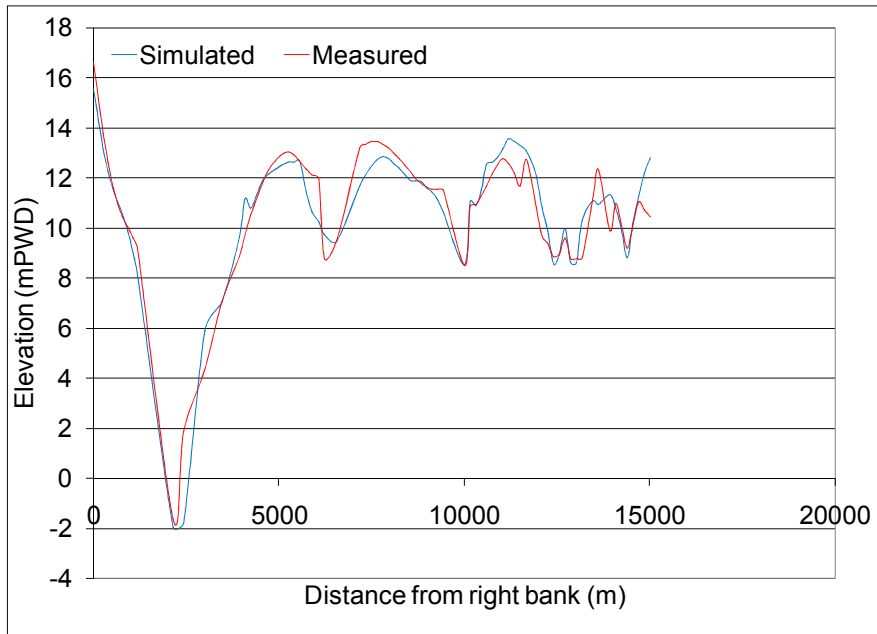


Figure 5.6: Comparison of Cross-Section at (Sec c-c)

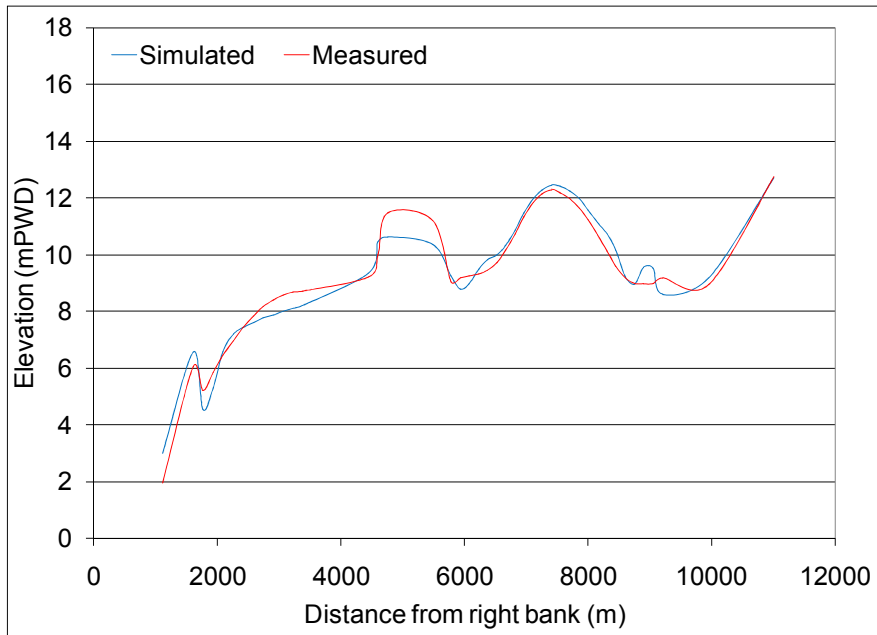


Figure 5.7: Comparison of Cross-Section at (Sec d-d)

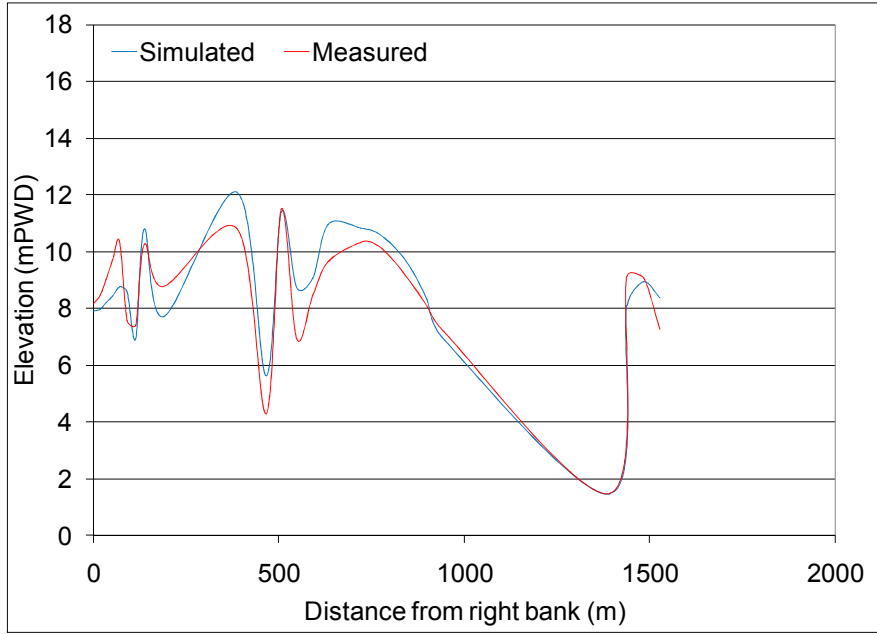


Figure 5.8: Comparison of Cross-Section at (Sec e-e)

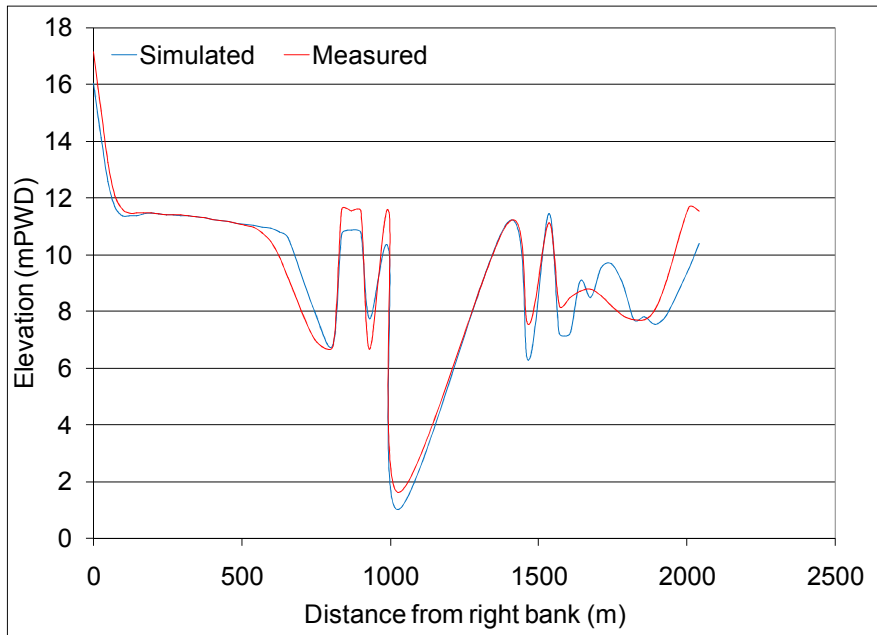


Figure 5.9: Comparison of Cross-Section at (Sec f-f)

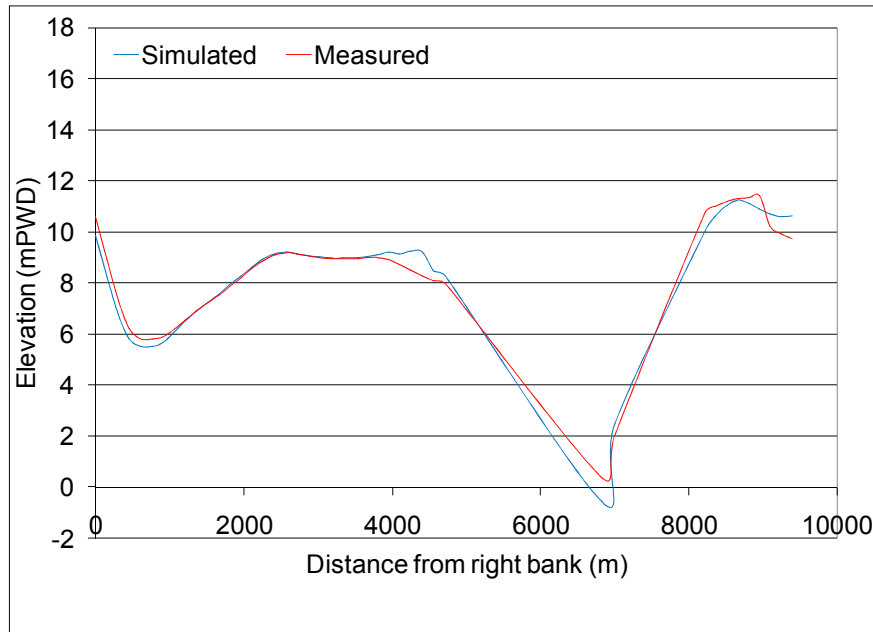


Figure 5.10: Comparison of Cross-Section at (Sec g-g)

5.4.2 Variation in Velocity and Sediment Transport

The series of figures below show the depth average velocity and the consequent total transport of sediment of the study reach of the river Jamuna in both dry and wet seasons. It can be visualized from the figures that during monsoon 2011 and 2012, there is a higher velocity of flow in the main channels of the selected reach compared to the dry period of 2011 and 2012. A light and deep blue area of (Figure 5.11 to 5.20) indicates relatively the lower erosion areas, while yellow and red colors indicate higher erosion areas. The velocity seems to be high mainly near Sirajganj Hard Point, Bangabandhu Bridge area (near East and West Guide Band), Bahadurabad Hard point, Shubaghacha during both the monsoon and dry season. These are the zones seem to get eroded. It is evident from the figures that the zones with higher velocity carry more sediment than the other zones. From (Figure 5.11 to 5.20), it also can be noticed that the flow velocity increased in the successive years similarly the amount of sediment transport has been increased. In eastern part of the study reach, specifically near Bahadurabad it can be observed that the velocity of flow is high in 2011 and respectively low in 2012 as a result the rate of sediment

transport decreases hence some amount of deposition took place on that location. Appearance of many distributary channel can be observed in 2011 and 2012, which is much clearer in July 2012 due to higher flow velocity erosion took place and many distributary channels appeared. The channels bifurcated from the Sirajganj station; show lower flow velocity compared to other locations and consequently possesses lower sediment transport capacity. Similar phenomena can be observed in the downstream portion of the channel. In this zone the flow velocity increased in the subsequent years as well as the sediment transport capacity.

Sediment transport capacities of the river are also responsible for the morphological changes induced by erosion-deposition. If discharge is higher it produces greater velocities as well as carries huge amount of sediment and there by increases the sediment transport capacities of the river. The sediments are deposited in where the velocity is low. As a result the bed level rises of the channel as observed in the previous figures.

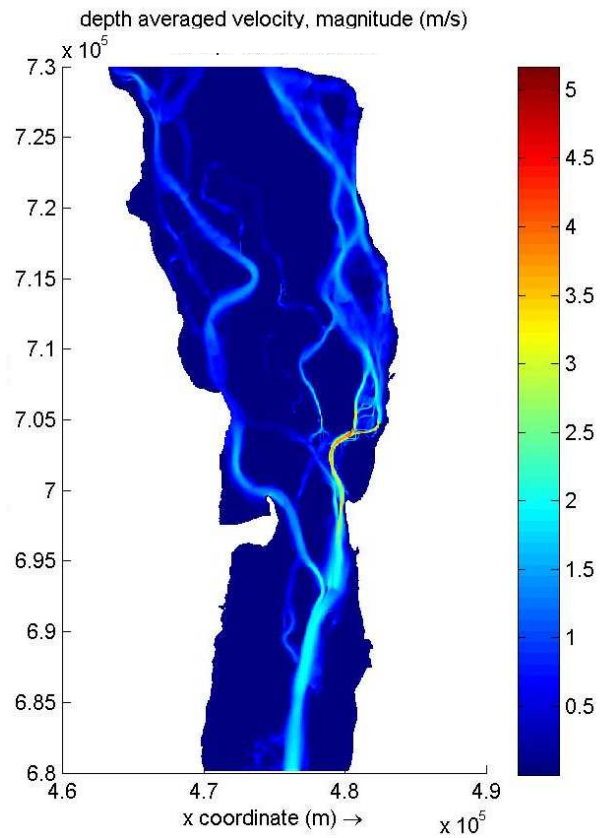


Figure 5.11: Depth Averaged Velocity in 29/7/2010

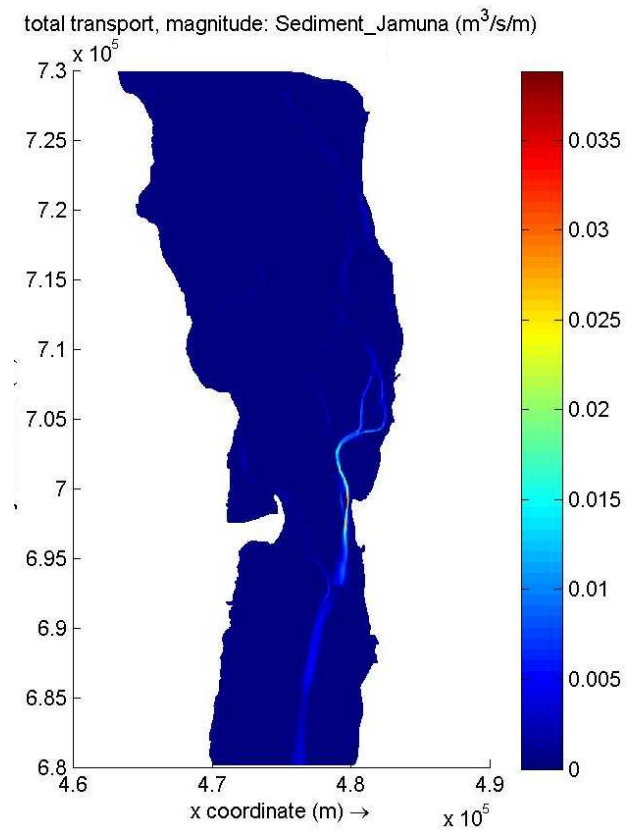


Figure 5.12: Total Sediment Transport in 29/7/2010

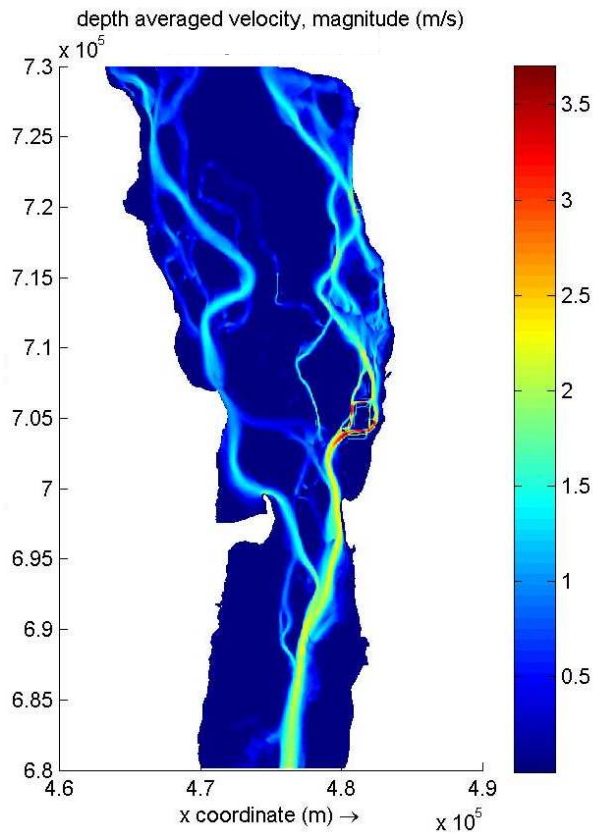


Figure 5.13: Depth Averaged Velocity in 27/1/2011

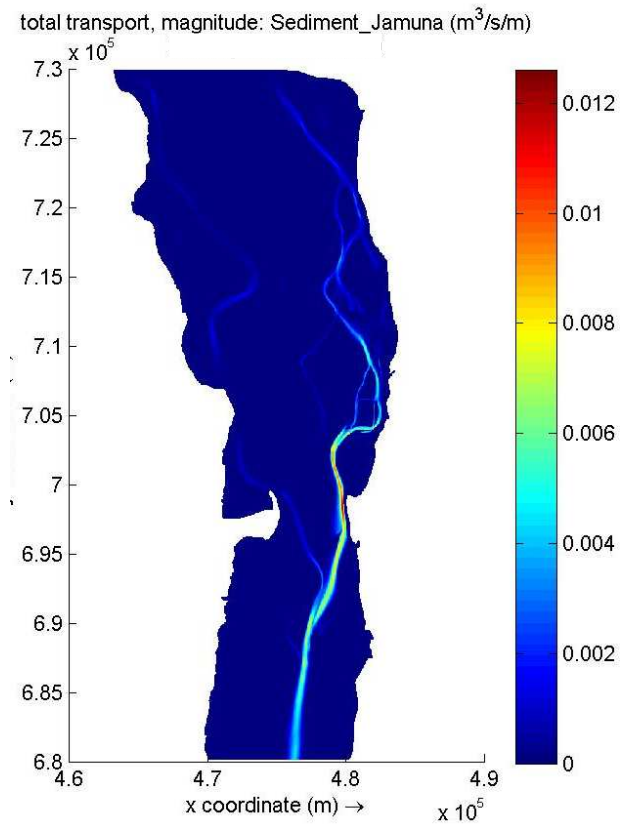


Figure 5.14: Total Sediment Transport in 27/1/2011

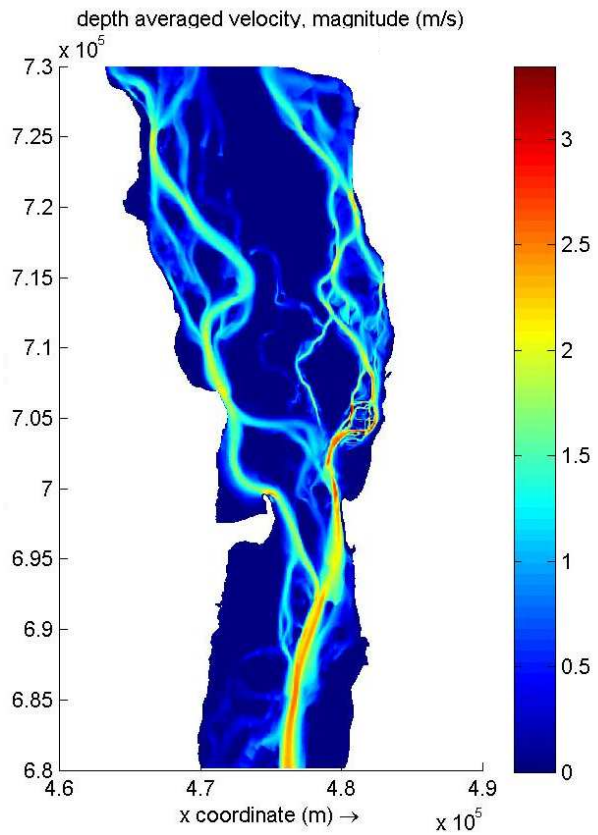


Figure 5.15: Depth Averaged Velocity in 27/7/2011

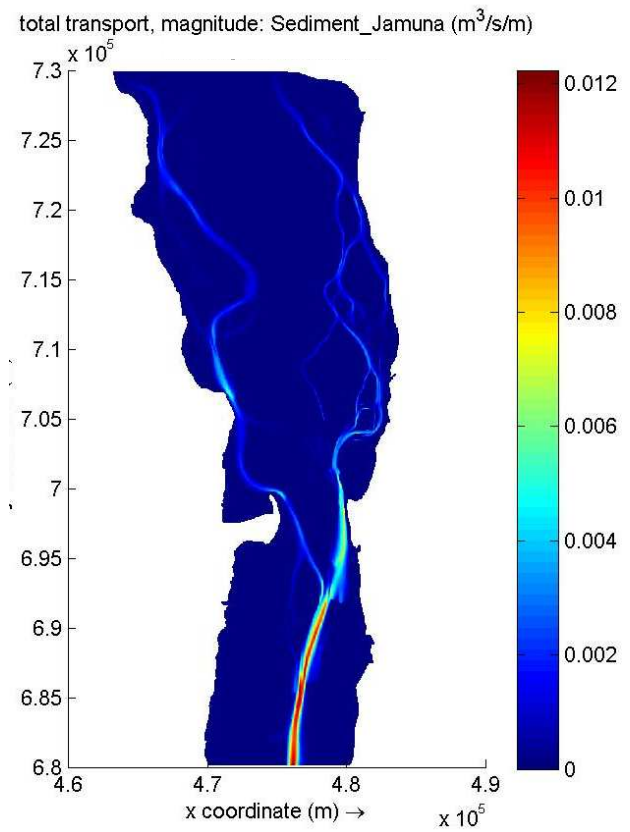


Figure 5.16: Total Sediment Transport in 27/7/2011

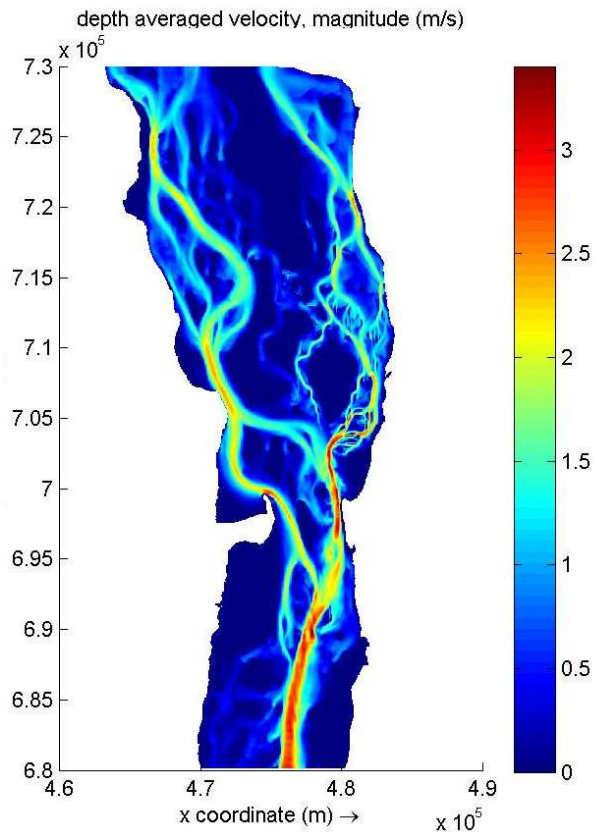


Figure 5.17: Depth Averaged Velocity in 25/1/2012

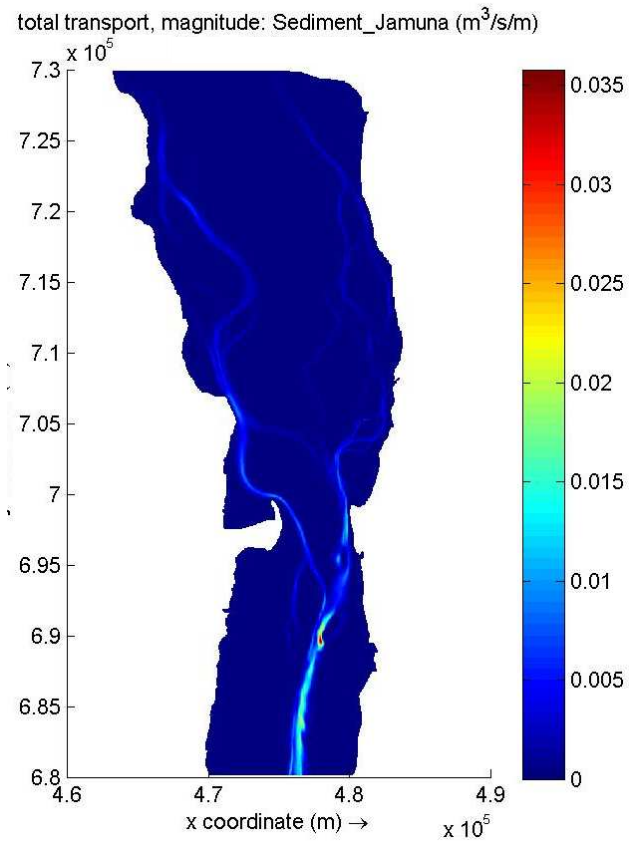


Figure 5.18: Total Sediment Transport in 25/1/2012

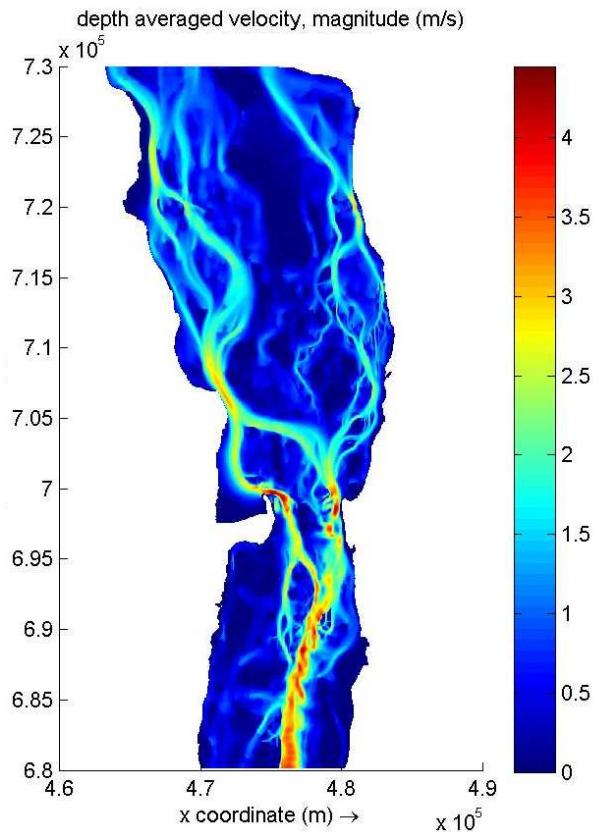


Figure 5.19: Depth Averaged Velocity in 24/7/2012

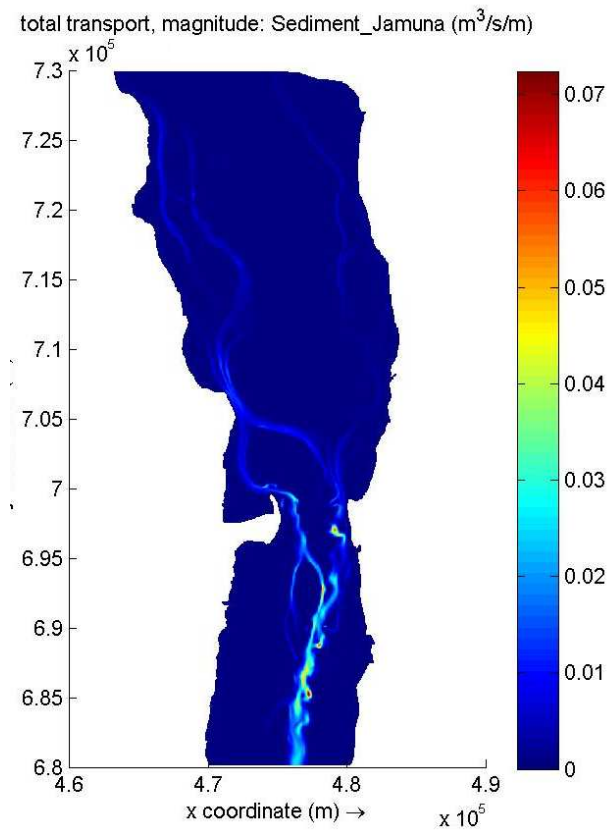


Figure 5.20: Total Sediment Transport in 24/7/2012

The results obtained from the numerical modeling Delft3D shows that the depth average velocities in the both east and west channel during the monsoon season of the stated years are significantly higher compared to dry season.

The above figures show that the sediment transport of the river varies spatially and this process is influenced by the local bathymetry and associated discharge and velocity. In July 2010, the transport rate varies approximately between 0.005 m³/s/m to 0.038 m³/s/m with an average of 0.0215 m³/s/m. The average sediment transport rates of the selected reach of the Jamuna River for various seasons are shown in Table 5.1.

Table 5.1: Average Sediment transport rate of the river for various seasons

Seasons	Sediment Transport Rate (m ³ /s/m)	
	2011	2012
Dry	0.0065	.018
Wet	0.0065	.036

The variation of discharge, velocity and sediment transport capacities as mentioned above affect the morphology of the Jamuna River. For various periods or seasons, these variables change resulting in different morphologic responses of the river.

Deposition near the char areas, formation of deep pockets and development of deep channels are the significant morphologic features. These processes can be better understood by analyzing the selected cross sections on the river. These sections along with their projected bed levels for different periods are shown in Figure 5.21.

The analysis was carried out for the river profile as well as for the selected cross sections. The selected cross sections are shown in Figure 5.21. The locations of each cross section measured from upstream boundary.

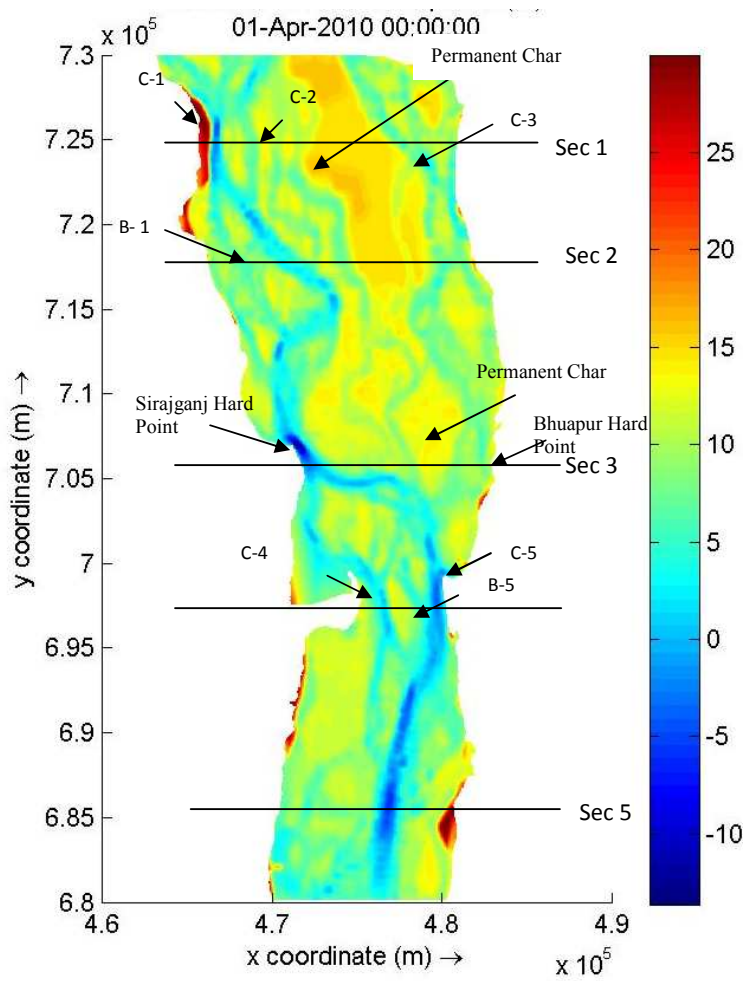


Figure 5.21: Bathymetry of selected reach of the Jamuna River in April 2010

The series of Figure (5.22-5.25) reveal that the three morphological years have much similar type of erosion and deposition patterns. Both erosion and deposition has been occurred mainly in monsoon season.

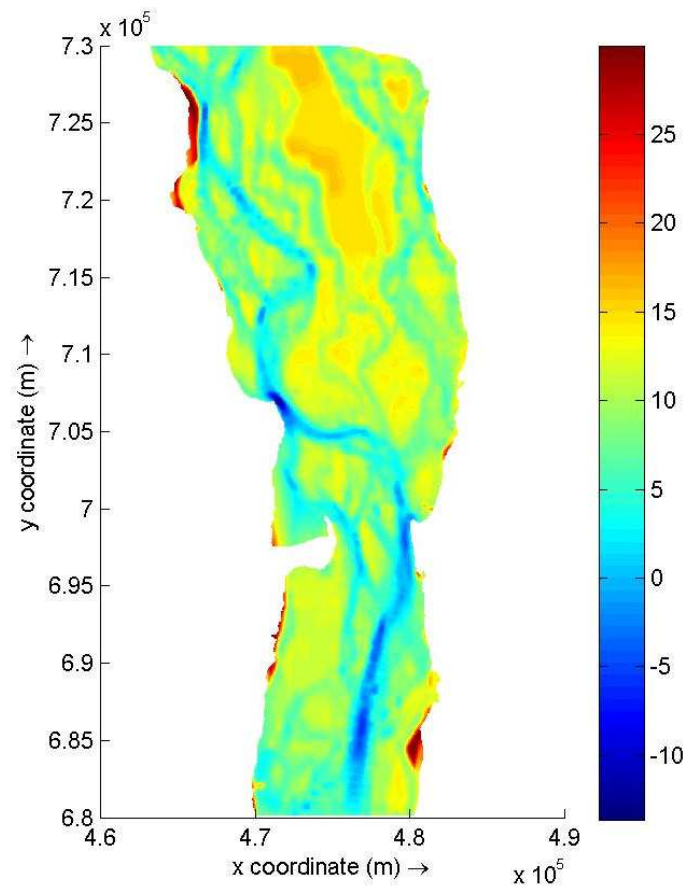


Figure 5.22: Initial bed level in (1 April 2010)

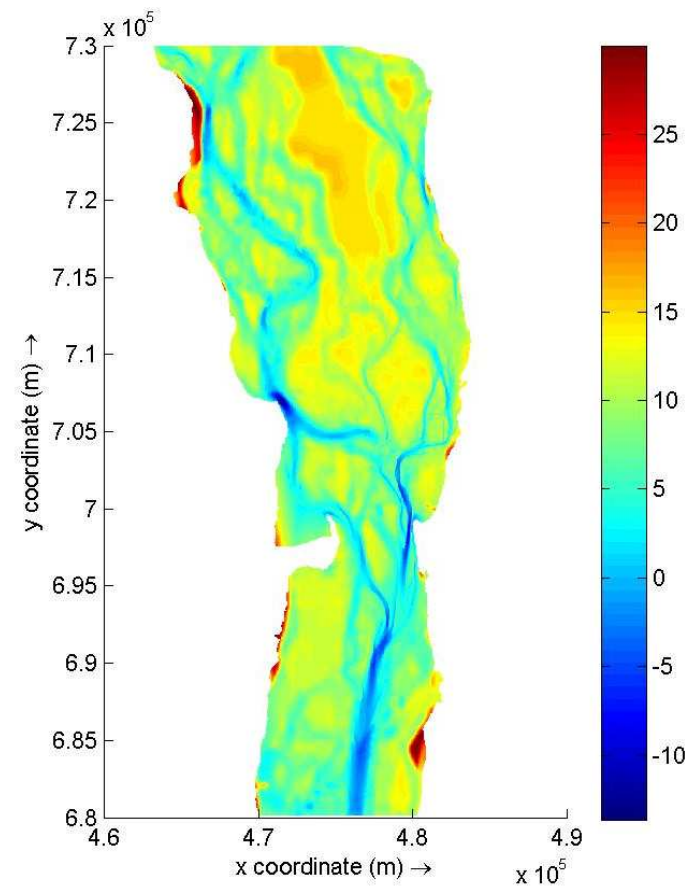


Figure 5.23: Simulated bed level in (25 September 2010)

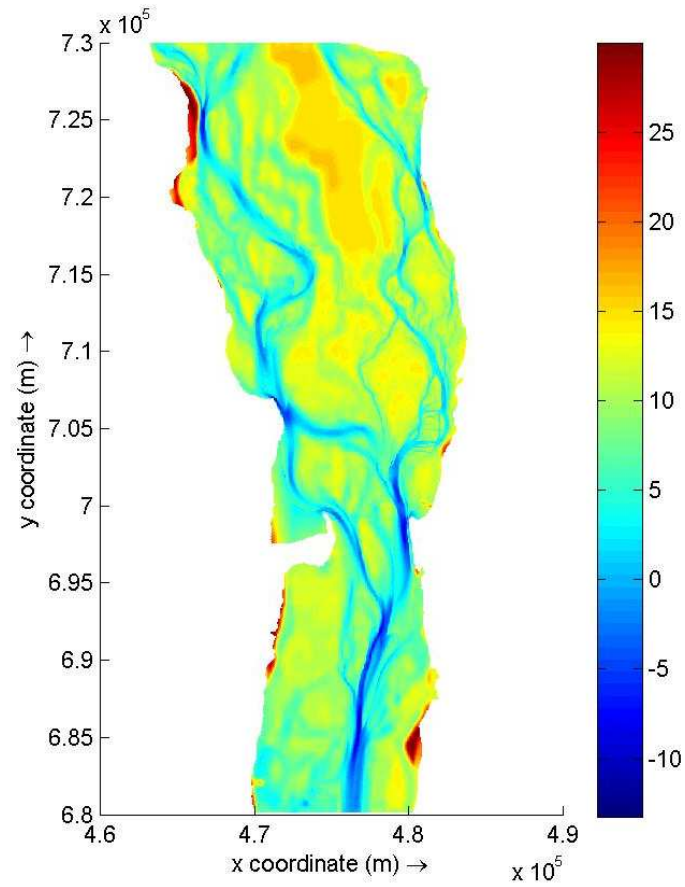


Figure 5.24: Simulated bed level (23 September 2011)

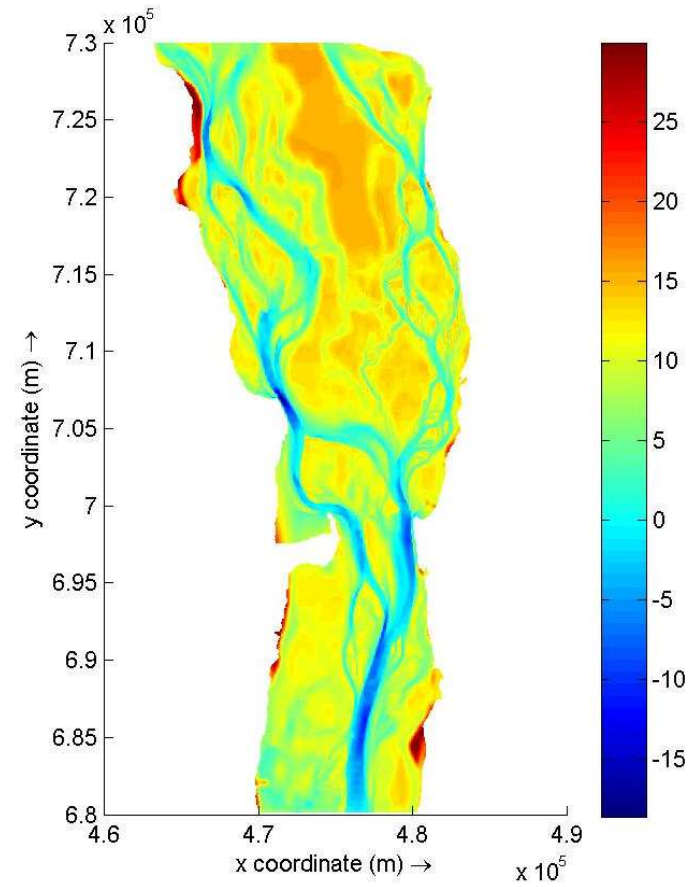


Figure 5.25: Simulated bed level (28 September 2012)

SECTION 1

Section 1 is located near upstream boundary at Kazipur (Figure 5.21). The main channel is situated at the west side of the reach. A char has divided the channel into two branch channel, indicated as C-1 and C-2. During the dry season this char normally remains dry and flooded during monsoon season. There is also a permanent char situated at the middle location of this section.

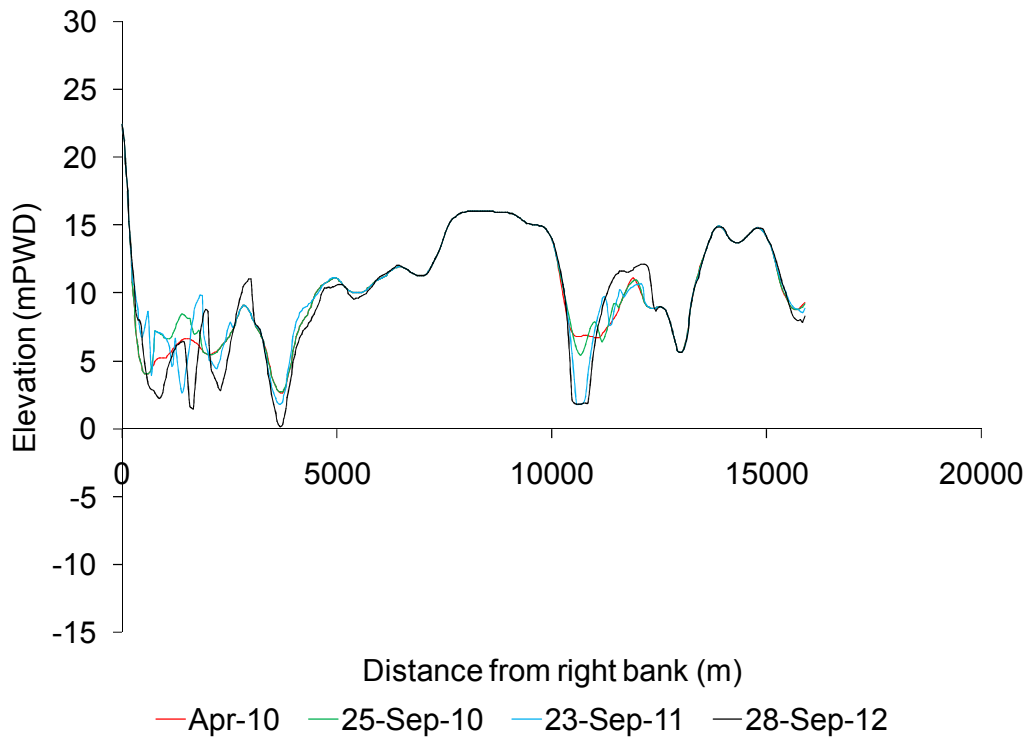


Figure 5.26: Cross-section at Section 1

In the beginning of the simulation in April 2010, it can be seen from the (Figure 5.22), that most of the flow was passing through the channel C-1. It is clear from the Figures (5.23 to 5.25) that small amount of deposition took place on both side of the char due to reduction of the velocity as well as increased the area and length of the char. Both of the channels have undergone severe erosion due to increased velocity, as a result they became relatively deeper and narrower. The bank of the channel C-1 has shifted westward and the bank of channel C-2 on eastward.

Cross Sections superimposed at section 1, shown in (Figure 5.26) for the period of April 2010 to Sept 2012, also indicates the same findings that both the channels C-1 and C-2 had undergone around 5 m of erosion due to increase in magnitude of the velocity from 2.38 m/s to 3.24 m/s and 1.6 m/s to 2.8 m/s respectively. Therefore both banks are vulnerable due to the erosion in this location.

Besides this main channel consecutively many shallower and narrower channel has been developed on the left side of the permanent char due to velocity fluctuations up to September 2011 but there is no change on the right side of the permanent char. Therefore no erosion and deposition took place up to September 2011, as there was no flow velocity. But in September 2012, it can be seen that both erosion and deposition took place on both side of the permanent char as some velocity of flow has been observed and consecutively shallower and narrower channel appeared.

SECTION 2

In section 2, the main channel C-1 due to meandering nature has taken a shifting in a sinuous manner from west to east direction (Figure 5.21). Also a branch channel formed from this channel indicated as B-1 and connected with this channel again in the downward direction. There is a char existing in between them (Fig 5.22).

Maximum flow is passing through the channel C-1 due to its bending nature and also due to higher velocity than that of the branch channel B-1. Severe erosion took place in both of the channels, thus relatively deeper and narrower channel has been created in the subsequent years. The channels became narrower due to deposition took place on both side of their banks as a result of reduction in flow velocity. From September 2011 to September 2012, erosion and deposition took place in between the main channels alternatively. Therefore a huge amount of deeper but narrower channel has been appeared in this location; another branch channel can be seen formed from channel C-1 in the year 2012. Also in the year 2012, due to increase in flow velocity, few small tributary channels can be observed in the east side of the reach. Both of the channels, C-1 and B-1 have shifted in westward from their bank lines.

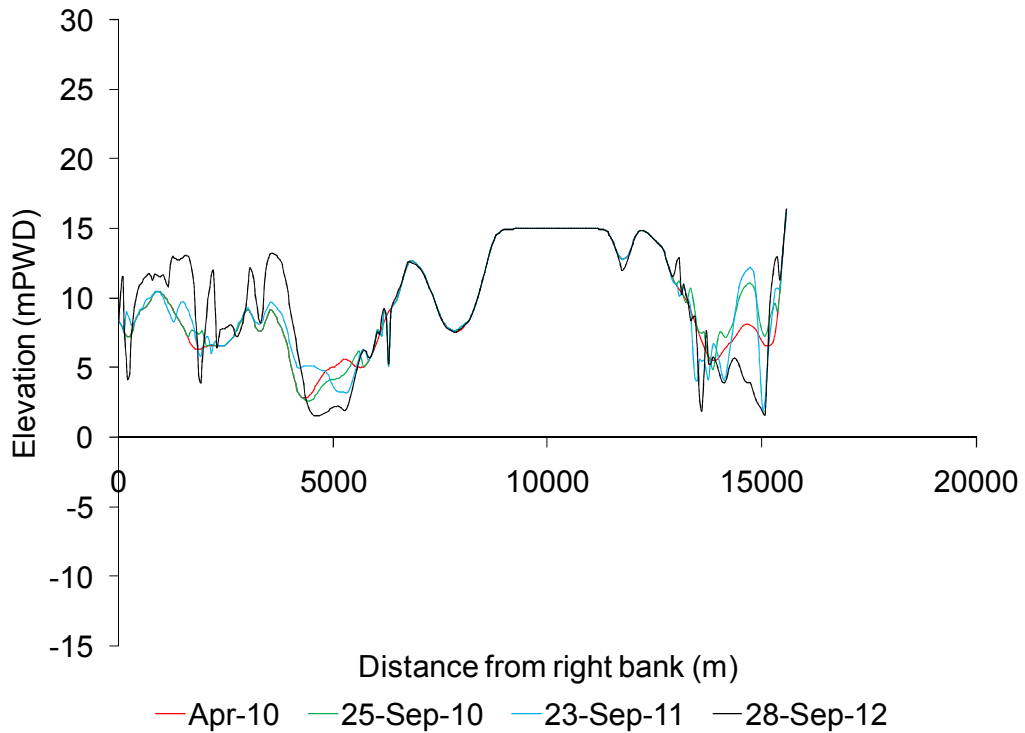


Figure 5.27: Cross-section at Section 2

From the superimposed cross sections at section 2 (Fig 5.27), it is clear that a maximum erosion of 5 m has taken place in the channel C-1 and C-2 due to increased velocity from 2.24 m/s to 2.98 m/s and 1.2 m/s to 2.3 m/s respectively.

SECTION 3

This section is located near Sirajgonj District (Figure 5.21). A major change can be observed in the main channel. At the starting of the simulation in April 2010, the channel was wide and shallow. A huge amount of erosion as well as shifting of the channel can be observed in westward in September 2011 and 2012 (Fig 5.24 and 5.25). Although the channel has been shifted in eastward in September 2010 as deposition took place on both of the bank lines, for reduction of the flow velocity (Fig 5.23).

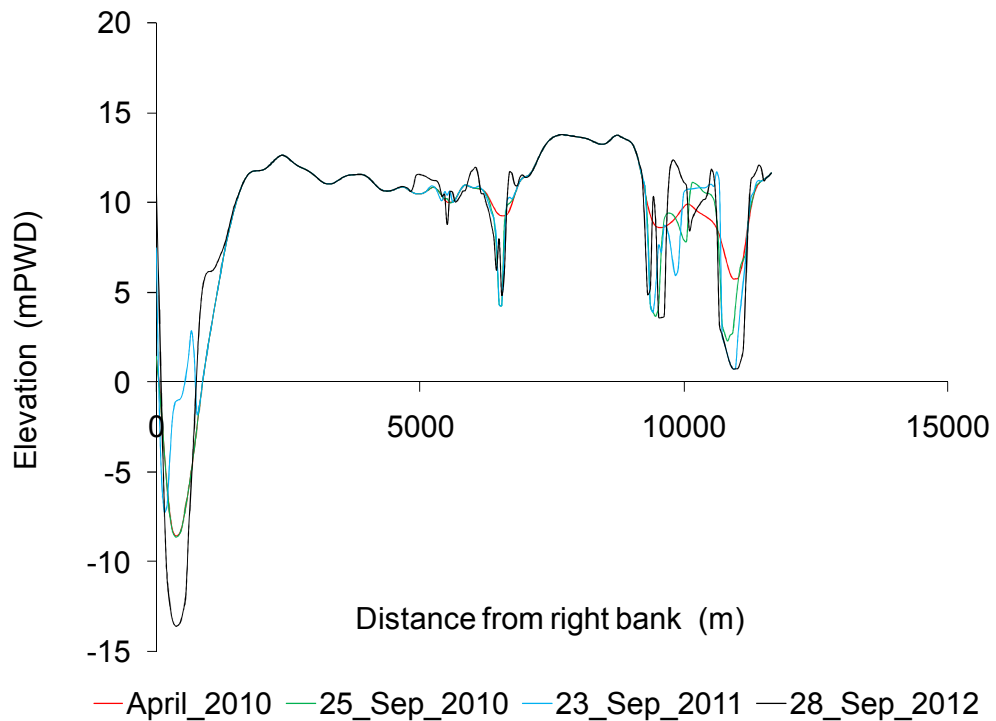


Figure 5.28: Cross-section at Section 3

Superimposed cross-sections in (Figure 5.28) also indicate the same findings. It is found that about 5 m of erosion took place in the channel due to increased velocity from 2.38 m/s to 3.77 m/s. In September 2012, a significant change has been observed in both sides of the permanent char. Alternatively huge number of erosion and deposition took place on both side of the chars due to continuous fluctuations of two velocities. Hence the width of the char has decreased as well as the area. In the location of erosions the existence of some tributary channel has been observed which seems to be relatively shallower and narrower.

SECTION 4

This section is close to the multipurpose Bangabandhu Bridge . There exist two branch channels created after passing the Sirajgonj indicated as C-3 and C-4. There is also a small branch channel, appeared from the branch channel C-4 and again connected with the same channel indicated as B-4 (Figure 5.21).

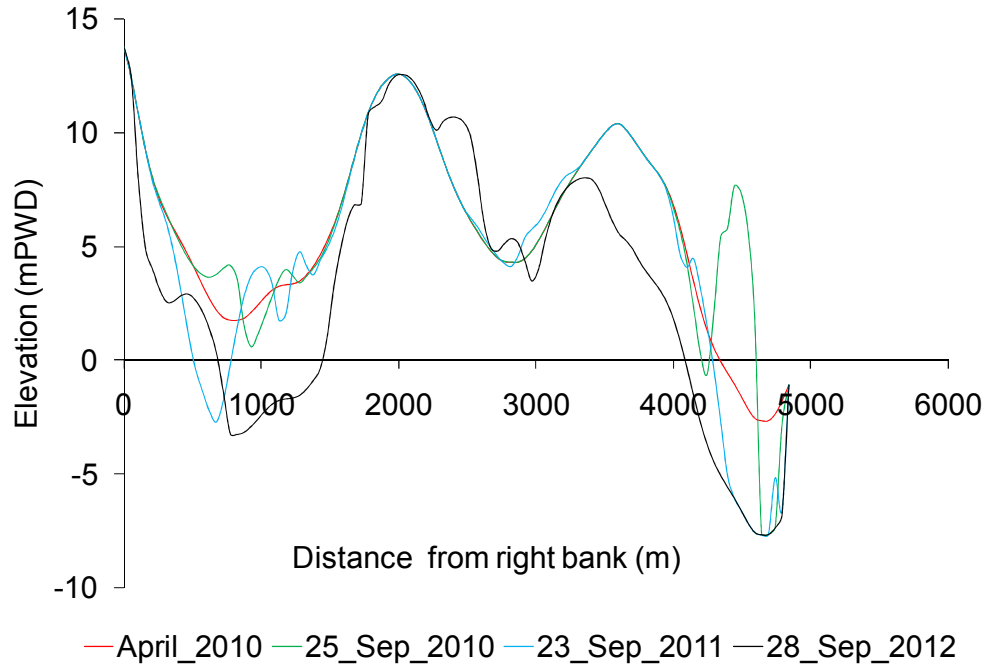


Figure 5.29: Cross-section at Section 4

At the beginning of the simulation, it can be observed that the flow velocity in both of the channels, C-3 and C-4 was low during the dry season. During the monsoon period in the year 2010 and 2011, the widths of both the channels have been reduced. Due to reduction of the velocity deposition took place on both of their respective banks. Both the channels, C-3 and C-4 have been shifted towards east and west respectively. But in 2012, the area influenced by the velocity is greater, thus much erosion took place and the bank line of both the banks seems to be shifted in west and east direction respectively. On the other hand, due to the tremendous flow velocity, huge erosion took place in both channels. Thus deeper and narrower channel has been formed up to 2011. A significant amount of erosion as well as deposition can be observed in the year 2012, for which the bank lines of all the channels have been shifted including the branch channel B-6 (Fig 5.25).

Superimposed cross-sections at section 4 (Fig 5.29) for the studied years also indicate the same findings. The channels C-3, C-4 and B-1 have undergone a severe

erosion of about 5 m in the year 2012 due to an increased flow velocity of about 2.34 m/s to 3.37 m/s, 2.36 m/s to 3.69 m/s and 0.84 m/s to 2.14 m/s respectively.

A char existed in between the channels C-3 and C-4. In September 2011, significant erosion took place on both side of the char and deepened the branch channel B-1. But in September 2012, it can be seen that a large amount of deposition of about 4 m took place at right side of the char due to the reduction of flow velocity and the branch channel has significantly shifted. Therefore the area of the char has been increased.

SECTION 5

Section 5 is situated near to the downstream of the study reach near to Chauhali (Figure 5.21). In this section, a major change has been observed in the main channel. Severe erosion took place in September 2012 due to increase in flow velocity. In September 2011, the magnitude of flow velocity is relatively lower than that of in the year 2010 and deposition took place in some amount and reduced the deepness of the channel compared to 2010 (Figure 5.30). It is evident from (Figure 5.23 and 5.24) that alternatively erosion and deposition took place in September 2010 and 2011. Hence there existed a temporary char in between them and divided the channel into two branch channels, which are relatively deeper and narrower. Huge amount of deposition took place in both side of the channel in September 2010 and consequently the channel has shifted towards east. The channel has shifted towards west in September 2011 and lastly in September 2012, due to more erosion and increased velocity the temporary char has been completely eroded and deeper and wider channel has been created.

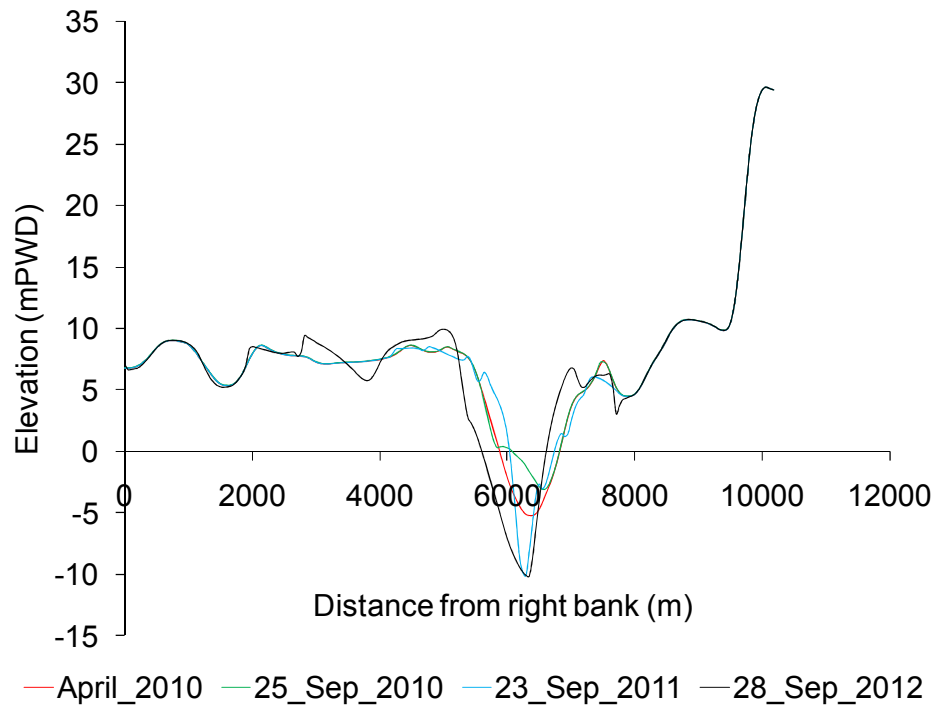


Figure 5.30: Cross-section at Section 5

From the cross section (Figure 5.30), it can be observed that around 5 m of erosion took place and the velocity was 2.36 m/s. This velocity reduced to 2.05 m/s and then increased abruptly to 3.22 m/s. In September 2010, a huge amount of deposition of around 7.5 m and 3 m took place on both the left and right side of the channel due to reduction of velocity at that location.

Table 5.2: Average Erosion and Deposition of Observed and Simulated Bathymetry

Cross-section	Dec-10		Sep-11	
	Observed (m)	Simulated (m)	Observed (m)	Simulated (m)
Section 1	-0.083	-0.003	-0.284	-0.182
Section 2	0.205	0.167	0.263	0.173
Section 3	0.002	0.003	-0.024	-0.039
Section 4	0.074	0.051	-0.882	-0.688
Section 5	-0.021	-0.052	-0.280	-0.354

The comparison of average erosion and deposition of observed and simulated cross-sections for September 2011 and December 2010 has been shown in Table 5.2. The result shows a very good agreement between observed and simulated bathymetry.

The maximum, minimum and net erosion and deposition of the study area of Jamuna River during the simulated time period are summarized in Table 5.3.

Table 5.3: Bed Level Changes for the selected sections

Section	Maximum Deposition (m)			Maximum Erosion (m)			NetDeposition/Erosion (m)		
	2010	2011	2012	2010	2011	2012	2010	2011	2012
1	2.23	5.91	5.41	-2.90	-4.99	-4.99	0.09	0.10	-.05
2	3.71	4.15	5.96	-3.90	-5.0	-5.0	0.14	0.16	0.28
3	2.53	8.58	9.74	-5.0	-5.0	-5.0	-0.17	-0.15	-0.17
4	10.36	3.73	5.22	-5.0	-5.0	-5.0	0.18	-0.46	-1.73
5	4.56	11.69	8.81	-1.69	-5.0	-5.0	0.06	0.07	-0.19

5.4.3 Comparison of the simulated bathymetry in September 2011 by Mike21 and Delft 3D

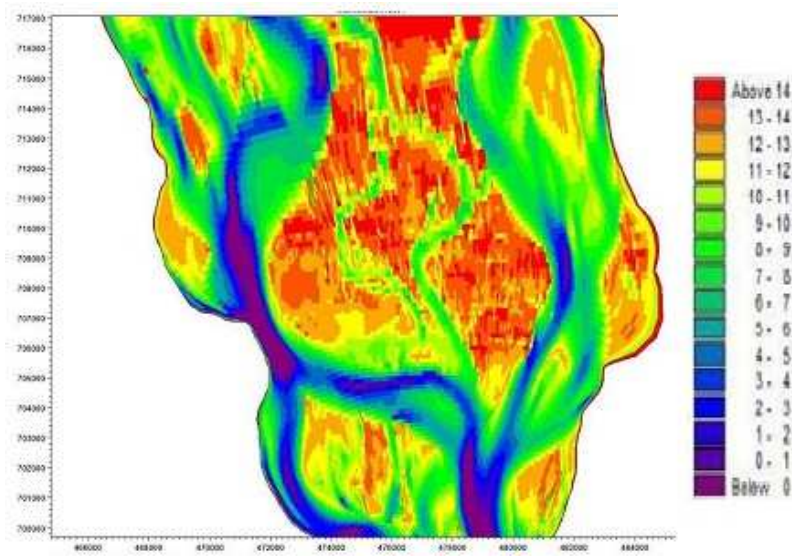


Figure 5.31: Simulated bathymetry by Mike 21 (September 2011)

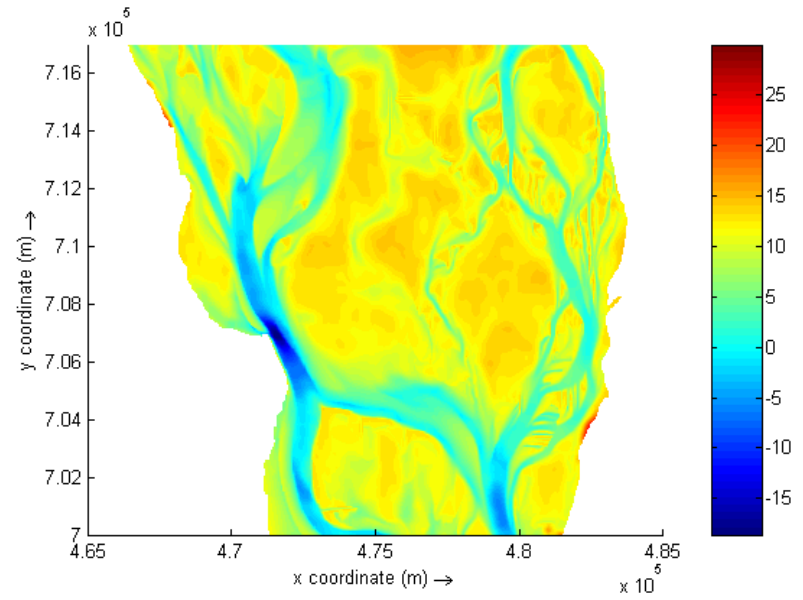


Figure 5.32: Simulated bathymetry by Delft 3D (September 2011)

The above figures (middle portion of the selected reach) show the simulated images of the bed level in September 2011. From Figure 5.32, it is found that Delft 3D model predicted river bed degradation patterns near Sirajganj Hard Point and East Guide Bund are very similar with the predicted river bed degradation of Mike 21 by IWM. From both pictures it can be revealed that the range of colors is well adjusted. Aggregation can be observed in the simulated bathymetry near the bank lines. But it can be observed that in both the picture that the highly erosion affected zone are at the same locations Shirajgonj and near the east guide bund of the main channel. In these zones according to the color bar the values are below 0mPWD indicating the violet and deep blue zone successively. The tributaries are in the range of 0 mPWD to 5 mPWD indicated by the light green color. Also the big char areas are indicated in red and deep yellow color successively ranging above 14mPWD.

5.5 Sensitivity Analysis

To determine the model's performance and how the model responds to several parameter settings a sensitivity analysis is performed. The sensitivity analysis consists of several stages. First several runs with the default parameter settings were made and the output is evaluated to check the general performance of the model. After these initial computations, several computations were made with different parameter settings, to see how these parameters influence the results. Parameter settings include:

- bottom roughness
- eddy viscosity.

5.5.1 Bottom roughness

In the Delft model the Manning parameter is varied to investigate the sensitivity of this parameter on the discharge. Three runs are made with a Manning parameter for char and channel (char 0.1 and channel .01; char 0.1 and channel .014; char .025 and channel .014). It is clear from figure 6.1 that the Manning parameter (n) has rather large influence on the water level, discharge constituents. When increasing the Manning

parameter the bottom roughness increases, mainly it can be seen that the water level height increases mainly due to the increase of the roughness of char rather than channel.

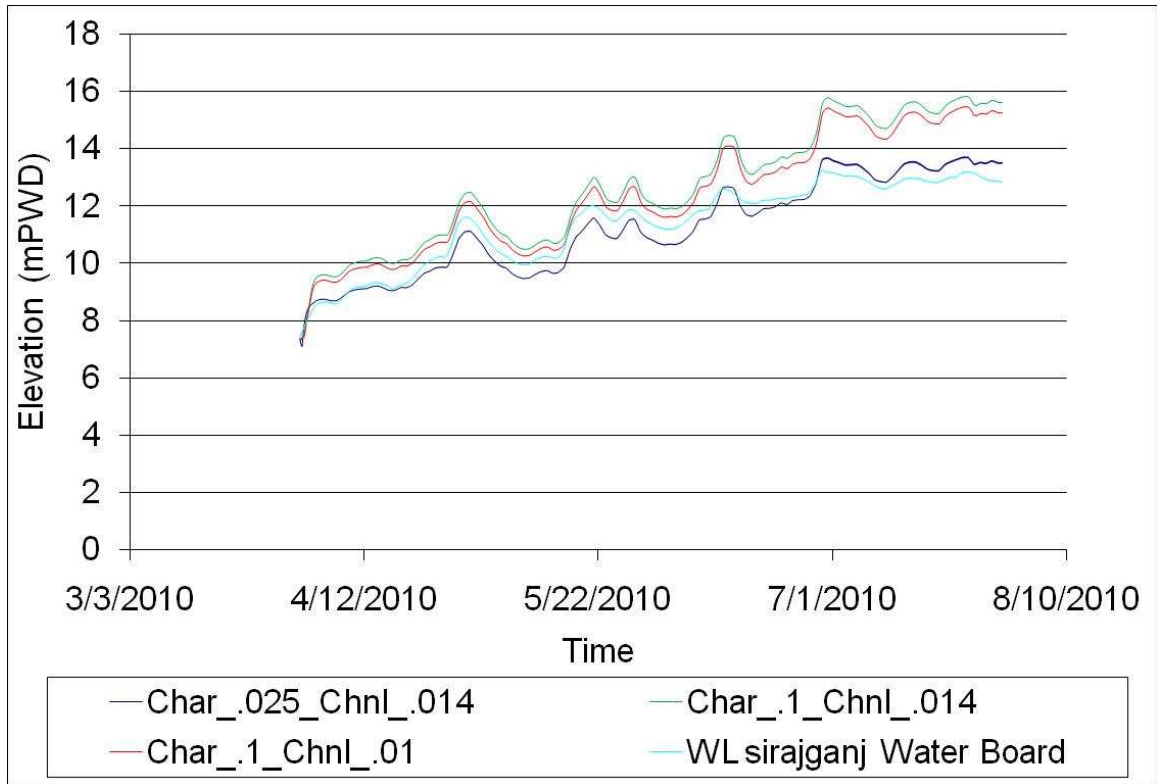


Fig. 5.33 Influence of Manning parameter on amplitudes of water level

The influence of the Manning parameter on of the water level in Shirajganj is also noticeable. In figure 5.33 it has been observed that the height of the water level after the run differ within 2.8m with the roughness $n=0.1$, $.014$, differ within 2.5m with $n=0.1$, $.01$ and differ within $.6m$ with $n=0.025$, $.014$. The run with $n=0.1$, $.014$ has the largest difference from the observed water level data and the run with $n=0.025$, $.014$ is relatively much close to the observed data.

5.5.2 Eddy Viscosity

The next important parameter that has been tested in tuning the run is the eddy viscosity. Three values have been taken to test the difference 1, 3 and 10. 10 is the default value and 1 is the value used for the alluvial river from various studies (IWM, 2011). The result for the three values has been shown in (figure 5.34). There is no such influence in the model as the water level variation is almost same. Hence we have considered the known used value 1.

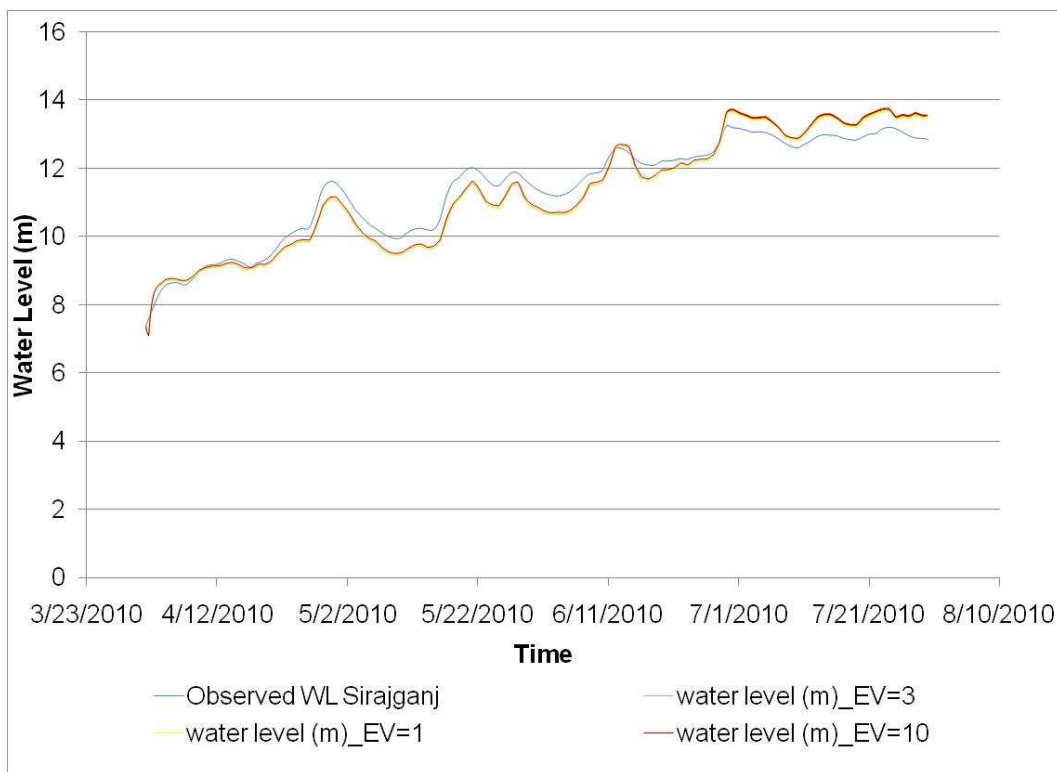


Fig. 5.34 Influence of Eddy Viscosity on amplitudes of water level

5.6 Summary

In general the model shows very reasonable results, especially considered the many uncertain factors in the model.

A further improvement of the model is considered not feasible with the available data. The most limiting factors are the lack of reliable bottom depths and reliable discharge data. For the purpose of the study the created model is accurate enough to draw conclusions.

CONCLUSIONS AND RECOMMENDATION

CHAPTER 6

6.1 General

The numerical technique Delft 3D developed in this study has been applied in the Jamuna river for a reach extending from Kazipara to Chauhali. Taking April 2010 field data of bed level as reference bed level, the changes of bed level in the two successive years within the reach has been computed by running the programme. The following conclusions has been drawn from the present study

6.2 Conclusions

The summary of the findings of the present study for the selected reach of the Jamuna River located at 30 km upstream and 20 km downstream from the Bangabandhu Bridge are as follows:

1. The model developed in this study has been calibrated against the observed water surface elevations at Shirajgonj. Attempt has been made to calibrate only the high flow data as most of the morphological activities occur during this period. Result obtained from the calibration process has shown adequate agreement with the observed values.
2. Next the model has been validated for two months (April to June) during the monsoon period with the water surface elevations of Shirajgonj. Result has shown satisfactory matches between observed and simulated values.
3. The erosion and deposition for one year and then two successive years have been computed, for the study reach using the present technique. It has been found that more materials have deposited mostly adjacent to the char areas which are surrounded by the channel branches. From the selected cross sections it can be revealed that maximum deposition took place on 2012 that

is about 9.97 m in section 1 near kazipur whereas maximum erosion took place on all the sections of about 5m.

4. In the present study the sediment transport rate, erosion and deposition and bed level changes has been analyzed for non cohesive sediment. The simulated average sediment transport rate is $0.0065\text{m}^3/\text{s}/\text{m}$ for dry season and $0.0065\text{m}^3/\text{s}/\text{m}$ for wet season in Sep 2011. In Sep 2012 the transport rate is $0.018\text{m}^3/\text{s}/\text{m}$ for dry season and $0.036\text{m}^3/\text{s}/\text{m}$ for wet season. Delft is capable of analyzing the above parameters in case of cohesive sediment also.
5. Overall there has been a very small amount of deposition. Considering the changes during the last two years and also along the total study reach of the Jamuna River it has been seen that appreciable deposition is absent but there has been a large amount of erosion in the west channel.
6. A relationship has been analyzed in variation of velocity and sediment transport. It can be seen that due to increased velocity the rate of sediment transport increases hence there forms erosion and the shifting characteristics of the channels can be observed.
7. The plan form analysis has revealed that during the past two years the river has shifted quite appreciable towards the east and west. The shifting process of river course and its subsequent erosion and accretion processes cause the loss and newly formation of land simultaneously.

6.3 Recommendations for further Study:

For getting better knowledge on the changes in the morphologic and hydrologic conditions of the Jamuna River the following suggestions are made for further study and to facilitate future studies:

1. There should be the availability of all types of data like discharge, water level, sediment concentration, cross section that covers shorter time interval and closer distance for both the dry and flood seasons.

2. The discharge and water level data should be measured at more stations all over the year to facilitate better understanding of morphological processes.
3. Nowadays the existence of multiple tools to model and evaluate all these aspects, such as Delft3D into the technical field, are supportive elements to generate numerous feasible scenarios and to select the optimal one
4. This type of morphological assessment studies can be carried out in most of the major rivers, estuaries and coastal regions of our countries by using the Delft Software.
5. There are some deficiencies in the functioning of the software which need to be improved. For instance, it has been needed to manually adjust some input files generated by the software tools RGFGRID and QUICKIN (e.g. delete some lines in grid files). Besides, any change in the grid configuration means the need to redo depths, cross- sections and observation points, which is time consuming.
6. It is also complicated to define obstacles such as jetties, groins and revetments, because they must be fitted to the grid points; thus it is impossible to accurately define the exact position of these obstacles. Besides, any change in the grid configuration means the need to redo depths, obstacles, cross-sections and observation points, which is time consuming.
7. In the present study the bridge has not been considered as the resolution of pier was difficult to adjust with the resolution of the grid.

REFERENCES

1. Alam, M. K. and Hosain, M. M., 1988, "Sediment transport in the River Jamuna", Journal of Institution of Engineers, Bangladesh, Vol. 16, Issue 1-2, pp. 17-26.
2. Allison, M. A., 1998. "Historical changes in the Ganges-Brahmaputra Delta front", Journal of Coastal Research, pp. 1269–1275.
3. Ali, Md. Hazrat and Kyotoh, Harumichi, 2002, "Instability Analysis of the Jamuna River, Bangladesh", Pertanika J.Sci. & Technol., Vol. 10, pp. 229-250.
4. Bhuiyan, Mohammad A. H., Rakib, M. A., Takashi, Kumamoto, Rahman, M. Julleh Jalalur, Suzuki, Shigeyuki, 2010, "Regulation of Brahmaputra-Jamuna River around Jamuna Bridge Site, Bangladesh: Geoenvironmental Impacts", Journal of Water Resource and Protection, Vol.2, pp. 123-130.
5. Bian, C., 1998, "Scientific exploration of Yarlung Zangbo River grand canyon", Beijing, Vol. 41, Issue 13, pp. 21-22.
6. BIWTA, 2003, "Hydraulic and morphological study for the selection of a site for ferry ghat alternative to Nagarbari/Notakhola", Final Report prepared by department of Water Resources Engineering, BRTC, BUET.
7. Bristow, C. S., 1987. "Brahmaputra River: Channel migration and deposition." In Ethridge et al. (1987), pp. 63–74.
8. BWDB, 1998, "Meghna Estuary Study", Draft Master Plan, Vol. 2: Morphological processes.
9. BWDB, 2011. "Bangladesh er Nod-Nodi", Bangladesh Water Development Board (BWDB), Dhaka, Bangladesh.
10. Coleman, J. M., 1969, "Brahmaputra River: channel processes and sedimentation," Sedimentary Geology 3 (2–3): pp.129–239.

11. DHI/SWMC., 1999, “Mathematical morphological model of Jamuna River at Jamuna bridge site”, Final Report, Phase II, prepared by Danish Hydraulic Institute in Association with SWMC.
12. DHI/SWMC., 1997, “Mathematical model study (Phase I) for optimizing of dredging, Gorai River Restoration Project”, Final Report, Phase I, Danish Hydraulic Institute in Association with SWMC.
13. EGIS, 1997, “Morphological dynamics of the Brahmaputra-Jamuna River”, Tech. Rep., EGIS, Dhaka, Bangladesh.
14. FAP 1, 1994 “River training studies of the Brahmaputra river”, Master Plan Report, Annex 4, Design and Construction, BWDB.
15. FAP21/22, 1994. Technical report No. 2: "Morphological predictions for test areas, Bank protection and river training pilot project FAP21/22. FAP21/22, Dhaka, Bangladesh.
16. FAP24, 1994. Study report No. 3: “Morphological studies phase 1”, Available data and characteristics. FAP24, Dhaka, Bangladesh.
17. Fergusson, J., 1863. “Delta of the Ganges.” The Quarterly Journal of the Geological Society of London 19: pp.321–354.
18. Goodbred, S. L. and S. A. Kuehl, 2000. “Enormous Ganges-Brahmaputra sediment discharge during strengthened early Holocene monsoon.” *Geology* 28 (12): pp. 1083–1086.
19. Habibullah, M. 1987, “Computer Modeling of River Chanel Changes in Alluvial Condition”, First Interim Report R 02/87, IFCDR, BUET, Dhaka.
20. Halcrow, 2002, “Jamuna-Meghna river erosion mitigation project”, Draft Inception report, Vol. 1. Options assessment, Halcrow.
21. Hayter, E.J., Mehta A.J., 1986, “Modelling cohesive sediment transport in estuarial waters”, Volume 10, Issue 4, pp. 294–303.

22. Hoque, N., 1999, "Application of remote-sensing and GIS for monitoring fluvial processes", PhD.Thesis, Physics Department, BUET.
23. Hossain, T. B., 1997, "A study on Aggradation and Degradation of the Khowai River", M. Engg. Project, Dept. of the Water Resources Engineering, BUET, Dhaka.
24. Reza, I., 2011, Term Paper on "Tracking the morphological change of a river extent of Bangladesh using satellite images in ArcGIS".
25. IWM Report, 2010-11 "Monitoring of Hydraulic and Morphological conditions of Jamuna River for the safety of Bangabandhu Bridge during the year", Final Report.
26. Jagers, H. R. A., 2003, "Modelling Planform Changes of Braided Rivers", ISBN 90-9016879-6.
27. Jain S.C., 1989, "Guide for Estimating Riverbed Degradation", J. Hydr. Division, ASCE, 1153(3), pp.356-366.
28. Jaramillo, W.F. and Jain, S.C., 1984, "Aggradation and Degradation of Alluvial Channel Beds", J. Hydr. Division, ASCE, 110(8), pp.1072-1085.
29. Klaassen, G.J., and Masselink, G., 1992, "Planform changes of a braided river with fine sand as bed and bank material", Proc. 5th International Symp. River Sedimentation, Karlsruhe, FR Germany, pp.459-471.
30. Klees, R. A. P., Hanssen, R. F., and Usai, S., 1997. "SAR-interferometry (1), a new geodetic technique for determining elevations and elevation changes." *Geodesia* 1997 (4): 155–162.
31. Kuehl, S. A., Hariu, T. M., and Moore, W. S., 1989. "Shelf sedimentation off the Ganges-Brahmaputra river system: evidence for sediment bypassing to the Bengal fan." *Geology* 17: pp. 1132–1135.
32. Lane, E.W., 1957, "A Study of the Shape of Channels Formed by natural Streams Flowing in Erodible Material", M.R.D. Sediment Series No.9, U.S. Army Engineers Division, Missouri River, Groups of Engineers, Omaha, Nebraska.

33. Leopold, L.B., Wolman, M.G, 1957, “River Channel Patterns: Braided, Meandering and Straight”, U.S. Geol. Survey, Prof. Paper 282-B.
34. Leopold, L.B., Wolman, M.G. and Miller, V.P., 1964, “Fluvial Processes in Geomorphology”, Freeman and Company, Sanfrancisco, California, U.S.A.
35. Luijendijk A.P., 2001, “Validation, calibration and evaluation of Delft3D FLOW model with ferry measurements”, M.Sc. Thesis, pp 4-1 to 4-5.
36. Montgomerie, T. G., 1885, “Report of a route survey made by Pandit Nain Sigh.” Proceedings of the Royal Geographical Society 7: pp. 188.
37. Mosselman, E., Huisink, M., Koomen, E., and Seymonsbergen, A. C., 1995, “Morphological changes in a large braided sand-bed river.” In Hickin, pp. 235–247.
38. Nguyen, K. D., Guillou, S., Chauchat, J., Barbry, N., 2009, “A two-phase numerical model for suspended-sediment transport in estuaries”, Volume 32, Issue 8, pp. 1187–1196.
39. National Geographic, 1999. “Lost waterfall discovered in remote Tibetan gorge.” Press Release Jan. 9, <http://www.geomag.com/events/releases/pr990111.html>, articles by among others Larson and Kilian.
40. River Survey Project, 1996. FAP24 Final report. Delft Hydraulics, Delft, The Netherlands.
41. Rahman, K. S., 1978, “A study on the erosion of the Padma”, M.Sc Engineering Thesis, Department of Water Resources Engineering, BUET, Dhaka.
42. Raju, K. G. R., 1980, “Aggradation and Degradation”, Proceedings of the International Workshop on Alluvial River Problems held at Roorkee, India, pp. 18-20.
43. Schumm, S.A. and Khan. H.R., 1972, “Experimental Study of Channel Patterns”, Geol. Soc. Am. Bull., Vol.83, pp. 1755-1770.

44. Shields, A., 1936. "Application of similitude mechanics and the research on turbulence to bedload movement." *Mitteilungen der Preussischer Versuchsanstalt für Wasserbau und Schiffbau* 26. In German (Anwendung der Ähnlichkeitsmechanik und der Turbulenzforschung auf die Geschiebebewegung)."
45. Shimizu, Y. and Itakura, T., 1989, "Calculation of Bed Variation in Alluvial Channels", *J. Hydr. Division, ASCE*, 1153(3), pp. 367-384.
46. Simons, D.B. and Senturk, F., 1971, "Sediment Transport Technology", *Water Resources Publications Fort Collins, Colorado, 80522, U.S.A.*, pp. 24-72.
47. Soni, J.P.; Garde, R.J.; and Raju, K.G.R., 1980. "Aggradation in streams due to overloading." *Journal of the Hydraulics Division, ASCE*, Vol. 106, No. HY1, pp. 117-132.
48. SWMC., 1999, "2-D Hydraulic model (FESWMS-2DH/SMS) of the river Ganges for Pakshey Bridge Construction Project", *Final Report prepared by SWMC, Vol. 1.*
49. Thorne, C.R., and Osman, A.M., 1988, "Riverbank stability analysis:II Applications", *Journal of Hydraulic Engineering, ASCE*, 114(2), pp. 151-172.
50. Thorne, C. R. and Russel, A. P. G., 1993, "Geomorphic study of bankline movement of the Brahmaputra River in Bangladesh," In 5th annual seminar of Scottish Hydraulics Study Group on sediment transports processes and phenomena, Edinburgh, U.K.
51. Thorne, C. R., Russel, A. P. G. and Alam, M. K., 1993. "Planform pattern and channel evolution of the Brahmaputra River, Bangladesh." In Best and Bristow, pp. 257–276.
52. Van K. T., 1999, "3D sediment transport in DELFT3D-FLOW Test calculations with sediment release". Report No. Z2534.10, WL | DELFT HYDRAULICS.
53. Van, L. C. R, 1984, "Sediment transport, Part III: Alluvial Roughness", *Journal of Hydraulic Engineering, Vol 110, No.12.*

54. Winterwerp, J. C., 1999. "On the dynamics of high-concentrated mud suspensions". Delft University of Technology, Delft, The Netherlands. Ph.D. thesis.
55. WL | Delft Hydraulics, 2000, "Morphological and navigable effects of groyne lowering", <http://www.wldelft.nl/cons/area/rem/index.html>.
56. WL | Delft Hydraulics, 2000, "Two-dimensional hydraulic and morphological model of the Tenryuu River", Japan, <http://www.wldelft.nl/cons/area/rem/index.html>.
57. WL | Delft Hydraulics, 2002, "Meander migration and scour of the Roer river", <http://www.wldelft.nl/cons/area/rem/index.html>.
58. WL | Delft Hydraulics, 2005, User Manual Delft3D-FLOW. The Netherlands.
59. WL | Delft Hydraulics, 2005, User Manual Delft3D-QUICKIN. The Netherlands.
60. WL | Delft Hydraulics, 2005, User Manual Delft3D-RGFGRID. The Netherlands.

Appendix: A

Table : A.1 (Observed and simulated water level data for Calibration)

Date	Observed Water Level (m)	Simulated water level (m)
4/1/2010	7.37	7.37
4/5/2010	8.64	9.25
4/10/2010	9.11	9.63
4/15/2010	9.29	9.61
4/20/2010	9.42	9.92
4/25/2010	10.24	10.30
4/30/2010	11.59	11.22
5/5/2010	10.40	10.30
5/10/2010	9.95	10.06
5/15/2010	10.19	10.26
5/20/2010	11.93	11.77
5/25/2010	11.48	11.34
5/31/2010	11.38	11.04
6/5/2010	11.31	11.15
6/10/2010	11.94	12.13
6/15/2010	12.28	11.91
6/20/2010	12.21	12.10
6/25/2010	12.36	12.36
6/27/2010	12.47	12.76
7/1/2010	13.17	13.58
7/5/2010	13.05	13.34
7/10/2010	12.6	12.8
7/15/2010	12.97	13.52
7/20/2010	12.92	13.4
7/25/2010	13.17	13.43
7/30/2010	12.85	13.47

Table A.2: (Observed and simulated water level data for Validation)

Date	Observed Water Level (m)	Simulated Water Level (m)
4/1/2011	8.36	8.36
4/10/2011	7.82	8.18
4/15/2011	7.78	8.12
4/20/2011	7.87	8.19
4/25/2011	8.00	8.25
4/30/2011	8.88	8.83
5/5/2011	8.64	8.56
5/10/2011	8.88	8.93
5/15/2011	8.87	8.73
5/20/2011	8.90	8.82
5/25/2011	9.05	9.05
5/31/2011	9.75	9.72
6/5/2011	9.81	9.84
6/10/2011	11.01	10.81
6/15/2011	10.68	10.36
6/20/2011	10.73	10.47
6/25/2011	10.97	10.72
6/30/2011	11.54	11.20
7/5/2011	12.05	11.76
7/10/2011	12.64	12.70
7/15/2011	12.80	13.01
7/20/2011	13.03	13.42
7/25/2011	13.41	13.51
7/31/2011	13.19	13.07
8/5/2011	13.24	12.93
8/10/2011	13.28	13.16
8/15/2011	12.98	12.35
8/20/2011	13.33	12.80
8/25/2011	13.18	12.48
8/31/2011	12.63	11.57